European Journal of Taxonomy 933: 1–98
https://doi.org/10.5852/ejt.2024.933.2525
ISSN 2118-9773
www.europeanjournaloftaxonomy.eu
2024 · Stöhr S.

Monograph

urn:lsid:zoobank.org:pub:8F720F2B-BFBC-4CA1-BFF2-A2B8C7C8D3E1

Taxonomic analysis of the genital plates and associated structures in Ophiuroidea (Echinodermata)

Sabine STÖHR

Swedish Museum of Natural History, Department of Zoology, Box 50007, 10405 Stockholm, Sweden.
Email: sabine.stohr@nrm.se

urn:lsid:zoobank.org:author:412800EB-AACE-4313-9810-61F89B740405

Abstract. Recently, new insights have been gained from the ophiuroid skeleton that were instrumental in the inference of a new phylogeny. The so far least studied ossicles are the adradial and abradial genital plates and the radial shields, which articulate with each other and support the genital slit and disc. In addition, the inner sides of the oral shields and madreporites have never been examined in detail. The present study utilized SEM, micro-CT and digital photography to document and examine these structures in 57 species from 28 of the currently accepted 34 families of Ophiuroidea. Early ontogeny and fossils were also considered. Previously, mainly the articular structures had been analysed, but the overall shape of the genital plates was here found to hold important phylogenetic signals. A long-neglected ossicle was re-discovered and studied in detail for the first time, here named the oral genital plate. It was recognized in all Ophintegrida, but was found to be absent in all Euryophiurida. The oral genital plate articulates with the oral shield and supports the proximal part of the genital slit wall. Abradial and oral genital plates were found to be absent in species that lack genital slits, but the adradial genital plate was always present. Numerous new morphological characters with potential phylogenetic signals were identified, described and figured in detail. A pre-existing character matrix was extended and revised with these new data, as well as with recently revised data on oral papillae, and a Bayesian phylogenetic analysis was performed. This phylogeny largely agrees with the current molecular hypothesis, but some branches were not supported.

Keywords. Brittle stars, SEM, micro-CT, radial shield, oral shield, madreporite, phylogeny.

Stöhr S. 2024. Taxonomic analysis of the genital plates and associated structures in Ophiuroidea (Echinodermata). *European Journal of Taxonomy* 933: 1–98. https://doi.org/10.5852/ejt.2024.933.2525

Introduction

Ophiuroidea Gray, 1840 is the most speciose class of Echinodermata Klein, 1778, with about 2100 valid species (Stöhr *et al*. 2022). Like all echinoderms, ophiuroids possess a (mesodermal) endoskeleton, consisting of magnesium-rich calcite (Kokorin *et al*. 2014) that forms a mesh-like structure known as stereom, infused with an organic matrix with components from dermis and epidermis (Byrne 1994). The ophiuroid skeleton is composed of various elements (ossicles) that show a high degree of specialisation and a diverse morphology, which holds phylogenetic signals (Thuy & Stöhr 2016). The Ophiuroidea originated about 480 million years ago, and their modern bauplan evolved between 444 and 419 Ma

(Thuy *et al.* 2022). The crown group was long believed to have radiated after the Permian-Triassic extinction event (250 Ma), but Thuy *et al*. (2023) suggested a much earlier origin of the main clades (≥ 313 Ma). Several of the currently accepted families of Ophiuroidea had been proposed by Matsumoto (1915), based mainly on skeletal structures, but were later rejected or synonymized, until they were re-affirmed by an extensive molecular study (O'Hara *et al.* 2017) that completely revised the ophiuroid phylogeny. Based on this phylogeny, a new classification (O'Hara *et al.* 2018) with brief morphological diagnoses for 33 families was proposed. Goharimanesh *et al*. (2021) analysed 76 diagnostic morphological (mostly skeletal) characters for all families, except the most recently discovered Ophiojuridae O'Hara, Thuy & Hugall, 2021 that is currently known from a single damaged specimen (O'Hara *et al*. 2021), and compiled detailed descriptions. Only morphological data allow the inclusion of extinct species, known only from fossils, in a phylogenetic analysis, and although the current molecular phylogeny is broadly supported by morphological data (Thuy & Stöhr 2016), palaeontological data can affect branch length, tree topology and node age estimates (Ware & Barden 2016), which has been demonstrated by Thuy *et al*. (2022, 2023). Yet, the morphological dataset is still rather limited and it is desirable to explore the internal (not externally visible) skeleton of brittle stars in greater detail to expand the morphological data matrix compiled for phylogenetic inference by Thuy & Stöhr (2016).

The internal brittle star skeleton was described and superbly figured by Lyman (1882). He discussed only a limited set of features, but the oral skeleton and its relationship to the arm skeleton had been analysed previously by him (Lyman 1874). Matsumoto (1915, 1917) studied internal skeletal structures such as arm vertebrae, dental plates, oral plates and genital plates. Murakami (1963) studied dental and oral plates, and Hendler (2018) performed a detailed comparison of the mouth skeleton of all major groups of brittle stars, greatly advancing our understanding of the homologies of these parts. LeClair (1996) analysed the functional morphology of arm vertebrae and their articular structures, which was further elaborated by Clark *et al*. (2018) and Goharimanesh *et al*. (2021, 2022). Martynov (2010) performed a large comparative study of spine articular structures on lateral arm plates and included brief descriptions and images of dental, oral and genital plates. Thuy & Stöhr (2011) studied the lateral arm plate shape and micromorphology and later identified 42 phylogenetically informative characters on these plates (Thuy & Stöhr 2016). Wilkie & Brogger (2018) studied the peristomial plates and found them to be

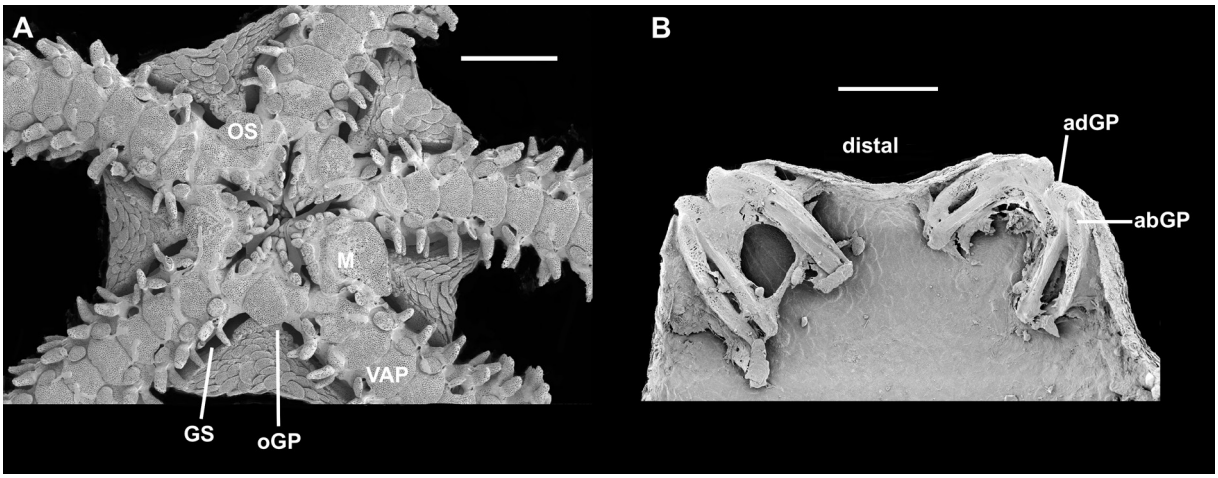

Fig. 1. Ventral and inner disc morphology of Ophiuroidea, SEM. **A**. *Ophionereis porrecta* Lyman, 1860, ventral side. **B**. Inside of dorsal disc of *Amphiura filiformis* (O.F. Müller, 1776), cast off during collecting, adradial and abradial genital plates attached to each other and to underside of radial shields. Abbreviations: abGP = abradial genital plate; adGP = adradial genital plate; GS = genital slit; M = madreporite; oGP = oral genital plate; OS = oral shield; VAP = ventral arm plate. Scale bars: 1 mm.

taxonomically useful at family level, although their main characters (size and fragmentation) were found in families of several orders (thus, homeoplaseous on different major branches of the tree). Ezhova *et al*. (2016) found the madreporite not to be phylogenetically informative, although they did not examine the inner surface of the madreporite.

Ossicles that have not yet received similar attention as the arm and mouth parts are the genital plates. These are part of the internal disc skeleton, largely invisible from the outside (Fig. 1A). They may be lost when the dorsal disc is autotomized or ripped off during collecting, as is often observed in species with scale-less disc parts, e.g., in *Amphiura filiformis* (O.F. Müller, 1776) (Fig. 1B) in contrast to its fully scaled congener *Amphiura chiajei* Forbes, 1843. This suggests that the genital plates may be more firmly attached to the dorsal disc than to the arm or ventral disc. Lyman (1882) and Matsumoto (1915, 1917) described two different ossicles as associated with and supporting the genital slit: the genital plate and genital scale present in almost all ophiuroids (Table 1). Matsumoto (1915, 1917) also mentioned two small "leaf-like scales" at the oral shield, found by him only in his order Gnathophiurida Matsumoto, 1915 (currently accepted as suborder Gnathophiurina). The leaf-like scales at the oral shield in *Macrophiothrix* H.L. Clark, 1938 were named "wing-like genital plates" by Hoggett (1991), which may cause confusion with Matsumoto's genital plate. Since the term "scale" may suggest a particular shape that is not always present in the genital scale, Martynov (2010) introduced the term *abradial genital plate* for the genital scale and correspondingly the term *adradial genital plate* for previous authors' genital plate, based on the position of these ossicles in relation to the arm (= radius). Here, I propose the term *oral genital plates* for Matsumoto's leaf-like scales at the oral shield, following the same logic. Martynov (2010) did not mention the oral genital plates and they seem to have been ignored in most morphological studies on brittle stars since Matsumoto (1915, 1917). Genital plates show a high morphological diversity with taxonomic significance (Stöhr *et al.* 2012a), but they have so far only been analysed superficially for phylogenetically informative characters (Table 1). Of the 130 characters in the matrix by Thuy & Stöhr (2016), only four pertained to the size and shape of the abradial genital plate, none to the adradial plate. The shape and microscopic structures of the oral genital plates have never been examined before.

The adradial genital plate is present in all ophiuroid species that have been examined, but the abradial plate appears to be missing in some Ophioscolecidae Lütken, 1869 (Martynov 2010). Martynov (2010) described both plates as about equal in size for most examined species (Table 1), but the adradial plate often has a thickened bulbous distal end and is usually stronger than the abradial plate, which is often flat and without a distinctly enlarged end. The adradial plate is usually positioned parallel to the arm, next to the vertebrae, and Matsumoto (1915) described it as affixed to the vertebrae in Gnathophiurina (contradicted by the easy loss of the genital plates in *A. filiformis*), but free in other groups, or attached by muscles, observations that have not been verified by later researchers. The adradial and abradial genital plates articulate with each other distally and the distal head of the adradial plate articulates with the distal end of the radial shield from below. There are specific articular structures on all these ossicles that have been described in terms of condyles and pits/sockets (Matsumoto 1915; Martynov 2010). In some taxa (e.g., *Ophiochondrus* Lyman, 1869, *Ophioderma* Müller & Troschel, 1840, *Ophiolepis* Müller & Troschel, 1840) the adradial and abradial genital plates were believed to be firmly affixed to each other, described as "soldered together" (Lyman 1882; Matsumoto 1915). Recent studies found that the plates separate readily when subjected to bleach (Martynov 2010; Stöhr *et al.* 2020). The term "soldered together" has also been applied by Matsumoto (1915) to the more firmly combined ambulacral ossicles that form the arm vertebrae and to the two ossicles that form the oral plate (half-jaw), both of which separate in bleach in some species (considered paedomorphic) and in juveniles (Stöhr & Martynov 2016). Thus, the exact meaning of this term is not as clear as it may have been over a century ago, and the relationship between the genital plates and adjacent structures needs to be re-examined.

Table 1 (continued on next three pages). Characterisation of genital plates by previous authors, per family. When no family characters were recorded, the type genus characters are given here, and if other genera were used, these are listed. The monospecific Ophiojuridae O'Hara, Thuy & Hugall, 2021 is omitted here, because it was not known to these previous authors. The terminology was translated into the terms used in the present study, and the information was adapted to the current classification, but most original phrases were kept. Abbreviations: see list on page 13.

Scientific name	Genital plate/radial shield articular characteristics		
	Lyman (1882)	**Matsumoto (1915, 1917)**	**Martynov (2010)**
Amphilepididae	adGP with very long cylindroid head, abruptly changing into short flat shaft, where short flat abGP attaches (like a "lobster's claw")	RS with socket, adGP with large, ball-like condyle; adGP not fixed to basal vertebrae; abGP short, flat, thin leaf-like; oGP short, wide, flattened, leaf-like, firmly attached to oral shield	RS with single compact, well-defined condyle; abGP similar in size to slightly smaller than adGP, both weakly developed, articulating below level of adGP condyle; ars of adGP: weakly defined symmetrically placed condyle bordered by low ridge; adGPs over proximal vertebrae not in contact
Amphilimnidae [formerly in Amphiuridae]	not mentioned	as in Amphiuridae.	not mentioned
Amphiuridae	RS with small distal knob; adGP long, slender, flattened, club-headed, abGP equally long or shorter, slender, blade-like	RS with socket, adGP with ball-like condyle; adGP firmly fixed to basal vertebrae; abGP short, very wide, flattened, leaf-like; oGP short, wide, flattened, leaf-like firmly attached to oral shield	RS with single, compact, well-defined condyle; abGP similar in size or slightly smaller than adGP and articulating below level of the adGP condyle; ars of adGP with well-defined symmetrically placed condyle, bordered by a low ridge; adGPs over proximal vertebrae in contact with each other
Asteronychidae [Trichasteridae in Matsumoto 1915,1917]	RS long, narrow, in pieces; adGP very wide, flat, proximally attaches to a small abGP	RS long, bar-like; RS and adGP with transverse ridge; adGP long and stout, abGP are rather very small; abGP articulates with adGP near the inner ends of the latter	adGP with moderate condyle; abGP much smaller than adGP
Astrophiuridae [formerly in Ophiuridae]	not mentioned	no condyles or sockets; adGP and abGP entirely internal, very slender, articulating with each other at the end	not mentioned
Clarkcomidae [formerly in Ophiocomidae]	not mentioned	not mentioned	not mentioned
Euryalidae	RS stout, solid; adGP stout; abGP short, very stout	transverse ridge, long, stout, no condyles or sockets; abGP small	adGP with moderate condyle; abGP much smaller than adGP
Gorgonocephalidae	RS of soldered overlapping plates; adGP and abGP are specialised scales of ventral interradial disc, folded in; RS and GP regulate roof of disc as it is lowered or raised	transverse ridge; adGP long, stout, abGP small, at distal end of adGP	moderate condyle; abGP much smaller than adGP
Hemieuryalidae	RS large, with thickened margins; adGP massive, shapeless, extending to oral shield; small abGP soldered to adGP	adGP and abGP of either side of a radius firmly soldered together	not mentioned

Table 1 (continued).

Scientific name	Genital plate/radial shield articular characteristics		
	Lyman (1882)	**Matsumoto (1915, 1917)**	**Martynov (2010)**
Ophiacanthidae	RS slightly enlarged distally; adGP thick, club-headed, somewhat rounded; abGP short, blade-like	transverse ridge or simple face; adGP and abGP not soldered	RS with single weakly defined condyle; abGP similar in size or slightly smaller than adGP and articulating below level of adGP condyle; ars of adGP vary from slightly elevated elongated condyle to well-defined asymmetrically placed condyle
Ophiactidae	adGP stout, long, slender, cylindrical, abGP much shorter	RS socket; adGP large, ball-like condyle; adGP firmly fixed to basal vertebrae, abGP short, very wide, flattened, leaf-like; oGP short, wide, flattened, leaf-like scale, firmly attached to oral shield	RS with single, compact, well-defined condyle; abGP similar in size or slightly smaller than adGP and articulating below level of adGP condyle; ars of adGP with well-defined symmetrically placed condyle, bordered by low ridge; adGPs over proximal vertebrae in contact to each other
Ophiernidae [formerly in Ophioleucidae]	RS short, circular; adGP flat, attached to outer end of peristomial plate	essentially similar to *Ophioleuce*	not mentioned
Ophiobyrsidae	RS oblong, small, short; adGP small, oval, solid, plastron-like, close to arm, meeting on its upper mid-line; near its distal end attaches to abGP short, curved, slender, longer than adGP	adGP, abGP small, both only at distal genital slit	adGP and abGP well defined
Ophiocamacidae [formerly in Ophiacanthidae]	adGP flattened, with longish head; abGP long and blade-like	as in Ophiacanthidae	not mentioned
Ophiocomidae	adGP thick blade with rounded edges, slightly clubbed head articulating with RS; abGP short, thin, blade-like	RS and adGP with two condyles and one pit; both GPs bar-like	RS with single or few weakly defined condyles; abGP similar in size or slightly smaller than adGP and articulating below level of adGP condyle; ars of adGP with well-defined, asymmetrically placed condyle
Ophiodermatidae	[*Ophioderma* was included in *Ophiura*]	RS and adGP with two condyles and one pit; both GPs bar-like	RS with single or few weakly defined condyles; abGP similar in size or slightly smaller than adGP and articulating below level of the adGP condyle; ars of adGP with1–2 irregular massive condyles
Ophiohelidae [formerly in Ophiacanthidae]	RS absent; *Ophiomyces*: adGP and abGP thin, wide, long, curved over top of arm	adGP long, thin, curved over dorsal arm, abGP absent	not mentioned
Ophiolepididae	adGP strong, with long thick head, abGP attached at a point far inward, so that the genital opening is much shortened, may be soldered to the adGP for part of its length	[lumped with *Ophiomusa*, *Ophiura* and others]; two condyles, one pit	RS with 1–2 weakly defined condyles; abGP similar in size or slightly smaller than adGP and articulating below level of adGP condyle; ars of adGP with weakly defined condyle, bordered by low ridge

Table 1 (continued).

Scientific name	Genital plate/radial shield articular characteristics		
	Lyman (1882)	**Matsumoto (1915, 1917)**	**Martynov (2010)**
Ophioleucidae	not mentioned	RS and adGP with two condyles and one pit; abGP wide, thin, leaf-like	not mentioned
Ophiomusaidae [formerly in Ophiolepididae]	adGP and abGP stout, massive	[lumped with *Ophiolepis*, *Ophiura* and others]; two condyles, one pit	not mentioned
Ophiomyxidae	RS small, irregular; adGP long, stout, rounded; short abGP attached at point far inward, creating a "lobster claw"	simple face articular structure; abGP slender, articulates at distance from distal end of adGP	well-defined condyle; adGP and abGP small
Ophionereididae	adGP long, moderately stout, club-headed, at inner part of head thin abGP extending to oral shield	RS and adGP with two condyles and one pit	RS with single or few weakly defined condyles; abGP similar in size or slightly smaller than adGP and articulating below level of adGP condyle; ars of adGP with well-defined, asymmetrically placed condyle
Ophiopezidae [formerly in Ophiodermatidae]	adGP shorter, thicker than in *Ophiura*, abGP inserted inside head of adGP, shortening genital slit	not mentioned	not mentioned
Ophiopholidae [formerly in Ophiactidae]	adGP thick, tapering cylindrical, abGP small, very short, curved	RS socket, adGP large, ball-like condyle; adGP firmly fixed to basal vertebrae; abGP short, very wide, flattened, leaf-like; oGP short, wide, flattened, leaf-like scale, firmly attached to oral shield	not mentioned
Ophiopsilidae [formerly in Ophiocomidae]	RS curved, bar-like; adGP with cylindroid head, flat at ⅓ of its length, where flat abGP attaches, prolonged to RS by slender additional piece	RS and adGP each with 2 condyles and 1 pit; adGP entirely free from basal vertebrae; abGP long, narrow, bar-like	not mentioned
Ophiopteridae [formerly in Ophiocomidae]	not mentioned	as in Ophiocomidae	not mentioned
Ophiopyrgidae [formerly in Ophiuridae]	*Ophiuroglypha irrorata*: abGP small, proximally narrow, wider distally	[lumped with *Ophiura*, *Ophiolepis*, *Ophiomusa* and others]	not mentioned
Ophioscolecidae [formerly in Ophiomyxidae]	Minute curved RS; adGP with clubbed head, rounded tapering shaft; abGP minute, flat, curved	as in Ophiomyxidae	*Ophioscolex*: adGP without distinct condyle; *Ophiocymbium*: distinct condyle; abGP absent in several genera
Ophiosphalmidae [formerly in Ophiolepididae]	*Ophiolipus*: adGP with rounded shaft, large clubbed head, to which attaches a long thin abGP, sharing articulation with RS	not mentioned	not mentioned
Ophiothamnidae [formerly in Ophiacanthidae]	adGP above arm, long, bar-like, narrowest at outer end, curved; abGP absent	adGP long, club-shaped, above arm; abGP absent	not mentioned

Table 1 (continued).

Scientific name	Genital plate/radial shield articular characteristics		
	Lyman (1882)	**Matsumoto (1915, 1917)**	**Martynov (2010)**
Ophiotomidae [formerly in Ophiacanthidae]	not mentioned	as in Ophiacanthidae	RS with single weakly defined condyle; abGP similar in size or slightly smaller than adGP and articulating below level of adGP condyle; ars of adGP intermediate between slightly elevated elongated condyle and well-defined asymmetrically placed condyle
Ophiotrichidae	RS large, triangular, with projecting distal knobs, articulated with the clubbed knobby heads of long, stout, rounded, slightly curved adGP; abGP large, almost semicircular, continued to mouth shield by additional scale (= oGP)	RS socket, adGP large, ball-like condyle; Genital plates, as a rule, firmly fixed to the basal vertebrae; abGP short, very wide, flattened, leaf-like; oGP short, wide, flattened, leaf-like scale, firmly attached to oral shield	RS with single compact well-defined condyle; abGP similar in size or slightly smaller than adGP and articulating below level of adGP condyle; ars of adGP with well-defined condyle, bordered by low ridge
Ophiuridae	RS jointed to curved, rounded, club-headed adGP; abGP attached to outer end of adGP, both continued by ridge or thin plate to mouth shield	RS and adGP with two condyles and one pit; adGP and abGP bar-like	abGP similar in size or slightly smaller than adGP, at same level as adGP condyle forming lateral prolongation; ars of adGP with one well-defined condyle, bordered by rectangular low ridge; ars of RS vary across taxa (1–2 slightly conspicuous condyles, well-defined narrow ridges, or no distinct condyles)

Genital plates are non-symmetric ossicles that can appear highly different (as if from different species), when looked at from different angles (Stöhr *et al.* 2020), and their shape and morphological details are difficult to understand. In previous studies (e.g., Martynov 2010; Stöhr *et al.* 2012a, 2020), they have been examined with scanning electron microscopy (SEM), a technique that requires destruction of the specimen to isolate the ossicles. The images obtained by SEM are two-dimensional, which requires several identical ossicles to be mounted in different positions to cover all details. The exact position of ossicles in relation to each other is often lost during the preparation process. To overcome the limitations inherent in two-dimensional imaging, three-dimensional imaging techniques such as X-ray micro-computed tomography (micro-CT) have been explored, but so far rarely on brittle stars (Landschoff & Griffiths 2015; Okanishi *et al.* 2017; Stöhr *et al.* 2019).

Previous studies focused on the articular structures on genital plates and radial shields, often ignoring other details. The present study analyses the shape and in situ position of the three types of genital plates in relation to each other and to radial and oral shields, examined by micro-CT and SEM. The aim of this project is to document and collect new morphological data on the genital plates to refine and improve the morphological phylogenetic inference. The resulting information may also be used to improve family level identification keys. In addition, the descriptions of these ossicles are refinements of the taxonomic descriptions of the analysed species.

Material and methods

Preparation and imaging

Specimens of 57 species from 28 families were examined for this study (Table 2), preferably of the type species or genus of a family, when available. From each species, one or several individuals were selected in the upper size range of the species (in late ontogeny), to obtain well-developed ossicles. For scanning electron microscopy (SEM), genital plates, oral shields, madreporites and radial shields were isolated by submerging the animal in concentrated household bleach (NaOCl) until the soft tissues had dissolved, leaving the dissociated skeletal parts. These were then washed in tap water. After the oral genital plates were (re-)discovered, additional specimens were dissociated and the oral genital plates were hand picked from the specimen during the process. In these specimens, intermediate stages during bleaching were photographed with an Olympus TG-4 digital camera with macro settings and image stacking function. The ossicles were mounted on aluminium stubs that had been covered with spray glue. Mounting in a drop of water allowed to arrange the tiny ossicles in different positions. The stubs were then left to dry in room air, coated with gold and examined with a Quanta FEG 650 scanning electron microscope at 5 kV current in high vacuum. Pre-existing (mostly unpublished) images from other projects (Stöhr 2005, 2011; Stöhr *et al.* 2013, 2020; Thuy & Stöhr 2016; Stöhr & Martynov 2016; Stöhr & O'Hara 2021) were also utilized (obtained with a Hitachi S-4300 SEM), although these did not always include all target structures, but when additional specimens were not available for dissection, limited data were still considered valuable. Pre-existing SEM images of some juveniles and paedomorphic species (Stöhr & Martynov 2016) were examined to include insights from early ontogeny. Observations from fossil species (Thuy & Stöhr 2016) were also included for evolutionary considerations.

Complete specimens of 23 species from 23 families were examined by micro-CT (Table 3) with a Zeiss Xradia Versa 520 X-ray microscope (XRM), at SUBIC (Stockholm University Brain Imaging Center) at voxel sizes of 1–23 µm. It was attempted to scan a section of each animal including an arm and part of an interradius with adradial and abradial genital plates, to reduce scan time and increase resolution. The largest specimens could not be scanned at high resolution, because the magnification had to be kept low to fit the complete target section in the beam area. When the oral genital plates were discovered, additional scans were performed to cover a section of the interradius with an oral shield. Image slices were reconstructed from the µCT scans with the Dragonfly software (Object Research Systems Inc., Canada). Volume rendering was performed with the software package Drishti (Limaye 2012). Large files were binned by a factor 2 to enhance computing performance. All micro-CT files were uploaded to the data repository Zenodo (https://zenodo.org/) and are freely accessible (https://doi.org/10.5281/zenodo.8138454).

Morphology and phylogenetic analysis

The characters observed on the target structures of this study were used to update the family level dataset by Thuy & Stöhr (2016, 2018), using the software Xper2 (Ung *et al.* 2010). New character statements were formed (see Appendix) as D-RS-9–D-RS-12 for the inner side of the radial shields, OR-GP-1–OR-GP-4 for the oral genital plates and AD-GP-1–AD-GP-4 for the adradial genital plates; the previous character statements GP-1–GP-9 were renamed as AB-GP-1–AB-GP-9 for the abradial genital plates; new characters AB-GP-11–AB-GP-13 were added and the states of *AB-GP-2: Abradial genital plate, shape* were modified. The characters M-PaT-2, M-PaT-4, M-PaT-6 and M-PaT-7 for the oral papillae were revised following Hendler (2018) and the new characters M-PaT-9–M-PaT-13 were added, differently from Thuy *et al*. (2021). A new state was added to *LAP-O-8: Outer surface structure: with pointed thorns (3)* and the new characters for vertebrae, *A-V-7: Needle-like thorns in dorsal groove: absent (0), present (1)*, and for lateral arm plates, *LAP-G-7: First LAPs, shape: like following LAPs (0), wing-like folded (1)*, were created. The character statements LAP-G-6, LAP-I-7 and LAP-I-8, introduced by Thuy *et al*. (2021), were also added to the matrix. The character statement *D-P-8: Outer*

Table 2 (continued on next page). Specimens of ophiuroid species examined by SEM and/or micro-CT. Locality, disc diameter (DD), and ID numbers of the samples are given, as far as known. MnhnL, Natural History Museum Luxembourg, SMNH, Swedish Museum of Natural History. Species marked with an asterisk were prepared specifically for this project; of others, images or dissociated ossicles existed prior to this study.

Family	Species	Locality	DD [mm]	ID
Amphilepididae	*Amphilepis norvegica**	Sweden, Skagerrak	7	SMNH-166617, 218820
Amphilimnidae	*Amphilimna olivacea*	West Africa, Gulf of Guinea	7.5	SMNH-108766, 133293, 218846–47, 218871
Amphiuridae	*Amphiura chiajei**	Sweden, Gullmarsfjord	7.2	SMNH-218888
Amphiuridae	*Amphiura filiformis*	Sweden, Kattegatt, off Värö	6	SMNH-218855
Amphiuridae	*Amphipholis squamata*	France, Mediterranean Sea, Port Cros	1, 1.12, 2.9	SMNH-99942, 99944, 218906
Asteronychidae	*Asteronyx loveni**	Iceland	13.6	SMNH-218899, 218901–02
Astrophiuridae	*Astrophiura* cf. *tiki*	Andaman Back-Arc basin	6.4	SMNH-120685
Euryalidae	*Euryale aspera*	New Caledonia, Lifou	22	SMNH-109400, 218856, 218857, 218859, 218870
Gorgonocephalidae	*Gorgonocephalus caputmedusae*	Atlantic Ocean	75	SMNH-130501–02, 131548–52, 131567–70, 218806–09, 218869–70
Hemieuryalidae	*Ophiozonella longispina*	Japan, Tokyo Bay	10	SMNH-111037–38, 127070, 218853–54
Ophiacanthidae	*Ophiacantha bidentata**	Svalbard	11.5, 13	SMNH-111042–44, 21889
Ophiacanthidae	*Ophiacantha abyssicola*	Iceland	13	SMNH-111014–16
Ophiactidae	*Ophiactis abyssicola**	Iceland	5.3, 7.6	SMNH-218897, 218900, 218903
Ophiactidae	*Ophiactis savignyi*	Lebanon, Mediterranean Sea Ramkine Island	–	SMNH-44323
Ophiernidae	*Ophiernus vallincola*	Iceland	10	SMNH-218827–28, 218849–50
Ophiocamacidae	*Ophiocamax vitrea**	Fiji, Lau Ridge, Yangasa cluster	10.9	SMNH-218891–92, 218896, 218898
Ophiocomidae	*Ophiocoma scolopendrina**	New Caledonia, Lifou, Baie de Chateaubriand, Wé	12	SMNH-218817–19
Ophiocomidae	*Ophiocoma echinata*	Tropical Atlantic, Saint Barthelemy	–	MnhnL OPH002
Ophiocomidae	*Ophiocoma schoenleinii*	New Caledonia, Lifou, Baie du Santal, Pte de Chépénéhé	15	SMNH-111020–22
Ophiocomidae	*Ophiocoma erinaceus*	New Caledonia, Lifou, Baie du Santal, Pte de Chépénéhé	16	SMNH-111017–19
Ophiocomidae	*Breviturma krohi*	La Réunion	13	SMNH-Type-8535
Ophiocomidae	*Breviturma dentata*	La Réunion, Etang Salé	11	SMNH-133232–33
Ophiocomidae	*Breviturma doederleini*	French Polynesia, Moorea	13	SMNH-133225, 133296–97
Ophiodermatidae	*Ophioderma longicaudum**	France, E of Marseille, Port d'Alon	25.2	SMNH-218880, 218884, 218907
Ophiodermatidae	*Ophioderma africanum*	Senegal, Dakar, Gorée Island, shipwreck Tacoma	11.72	SMNH-Type-7486
Ophiodermatidae	*Ophioderma zibrowii*	Mediterranean Sea, Cyprus	12	SMNH-112870, 218911
Ophiohelidae	*Ophiomyces delata*	Tonga, Eua	–	SMNH-131572, 133592, 218875
Ophiohelidae	*Ophiomyces frutectosus*	North Atlantic, Josephine Bank	5.4	SMNH-162465
Ophiolepididae	*Ophiolepis variegata**	Panama	16.4	SMNH-202613, 218824–26, 218893–95

Table 2 (continued).

Family	Species	Locality	DD [mm]	ID
Ophiolepididae	*Ophiotypa simplex*	Indonesia, N of Java	5.1	SMNH-99539
Ophioleucidae	*Ophiopallas paradoxa**	New Caledonia, Lifou	7	SMNH-218863–64
Ophiomusaidae	*Ophiomusa lymani*	Iceland	24.3	SMNH-130490, 130493, 130500, 218877–78
Ophiomyxidae	*Ophiomyxa serpentaria**	Iceland	17	SMNH-218815–16
Ophiomyxidae	*Ophiomyxa pentagona*	Mediterranean Sea, Italy	15	SMNH-111004–06, 111024, 160597
Ophionereididae	*Ophioplax lamellosa*	Australia, Pieman Canyon	8.5	SMNH-130491–92, 130497, 131575–77, 218867
Ophionereididae	*Ophiochiton fastigatus*	Bay of Bengal	–	MnhnL OPH025
Ophionereididae	*Ophionereis reticulata**	West Indies, Saint Thomas	12.2	SMNH-218822–23, 218835, 218852, 218858, 218874
Ophionereididae	*Ophionereis porrecta*	New Caledonia, Lifou, Pte Easo	4.5	SMNH-11100809, 111047, 218905
Ophionereididae	*Ophionereis degeneri*	New Caledonia, Lifou, Pte Easo	4.5	SMNH-111010
Ophiopholidae	*Ophiopholis aculeata**	Norway, Bergen area, NW of Siggen	15	SMNH-218848, 218881
Ophiopsilidae	*Ophiopsila guineensis**	Mediterranean Sea, France	10.9	SMNH-218839–40, 218866
Ophiopyrgidae	*Ophiopleura borealis*	Svalbard	32	SMNH-21881114, 218872
Ophiopyrgidae	*Ophiopyrgus saccharatus*	Indian Ocean, Australia	5.1	SMNH-99530
Ophiopyrgidae	*Ophiopyrgus wyvillethomsoni*	Mid-Pacific Ocean	2.56	SMNH-102149
Ophiopyrgidae	*Amphiophiura latro*	Fiji, Lau Ridge	6	SMHN-154489, 218841–42, 218865, 218950
Ophiopyrgidae	*Amphiophiura insolita*	New Caledonia, Lifou	12	SMNH-108774, 111033 –34, 218832–34, 218845
Ophioscolecidae	*Ophioscolex glacialis**	Svalbard and Jan Mayen, Kong Karls Land, Kongsöya, S of Tömmernäset	20.6	SMNH-218860–62, 218890
Ophioscolecidae	*Ophiolycus purpureus**	Iceland	11.6	SMNH-21886
Ophiothamnidae	*Histampica duplicata*	Iceland	5.5	SMNH-131574
Ophiotomidae	*Ophiocomina nigra**	Mediterranean Sea, Marseille	8.9	SMNH-218879, 218887
Ophiotomidae	*Ophiotreta valenciennesi*	Tonga, N Ha'apai group	14	SMNH-201475
Ophiotomidae	*Ophiocopa spatula*	Tonga, Central Ha'apai group	–	SMNH-131565–66
Ophiotrichidae	*Ophiothrix fragilis**	Sweden, Gullmarsfjord	14	SMNH-218883
Ophiuridae	*Ophiura sarsii**	Iceland	17.9	SMNH-218876, 218882
Ophiuridae	*Ophiura ophiura**	Sweden, Gullmarsfjord	15.8	SMNH-218829–31, 218836, 218873
Amphilepidida incertae sedis	*Ophiopus arcticus**	Iceland	5.2	SMNH-218843–44
Amphilepidida incertae sedis	*Ophienigma spinilimbatum*	USA, Atwater Canyon	–	SMNH-131562–63

Table 3. Scanning parameters for specimens of ophiuroids examined by micro-CT with a Zeiss Xradia Versa 520 x-ray microscope. Abbreviations: Exp = exposure time per image; Opt = optical magnification. For specimen data see Table 2.

Family	Species	Voltage (kV)	Voxel (µm)	Opt.	Filter	Exp. (s)	No. of images
Amphilepididae	*Amphilepis norvegica*	100	2.90	4	LE1	1	991
Amphilimnidae	*Amphilimna olivacea*	100	3.68	4	LE2	1	991
Amphiuridae	*Amphiura chiajei*	80	3.52	4	LE1	0.7	992
Asteronychidae	*Asteronyx loveni*	100	5.07	4	LE1	2	2026
Hemieuryalidae	*Actinozonella texturata*	100	2.61	4	LE2	1	991
Ophiacanthidae	*Ophiacantha bidentata*	100	4.15	4	LE2	1	990
Ophiactidae	*Ophiactis savignyi*	80	1.19	4	LE1	2	986
Ophiernidae	*Ophiernus vallincola*	100	3.27	4	LE2	1	990
Ophiocamacidae	*Ophiocamax vitrea*	100	4.1	4	LE2	3	989
Ophiocomidae	*Ophiocoma echinata*	100	5.61	4	LE1	4	2022
Ophiodermatidae	*Ophioderma longicaudum*	100	2.28	4	LE1	4	1982
Ophioleucidae	*Ophiopallas paradoxa*	80	2.77	4	LE1	0.7	991
Ophiomusaidae	*Ophiomusa lymani*	100	23.3	0.4	LE2	1	1024
Ophiomyxidae	*Ophiomyxa pentagona*	100	3.3	4	LE2	3	1008
Ophionereididae	*Ophionereis reticulata*	100	8.5	4	LE1	1	1014
Ophiopholidae	*Ophiopholis aculeata*	100	3.53	4	LE2	1	991
Ophiopsilidae	*Ophiopsila guineensis*	100	3.74	4	LE2	1	992
Ophiopyrgidae	*Amphiophiura insolita*	100	4.55	4	LE2	1.5	990
Ophioscolecidae	*Ophiolycus purpureus*	100	3.39	4	LE2	1	992
Ophiothamnidae	*Histampica duplicata*	100	3.36	4	LE2	0.6	992
Ophiotomidae	*Ophiocomina nigra*	100	4.2	4	LE2	1	990
Ophiotrichidae	*Ophiothrix fragilis*	140	6.02	0.4	HE1	5	2023
Ophiuridae	*Ophiura ophiura*	100	4.1	4	LE2	2	990

integument thickness was removed, because thickened integument is homoplasious at family level (e.g., found in Ophiopyrgidae, Ophioscolecidae, Ophiomyxidae) and variable among species within families (e.g., in Ophiopyrgidae: *Ophiopleura* and *Ophiosparte* but not *Amphiophiura* nor *Ophiopyrgus*). The assessment of all anatomical structures was based on adult specimens, which means that structures that develop in early ontogeny, but are lost later, were scored as unknown/absent.

A common problem in datasets designed to reconstruct higher-level phylogenies are character dependencies with large numbers of absent characters, because structures appear or disappear in major lineages (Simões *et al.* 2023). In the original matrix, such character dependencies were dealt with in an inconsistent way, i.e., character states defined as observed properties were combined with the state "absent" in the same character statement. Other characters were treated separately with a primary/neomorphic character (absent/present) and one or several dependent secondary/transformational characters (Sereno 2007), a coding strategy that has recently been shown to outcompete other coding methods with large datasets (Simões *et al.* 2023). Bayesian inference has been found to better handle the problems arising from character dependencies than maximum likelihood and parsimony methods (Simões *et al.* 2023), but it may fail with large amounts of missing data (King 2019), and increasing the number of secondary characters in a morphological matrix can reduce the accuracy of currently available algorithms (Simões *et al.* 2023). Sereno (2007) showed that coding "absent" as "unknown" in a transformational character delivers the same results in a phylogenetic analysis as coding it paired with a separate neomorphic character. Logically, "unknown" is appropriate, when we can't know if a

structure has been lost or not yet evolved. Although "unknown" is coded as missing and inapplicability as a gap, both are treated the same (as missing data) by most algorithms used by the available software for phylogenetic inference (Brazeau 2011). Multiple dependencies for absent characters can be treated as unknown data without creating a bias towards that character. Hence, absent structures were here scored as "unknown" in a secondary character, omitting the primary character, except in neomorphic characters without dependencies. When the absence of a structure was considered apomorphic it was scored as a state in a transformational character (e.g., number of dorsal arm plates in Asteronychidae scored as "none"). Since details of oral genital plates were not examined in all species needed for the phylogenetic inference and it is unknown if they existed in the common ancestor of Ophintegrida and Euryophiurida, a neomorphic character was included to allow at least scoring for the presence of these ossicles, although all dependencies needed to be scored as unknown. Character descriptions were revised to form proper character statements containing a structure, a variable and its properties (Appendix). All characters included from the previous matrix were verified and when necessary rescored. The final character matrix included 69 species (including eight fossils) and 153 characters. It was exported as a Nexus formatted file (Supp. file 1).

A Bayesian phylogenetic analysis was performed using the software package MrBayes (Huelsenbeck & Ronquist 2001) with the same parameters as in Thuy & Stöhr (2016), but with a partly different set of species (Supp. file 1). MrBayes uses a modified version of the Juke-Cantor model for morphological data as outlined by Lewis (2001) with character states from 2 to 10 (Wright & Hillis 2014; Ronquist *et al*. 2020). Only variable characters were sampled, omitting characters that have the same state for all examined taxa. Some parsimony non-informative character states were included, e.g., wing-like folded first lateral arm plates (Amphilimnidae) and needle-like thorns on the vertebrae (Ophiocamacidae), which are autapomorphies of monogeneric families, but also synapomorphies of the species in these families and were found to improve the tree. To compensate for this, the coding parameter was set to variable in the Bayesian analysis. Character states were assumed to have equal frequency, and prior probabilities were equal for all trees. As outgroup, *Aganaster gregarius* (Meek & Worthen, 1869) was used. Evolutionary rates were assumed to vary between sites according to a discrete gamma distribution. Branch lengths were unconstrained. Average standard deviations of split frequencies stabilized at about 0.005 after seven million generations, sampled every 1000 generations. The first 25% of the trees were discarded as burnin. The resulting consensus trees were examined with the software FigTree ver. 1.4.4 by Rambaut (http://tree.bio.ed.ac.uk/software/figtree/).

The taxonomy follows Stöhr *et al*. (2022). The terminology previously used to describe the articular structures of the genital plates was revised.

Terminology used

- Abradial genital plate = the ossicle farther from the arm (= radius), articulates laterodistally with the adradial genital plate.
- Adradial genital plate = the ossicle closest to the arm (= radius), articulates with the radial shield from below and with the adradial genital plate laterally.
- Articular structure = general term for the structures that form an articulation or joint between two ossicles.
- Condylar process = protuberance that ends in a condyle or other articular structure.
- Condyle = domed/convex prominence at the end of an ossicle, part of the articular structures of a joint between ossicles.
- Oral genital plate = smaller ossicle that articulates at the distal edge of the oral shield.

Abbreviations

abGP	=	abradial genital plate
adGP	=	adradial genital plate
ars	=	articular structure(s)
AS	=	adoral shield
co	=	condyle
cp	=	condylar process
DAP	=	dorsal arm plate
dd	=	disc diameter
dist	=	distal
do	=	dorsal
GP	=	genital plate
gpa	=	genital papillae
gr	=	groove
GS	=	genital slit
h	=	hydropore
LAP	=	lateral arm plate
M	=	madreporite
micro-CT	=	X-ray micro-computed tomography
n	=	notch
oGP	=	oral genital plate
OP	=	oral plate
OS	=	oral shield
p	=	muscle patch
PP	=	peristomial plates
prox	=	proximal
RS	=	radial shield
SEM	=	scanning electron microscopy
sp	=	spur
T	=	tooth
v	=	vertebra
VAP	=	ventral arm plate
vd	=	ventral disc
ve	=	ventral

Results

Morphology

The three types of genital plates are described below in taxonomic order per family and genus, followed by observations from juvenile stages and fossils. The genital plates, radial shields and oral shields vary in shape and size between the examined species and hold phylogenetic signals, as is summarized after the taxonomic treatment. Oral genital plates were found in almost all taxa, except in the Euryophiurida, but can be secondarily lost in some species. Abradial genital plates were also found to be absent in some species, presumably secondarily lost (see also Discussion). Computer generated tabular descriptions of all analysed species, based on the matrix of family level characters, can be found in Supp. file 2.

Superorder Euryophiurida O'Hara, Hugall, Thuy, Stöhr & Martynov, 2017
Order Ophiurida Müller & Troschel, 1840 sensu O'Hara *et al*., 2017
Family Ophiuridae Müller & Troschel, 1840

Genus ***Ophiura*** Lamarck, 1801
Fig. 2

Type species

Asterias ophiura Linnaeus, 1758.

Examined species

Ophiura ophiura, *O. sarsii* Lütken, 1855.

Oral GP

Row of nearly vertical scales lines abradial edge of genital slit, proximalmost scale overlapped by lateral edge of oral shield, appears not to articulate or form a pair with opposite scale, hence, oPGs considered absent.

Adradial GP

Club-like long rod with bulbous distal end, at least three arm segments long, parallel to arm, distal end curving upwards to meet radial shield. Dorsal part of rod-like part round and thickened, ventral part thinner and blade-like flattened. Distal end with two ball-like condyles, differing in size, one bordered adradially by a half-circle-shaped groove, abradially by flat edge. Several depressions between condyles, a rough patch proximal to condyles on dorsal adradial edge.

Abradial GP

Roughly triangular, cup-shaped (abradially convex), with dorsal beak-like extension, much wider than adGP, two thirds as long as adGP, almost completely exposed at disc edge. Ventral adradial edge with pores, where genital papillae attach (arm comb). Articulates to adGP at right angle, creating wide gap between both GPs.

Oral shield

Madreporite with hydropore in one lateral distal edge, inner surface flat, smooth stereom, finer along edges, large opening in proximal half.

Radial shield

With two weakly domed condyles, radial one bordered by distal half-circular groove, articulating with adGP.

Family Ophiopyrgidae Perrier, 1893

Genus ***Ophiopyrgus*** Lyman, 1878
Fig. 3

Type species

Ophiopyrgus wyvillethomsoni Lyman, 1878.

Examined species

Ophiopyrgus saccharatus Studer, 1882, *O. wyvillethomsoni*.

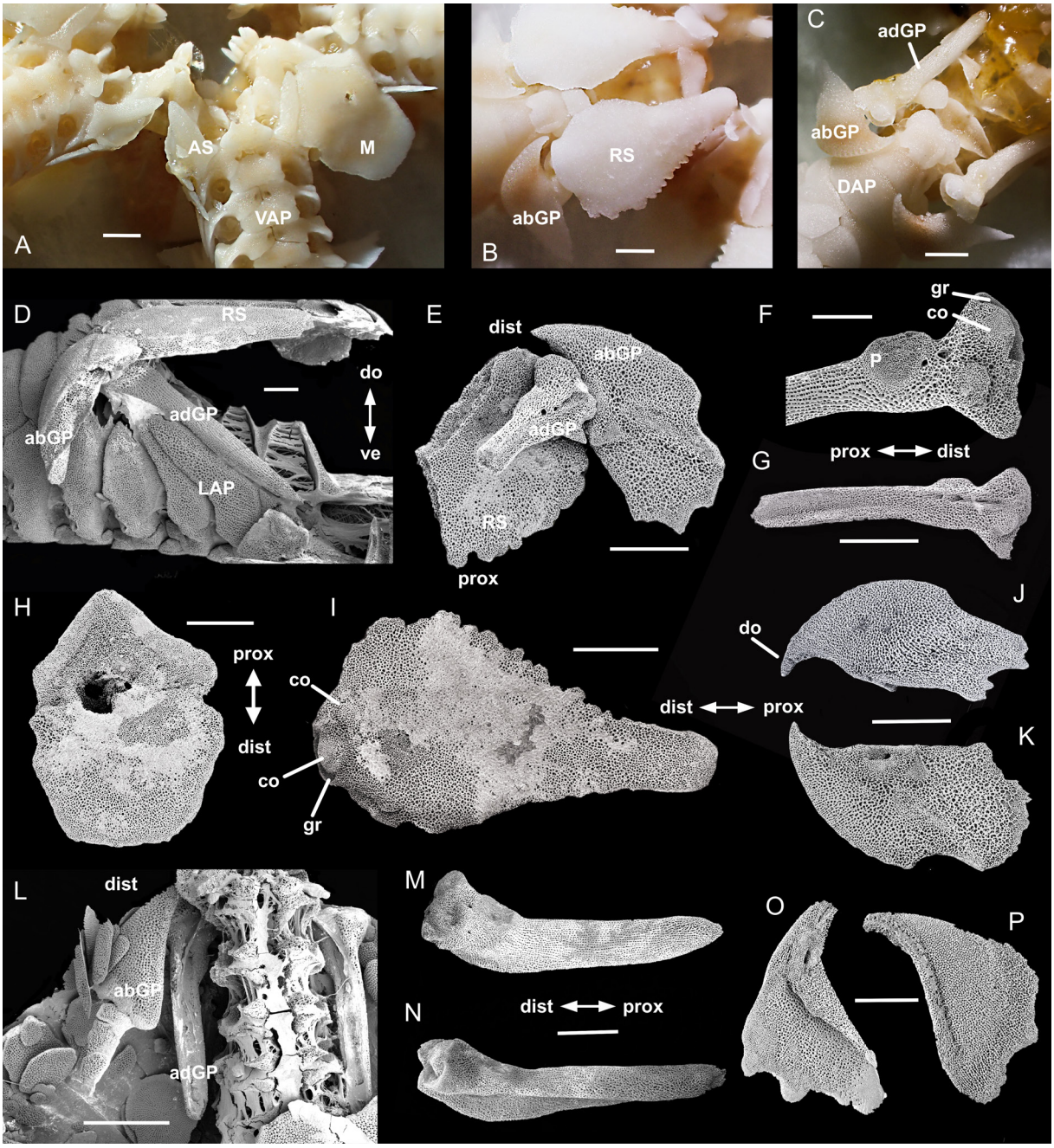

Fig. 2. Ophiuridae Müller & Troschel, 1840, digital (A–C) and SEM (D–P) images. **A–K**. *Ophiura ophiura* (Linnaeus, 1758). **A**. Mouth parts macerated in bleach, one jaw with oral shield removed, another with madreporite still attached, no oGP present. **B**. Radial shields and abGP in situ, dorsal view. **C**. adGP and abGP at arm base after removal of RS and disc, dorsal view. **D**. abGP, adGP, and RS, lateral view. **E**. abGP, adGP, RS, internal view. **F**. adGP, distal end, dorsal aspect. **G**. abGP, abradial aspect. **H**. Madreporite, inner aspect. **I**. Radial shield, inner aspect. **J**. abGP, outer aspect. **K**. abGP, inner aspect. **L–P**. *Ophiura sarsii* Lütken, 1855. **L**. adGP, abGP in situ, ventral view. **M**. adGP, abradial aspect. **N**. adGP, adradial aspect. **O**. abGP, inner aspect. **P**. abGP, outer aspect. Scale bars: A–E = 1 mm; F–P = 0.5 mm.

Oral GP

Absent.

Adradial GP

Ophiopyrgus saccharatus: rectangular, high, distally swollen, appears rounded axe-shaped in dorsal view, axe-head at abradial edge, adradial side straight, flat, large hole in distal dorsal part, articulates with RS at distal adradial point with round, finer meshed patch. As long as abGP, half as wide. *Ophiopyrgus wyvillethomsoni*: elongated, irregular, depression in distal abradial edge connects to abGP, flat distal end articulates with RS. Shorter than abGP, half as wide.

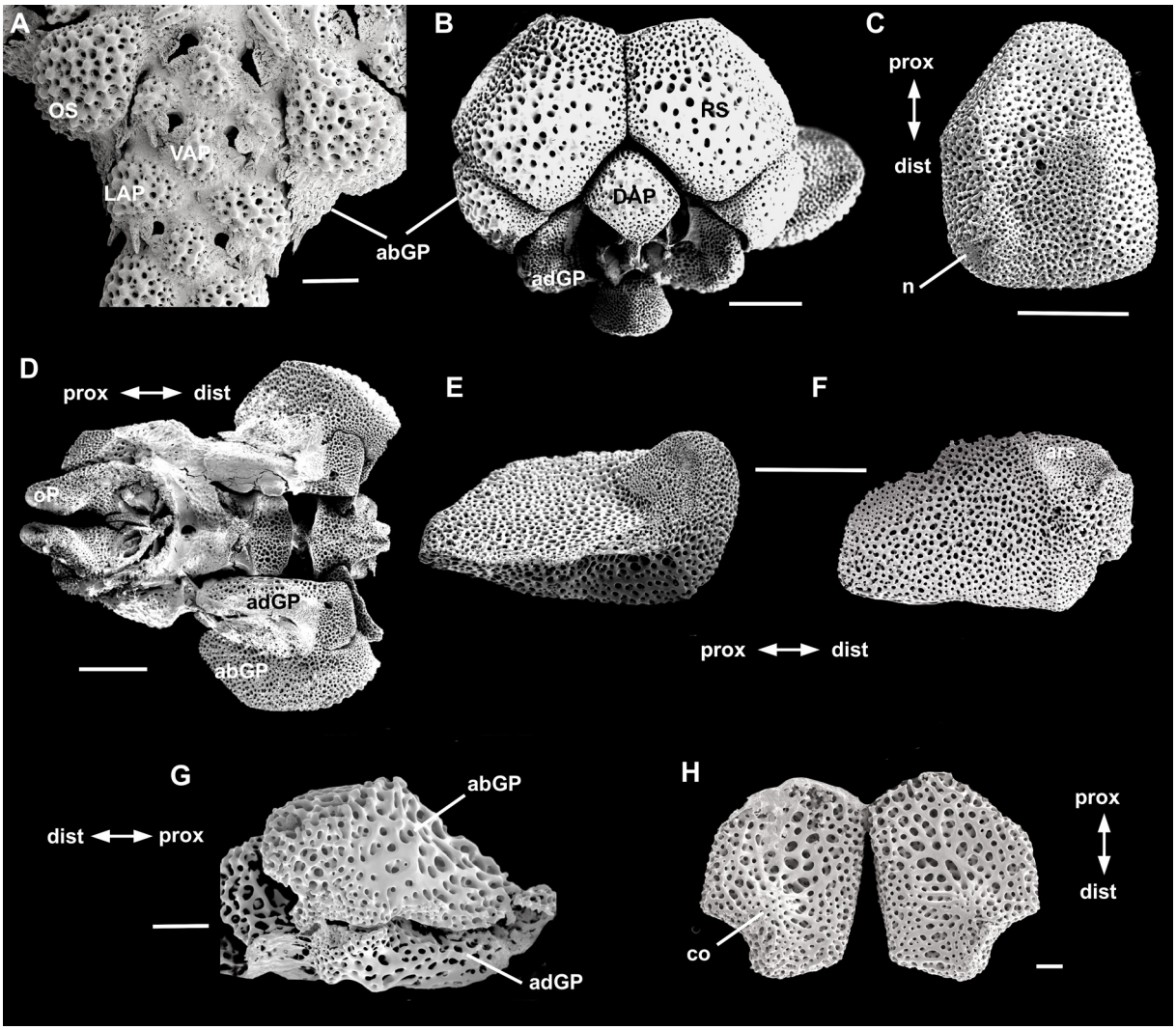

Fig. 3. Ophiopyrgidae Perrier, 1893, *Ophiopyrgus* Lyman, 1878, SEM images. **A–F**. *Ophiopyrgus saccharatus* Studer, 1882. **A**. Section of ventral disc and arm. **B**. Dorsodistal view of arm base with RS, adGP, abGP. **C**. RS, inner side. **D**. Oral plates with attached vertebrae, adGP and abGP. **E**. adGP, abradio-ventral view. **F**. abGP, surface connecting to RS. **G–H**. *Ophiopyrgus wyvillethomsoni*. **G**. adGP and abGP adjoined. **H**. Radial shield pair, inner side. Scale bars: A–F = 0.5 mm; G–H = 0.1 mm.

Abradial GP

Ophiopyrgus saccharatus: pear-shaped, stout, as long as but twice as wide as adGP, disto-dorsal depression connects to RS, adradial ventro-distal deep depression curves around adGP. *Ophiopyrgus wyvillethomsoni*: twice as wide as adGP, stout, distally wider than proximally, pear-shaped.

Oral shields

Externally, madreporite not distinguishable. Inner sides not examined.

Radial shield

Ophiopyrgus saccharatus: stout, articular notch in ventro-distal point articulates with adGP, central depression with hole, straight abradial distal edge connects to abGP. *Ophiopyrgus wyvillethomsoni*: articular structure a low knob/condyle in middle of distal end.

Remarks

The family Ophiopyrgidae contains several paedomorphic genera (Stöhr & Martynov 2016), including the type genus *Ophiopyrgus*, with a strongly juvenile appearance. Unusual among the studied species is that in *O. saccharatus* the abradial GP connects broadly to the radial shield, and apart from the oral shield, the abGPs are the only plates on the ventral disc. Externally, the radial shields resemble disc scales in shape and size. *Ophiosparte gigas* Koehler, 1922 was included in Ophiopyrgidae by molecular data (O'Hara *et al.* 2017), but its adGP is bar-like, distally inflated, and its abGP is cup-shaped, bearing comb papillae (Martynov 2010), and in combination with other characters, such as the superficial oral tentacle pore, oral papillae similar to *Ophiura* and the large number of tentacle scales, *Ophiosparte* is morphologically more similar to *Ophiura* than to any here analysed ophiopyrgid.

Genus ***Amphiophiura*** Matsumoto, 1915
Fig. 4

Type species

Ophioglypha bullata Thomson, 1877.

Examined species

Amphiophiura latro (Koehler, 1904), *A. insolita* (Koehler, 1904).

Oral GP

Absent.

Adradial GP

Amphiophiura latro: spatulate, stout, half as wide as long, proximally tapered, articular structures flat patches of finer meshed stereom. Abradial side with longitudinal groove and large hole in distal part. Twice as long as abGP. *Amphiophiura insolita*: stout, wedge-shaped, half as wide as long, dorsally concave, ventrally convex, proximally tapered, distal end widened, articular surface to RS flat, extending to middle of plate, protruding laterally. Abradial ventrodistal part with articular structure with abGP of coarse stereom.

Abradial GP

Amphiophiura latro: shorter than adGP, twice as high as long. Exposed distal end inflated, slightly curved, with tuberculous stereom, small round articular holes without lobes for genital papillae, inner

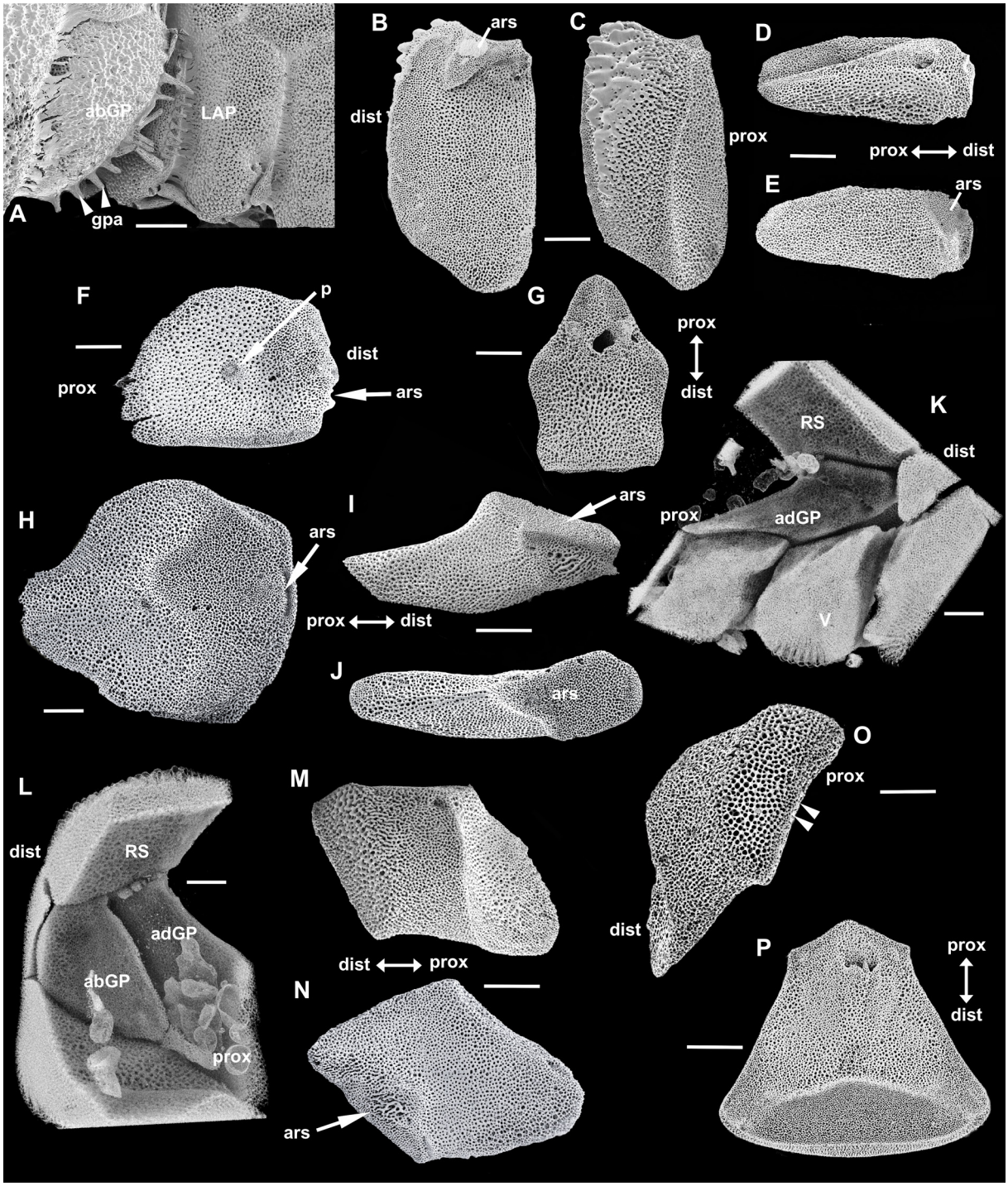

Fig. 4. Ophiopyrgidae Perrier, 1893, *Amphiophiura* Matsumoto, 1915, SEM images, unless otherwise noted. **A–G**. *A. latro* (Koehler, 1904). **A**. Arm base, lateral aspect. **B**. abGP, radial aspect. **C**. abGP, abradial aspect. **D**. adGP, abradial aspect. **E**. adGP, adradial aspect. **F**. Radial shield, inner (ventral) aspect. **G**. Madreporite, inner (dorsal) aspect. **H–P**. *A. insolita* (Koehler, 1904). **H**. Radial shield, inner aspect. **I**. adGP, abradial aspect. **J**. adGP, dorsal view. **K**. adGP in situ, micro-CT. **L**. abGP in situ, micro-CT. **M**. abGP, abradial aspect (distal part with larger pores is exposed at disc edge). **N**. abGP, adradial aspect. **O**. abGP, distal end, arrowheads mark articular structures for genital papillae. **P**. Madreporite, inner aspect. Scale bars: A–O = 0.5 mm; P = 1 mm.

part with simple stereom, as high and long as outer part, but much thinner. *Amphiophiura insolita*: shorter than adGP, broad diamond-shaped. Exposed distal end slightly curved, with weakly tuberculous stereom, small round articular holes without lobes for genital papillae; inner part with simple stereom, proximal end tapered, proximal third flat, thinner than inflated distal two thirds. Adradial edge slanting, a round depression with coarse stereom close to edge with articular structure to adGP.

Oral shields

Amphiophiura latro: covering large part of ventral disc, inner side with one round spur on either side of proximal part. Madreporite with large hole in proximal part between spurs, opening to one side. *Amphiophiura insolita*: covering all of ventral disc. Madreporite with large hole near proximal edge, no side opening.

Radial shield

Amphiophiura latro: articular structures a shallow depression and a small round, finer meshed patch at the distal internal edge. A round, finer meshed patch in the centre of the inner surface. *Amphiophiura insolita*: articular structure a wide flat surface extending from distal edge to middle of plate, thicker than proximal part. Lateral in distal edge a short slit.

Remarks

The genus *Amphiophiura* Matsumoto, 1915 is regarded as paedomorphic (Stöhr & Martynov 2016), but contrary to expectations, the genital plates are large and well differentiated. There is a stout conical adGP with a flat articular structure, and, in contrast to most other species, a much larger abGP, partially exposed at the disc edge, bearing an arm comb of genital papillae. Although the arm comb is similar to that of *Ophiura*, species in that genus have an exposed cup-shaped abGP that does not extend far into the disc. In several species of *Amphiophiura* the genital slit borders the large oral shield laterally.

Genus ***Ophiopleura*** Danielssen & Koren, 1877
Fig. 5

Type species

Ophiopleura borealis Danielssen & Koren, 1877.

Examined species

Ophiopleura borealis.

Oral GP

Absent.

Adradial GP

Blade-like long, dorsalwards curved, distally thicker with one weakly domed condyle and one condylar process with flat end, one circular smooth dorsal depression with thick rim (suction cup-shaped), one oval adradial embossed articular structure with coarser stereom. Ventral half thinner than dorsal.

Abradial GP

As long as adGP, weakly curved, concave dorsal surface articulating broadly to ventral abradial part and condylar process on adGP, proximal end strongly tapered to a point.

Oral shields

Inner side flat, coarse stereom. Madreporite externally with multiple small pores in distal part (not visible on inner side), inner side similar to that of regular oral shield, but large central opening, partially covered by stereom lobes.

Radial shield

Almost as long as disc radius (most of it covered by scales and thick skin in intact disc), narrow, thin, distal end widened, fragmented into several pieces of varying size during bleaching. Single low condyle on middle of distal end, distally bordered by deep groove; one nearly round, finer meshed depression proximal to condyle.

Remarks

Ophiopleura is one of the more completely developing genera of Ophiopyrgidae, not considered to be paedomorphic. In *O. borealis*, the adGP and abGP support the genital slit along its full length, between distal end of adoral shield and disc edge, which may explain the absence of oGPs. The radial shields are covered by disc scales, except for their distalmost part, and their appearance, rib-like and radiating from the disc center to the disc margin, as well as their tendency to break into several pieces, is similar to conditions in Euryalida, but they are considerably thinner. The shape of its genital plates is unusual among the here studied species and doesn't convey its phylogenetic relationships.

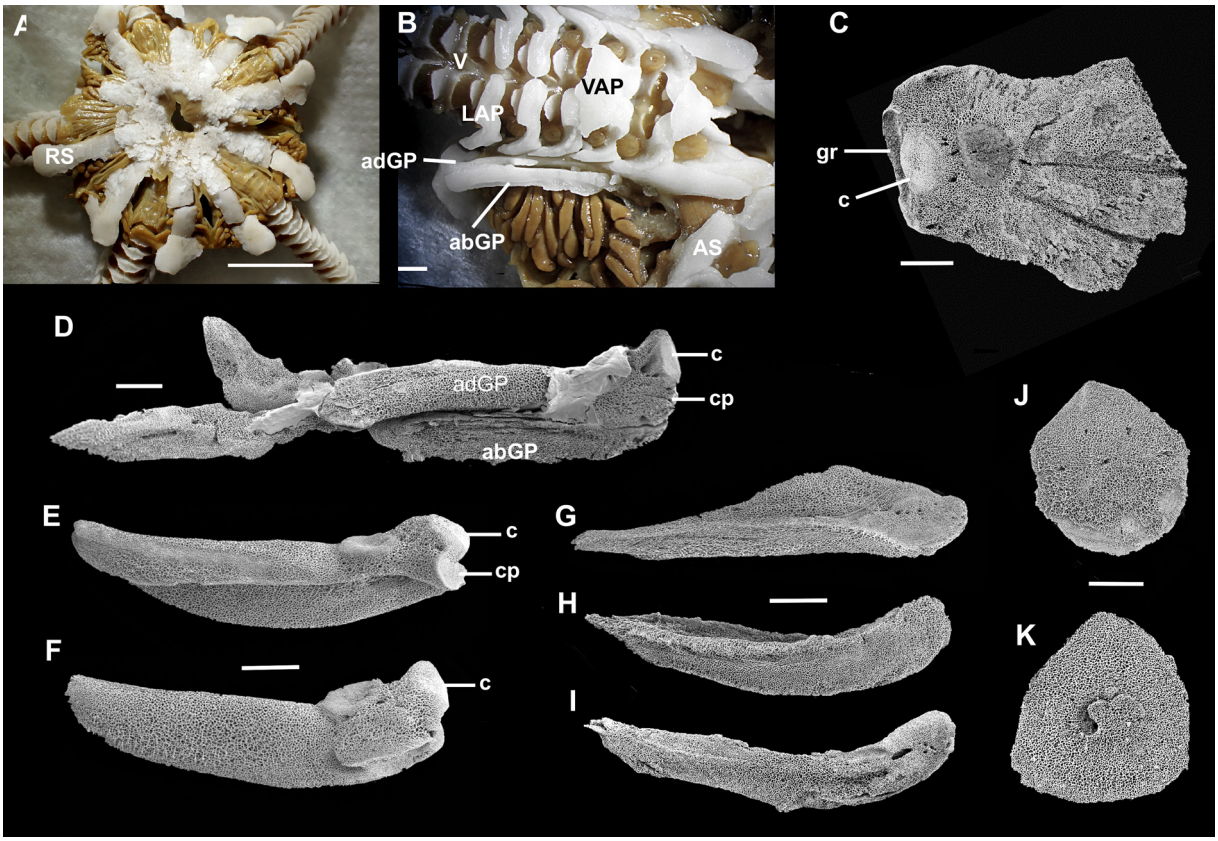

Fig. 5. Ophiopyrgidae Perrier, 1893, *Ophiopleura borealis* Danielssen & Koren, 1877, SEM images. **A**. Dorsal disc, scales removed by bleaching. **B**. Bleached arm with genital plates, ventral view. **C**. RS, distal part, ventral aspect. **D**. adGP and abGP attached to each other, abradial view. **E**. adGP, abradial view. **F**. adGP, adradial view. **G**. abGP, dorso-lateral view. **H**. abGP, ventral view. **I**. abGP, lateral view. **J**. Oral shield, inner side. **K**. Madreporite, inner side. Scale bars: A = 10 mm; B–K = 1 mm.

Family Ophiomusaidae O'Hara, Stöhr, Hugall, Thuy & Martynov, 2018

Genus ***Ophiomusa*** Hertz, 1927
Fig. 6A–G

Type species

Ophiumusium lymani Wyville-Thomson, 1873.

Examined species

Ophiomusa lymani.

Oral GP

Absent.

Adradial GP

Bar-like, dorsalwards curved, distal end flaring, with one large and one smaller, weakly domed or flat condylar process and curved groove; proximal to processes a large, nearly circular depression with coarser stereom. At middle of ventral edge, a fin-like process, which articulates with abGP.

Abradial GP

Large, as long as adGP, triangular, thick, a longitudinal ridge divides the plate in two slanting halves. Almost completely exposed on ventral disc.

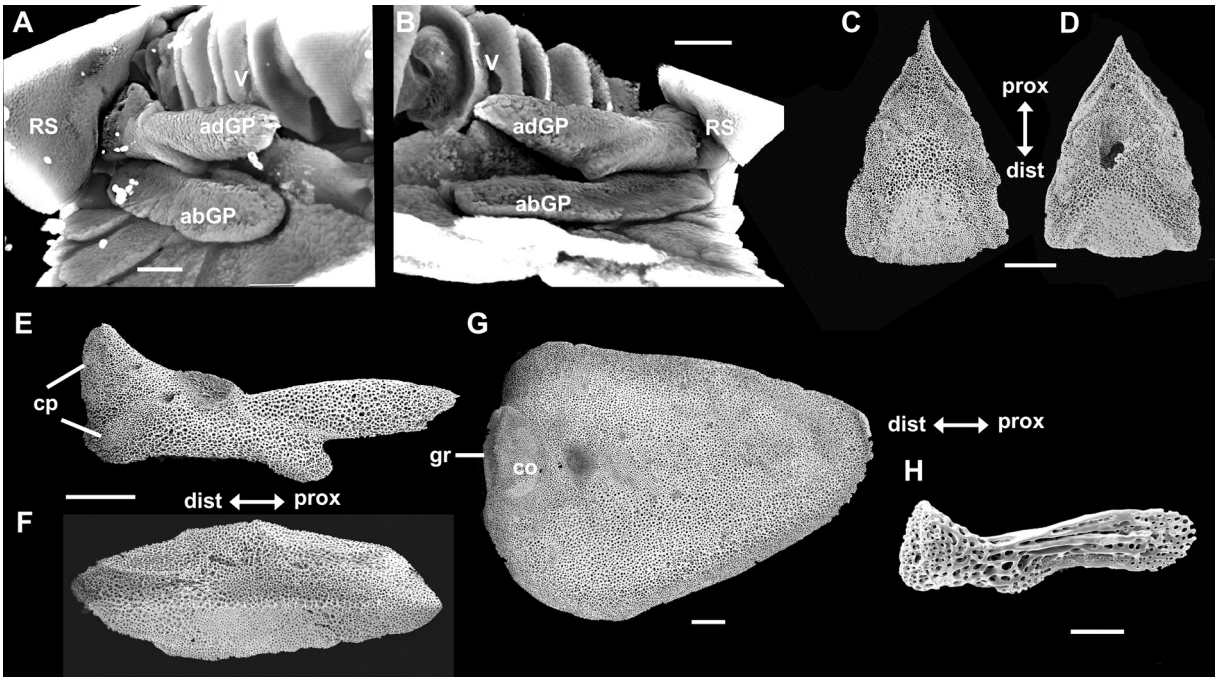

Fig. 6. A–G. Ophiomusaidae O'Hara, Stöhr, Hugall, Thuy & Martynov, 2018, *Ophiomusa lymani* (Wyville-Thomson, 1873), SEM, unless otherwise noted. **A–B**. Micro-CT, adGP and abGP in situ. **C**. Oral shield, inner aspect. **D**. Madreporite, inner aspect. **E**. adGP, abradial view. **F**. abGP, adradial view. **G**. RS, inner aspect. **H**. Astrophiuridae Sladen, 1879, *Astrophiura* sp., adGP. Scale bars: A–G = 1 mm; H = 0.1 mm.

Oral shields

Inner side flat, distally a triangular patch of smooth stereom with minute pores, in centre coarsely meshed stereom, proximally finer meshed. Madreporite strongly thickened, flatter smooth triangular patch distally, large central opening (externally no hydropore visible).

Radial shield

At middle of distal edge, a low condyle, bordered distally by narrow groove, proximal to condyle a circular patch with finer stereom.

Remarks

The disc skeleton of *Ophiomusa lymani* consists of a small number of large, tightly adjoining plates and few smaller dorsal scales. It is considered to be a paedomorphic species (Stöhr & Martynov 2016). The abGP makes up a considerable part of the ventral disc covering. The genital slits are not obvious. The rough patches on adGP and RS seem to be positioned opposite to each other and are likely connected by muscle fibres.

Family Astrophiuridae Sladen, 1879

Genus ***Astrophiura*** Sladen, 1879
Fig. 6H

Type species

Astrophiura permira Sladen, 1879.

Examined species

Astrophiura sp., *A.* cf. *tiki* Litvinova & Smirnov, 1981 (Stöhr *et al.* 2012b).

Oral GP

Absent.

Adradial GP

Bar-like, flat for most of its length, proximal end rounded, distal to midpoint a fin-like ventral process, distal end thicker, upwards curved, edge straight, depressed, no condyles.

Abradial GP

Not examined, possibly absent, since no genital slits were seen.

Oral shields

Madreporite large, pentagonal, externally domed, small hydropore near a lateral edge, inner side not examined. Other OS not identifiable, considered absent.

Radial shield

Inner side not examined.

Remarks

Astrophiura has a unique and specialized morphology, possibly affected by paedomorphosis.

Order Euryalida Lamarck, 1816
Family Gorgonocephalidae Ljungman, 1867

Genus ***Gorgonocephalus*** Leach, 1815
Fig. 7

Type species

Asterias caputmedusae Linnaeus, 1758.

Examined species

Gorgonocephalus caputmedusae.

Oral GP

Absent.

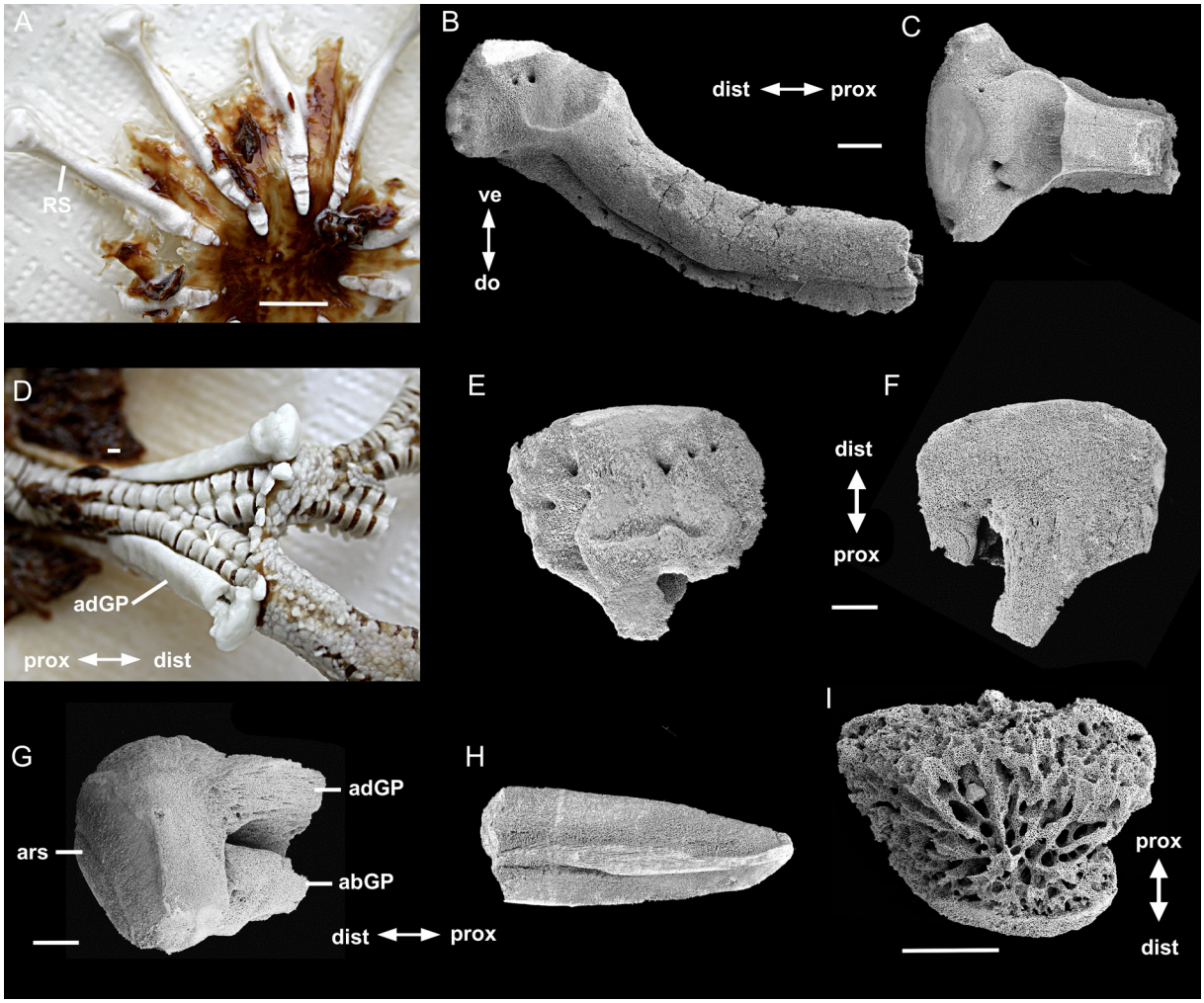

Fig. 7. Gorgonocephalidae Ljungman, 1867, *Gorgonocephalus caputmedusae* (Linnaeus, 1758), SEM images (except A, D, digital images). **A**. Dorsal disc inner side with radial shields exposed. **B**. Radial shield distal end, ventrolateral view. **C**. Radial shield, distal end, ventral view. **D**. adGP in situ. **E–G**. adGP, distal end fragments. **H**. adGP proximal part fragment. **I**. Madreporite, inner aspect. Scale bars: 1 mm.

Adradial GP

Long with bulbous distal end, extending in an L-shape or as a rounded structure fused to abGP; parallel to arm vertebrae, as long as at least nine segments. Distal edge large and flat, no special articular structures, a depression in dorsal surface. Proximal part with deep median furrow, in cross section u-shaped. Fragmented into multiple, different sized pieces during bleaching.

Abradial GP

Small, attaching under proximal edge of bulbous L-shaped part on adradial GP or both fused to form a single structure.

Oral shields

Regular OS absent, but one or several madreporites, thickened, externally with numerous scattered small pores (transverse row of 7–8 pores in *G. lamarcki* (Müller & Troschel, 1842), inner side a meshwork of irregular lamellae and openings.

Radial shield

Long, bar-like with widened distal end, ventral side with flat, smooth articular patch at distalmost end, proximal to widened part a concave patch. Dorsal surface wider than ventral bar, creating thin lateral overhanging edges, with scaly appearance and numerous pores where disc granules were attached. Fragmented into several different sized pieces during bleaching.

Remarks

Radial shields and genital plates broke easily during bleaching in *Gorgonocephalus*.

Family Asteronychidae Verrill, 1899

Genus ***Asteronyx*** Müller & Troschel, 1842
Fig. 8

Type species

Asteronyx loveni Müller & Troschel, 1842.

Examined species

Asteronyx loveni.

Oral GP

Absent.

Adradial GP

Half as long as in-disc part of arm. Flat, widest part half as wide as length, distally upwards curved, tapering to rounded proximal end. Terminating distally in a rounded condylar process with flat surface and at a small distance ventrally a half circle-shaped groove. Offset from fused abGP by longitudinal slits, not separating plates.

Abradial GP

Firmly fused to dorsal edge of adGP. Blade-like flat, longer than adGP, half as wide as adGP, abradial proximal half slightly depressed. Both GPs aligned along arm vertebrae with single flat surface.

Oral shields

Madreporite widely drop-shaped, externally with several small pores, inner side with deep middle depression, two irregular pores on either side. No regular oral shields.

Radial shield

Superficially appearing as long bar-like structures, consisting of a short distal part with widened end and for most of its length composed of multiple layers of thin, irregular, overlapping plates. Distal end with flat articular structure and a curved dorsal ledge. Proximally at a distance a round patch of finer mesh stereom. RS and adGP articulate by muscles and connective tissue, hard parts touching only at internal edge, evidenced by the wide gap between them in the relaxed disc.

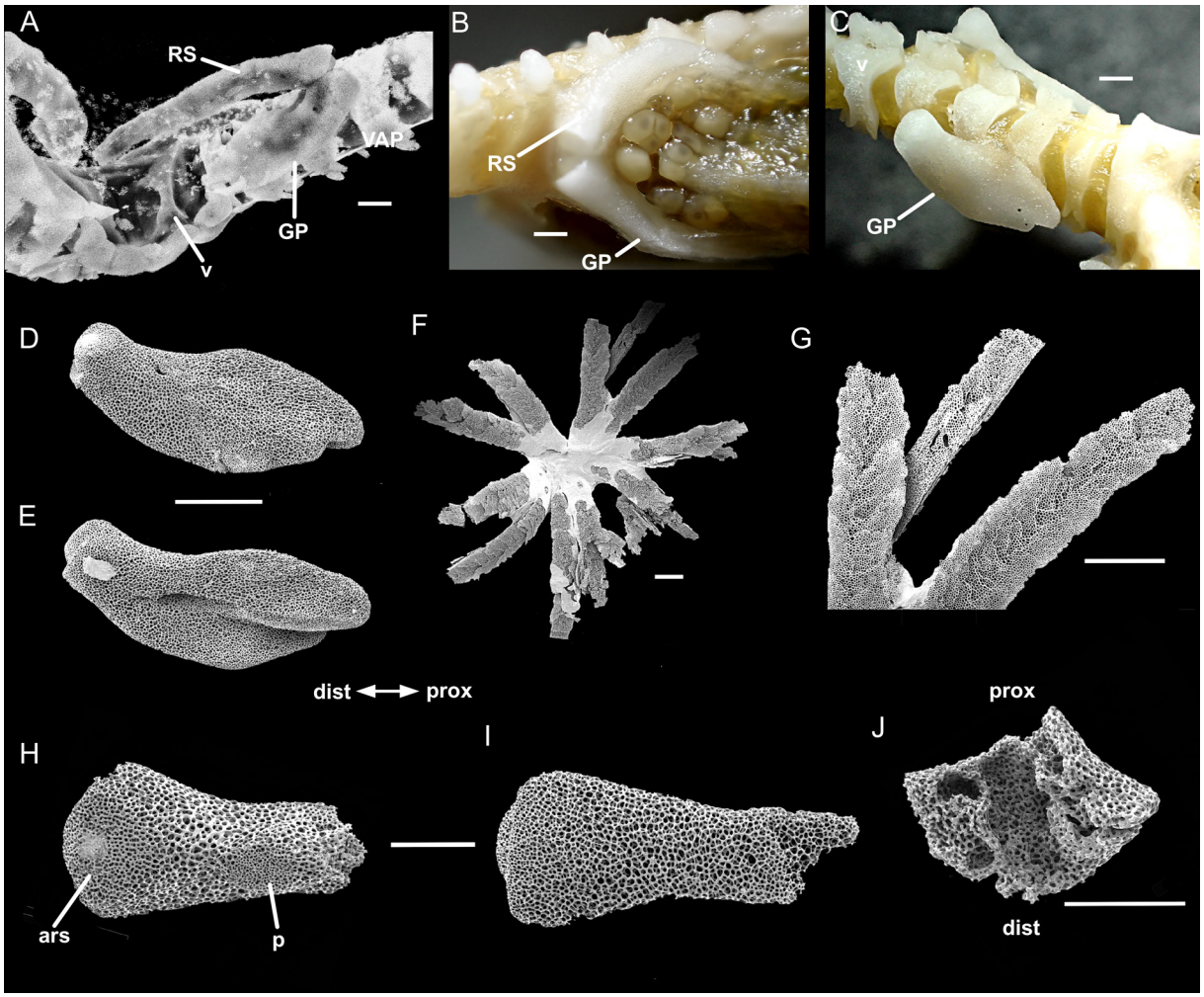

Fig. 8. Asteronychidae Verrill, 1899, *Asteronyx loveni* Müller & Troschel, 1842. A = micro-CT; B–C = digital photos; D–J = SEM images. **A–B**. Radial shield and fused adradial and abradial genital plates in situ. **C**. Genital plates in situ. **D**. Genital plates, adradial view. **E**. Genital plates, abradial view. **F**. Radial shields, dissected from disc, distal ends fallen off. **G**. Detail of F, separating layers of radial shields. **H**. Radial shield distal end, inner aspect. **I**. Radial shield, distal end, outer side. **J**. Madreporite, inner aspect. Scale bars: A–G = 1 mm; H–J = 0.5 mm.

Family Euryalidae Gray, 1840

Genus ***Euryale*** Lamarck, 1816
Fig. 9

Type species

Euryale aspera Lamarck, 1816.

Examined species

Euryale aspera.

Oral GP

Absent.

Adradial GP

Bar-like, distally thickened, curving upwards, flat articular structure and shallow groove.

Abradial GP

Isosceles triangular, thick, distal end straight, proximal end pointed, attaches along proximal dorsal edge of adGP.

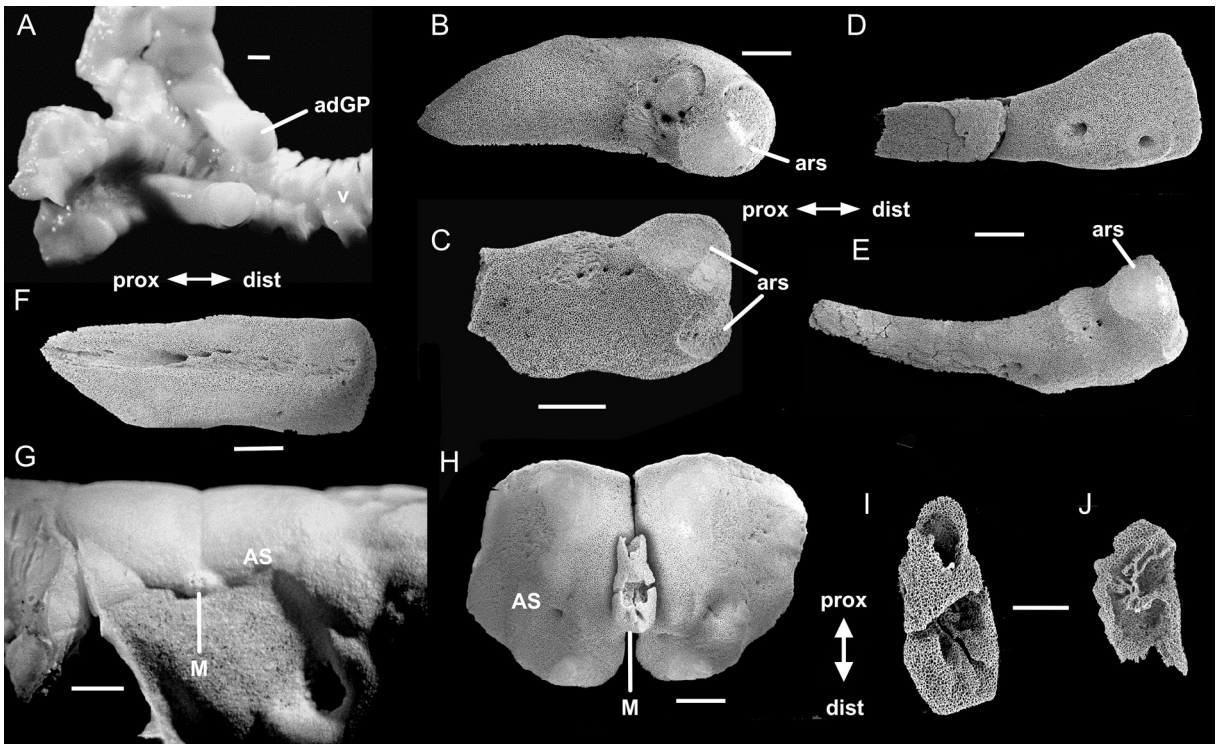

Fig. 9. Euryalidae Gray, 1840, *Euryale aspera* Lamarck, 1816. A, G = digital images; B–F, H–J = SEM images. **A**. adGP in situ. **B**. adGP abradial view. **C**. adGP, dorso-adradial view. **D**. Radial shield, dorsal view. **E**. Radial shield, latero-ventral view. **F**. abGP. **G**. Section of ventral disc. **H**. Adoral shields and madreporite, inner view. **I**. Madreporite, inner aspect. **J**. Other madreporite, inner aspect. Scale bars: A–H = 1 mm; I–J = 0.5 mm

Oral shields

All madreporic. At size 22 mm dd, minute, externally one or two pores visible. Internally, one madreporite elongated (slipper-shaped), proximally rounded and closed over, in middle a square opening, distal part narrower, tube-like closed, distal end open. Another madreporite internally not closed over, with deep openings and several septa. Only distal surface externally visible at vertical interradius, madreporite placed on inner side of two adradial shields, completely covered.

Radial shield

Bar-like, curved, distal end in dorsal aspect spatulate, widened, in ventral aspect rounded, gradually increasing in thickness from proximal to distal, articular structures as two flat patches, one on ventral side, one as distal surface. Proximal to articular structures a concave part with several holes.

Superorder Ophintegrida O'Hara, Hugall, Thuy, Stöhr & Martynov, 2017
Order Ophioscolecida O'Hara, Hugall, Thuy, Stöhr & Martynov, 2017
Family Ophioscolecidae Lütken, 1869

Genus ***Ophioscolex*** Müller & Troschel, 1842
Fig. 10

Type species

Ophioscolex glacialis Müller & Troschel, 1842.

Examined species

Ophioscolex glacialis.

Oral GP

Oval, thin, scale-like, articular notch at inner proximal edge, sitting slanted at proximal end of genital slit, pair widely separated, partly overlapped by oral shield, attached to oral and adoral shield.

Adradial GP

Bar-like, distal end slightly swollen, minute in relation to disc size, restricted to disc edge, far from oral shield. Articular structures not well defined, two or three ribs separated by grooves, a single condyle, proximal to it a process where abGP attaches.

Abradial GP

Flat, thin, elongated blade, dorsal edge straight, ventral edge convex. Proximally tapered, distally straight slanting edge without specific articular structures. ¾ as long as adGP. Attaching to adGP at a short distance from distal end, laying parallel.

Oral shields

Wider than long, externally with horizontal fold, internally with proximal horizontal ridge, demarcating distal portion, where oral GPs attach to a pore at each side. Madreporite as wide as long, folded horizontally, inner side with weak central horizontal ridge, and irregular processes extending into hollow interior, opening widely to one side.

Radial shield

Considered absent, but unidentified short ossicle present distal to abGP, attached to it, in ventral position.

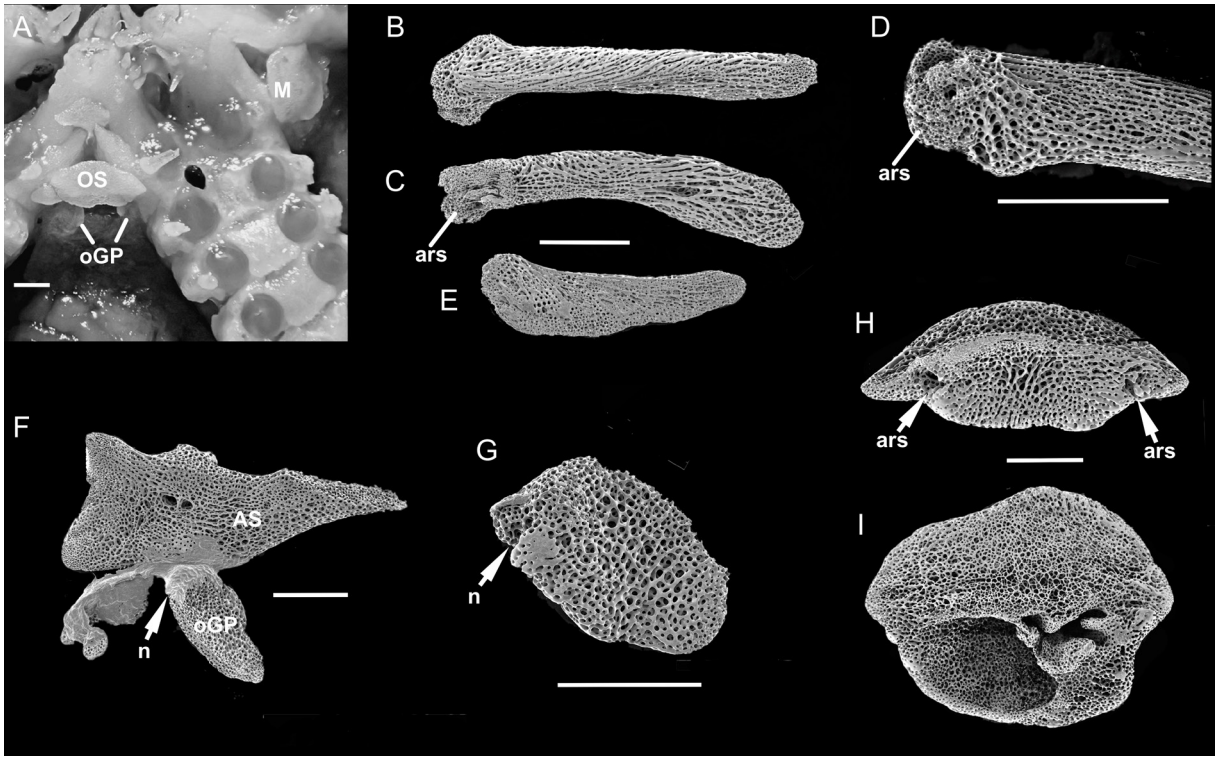

Fig. 10. Ophioscolecidae Lütken, 1869, *Ophioscolex glacialis* Müller & Troschel, 1842, SEM, unless otherwise noted. **A**. Oral shield, madreporite, oral genital plates in situ (lightly bleached), digital image. **B**. adGP, adradial aspect. **C**. adGP, abradial spect. **D**. adGP, distal end. **E**. abGP. **F**. adoral shield with oGP attached. **G**. oGP. **H**. Oral shield, inner aspect. **I**. Madreporite, inner aspect. Scale bars: 0.5 mm.

Genus ***Ophiolycus*** Mortensen, 1933
Fig. 11

Type species

Ophioscolex dentatus Mortensen, 1933.

Examined species

Ophiolycus purpureus (Düben & Koren, 1846).

Oral GP

Oval, twice as long as wide, flat, scale-like. Articulating with oral shield on latero-distal inner surface below horizontal ridge.

Adradial GP

Bar-like elongated, with middle kink, distal half thickened, wider than thinner proximal half. In middle an abradially protruding edge at which abGP attaches. Ventral edge thicker than dorsal edge. Distal end without specific articular structures.

Abradial GP

Half as long as adGP, blade-like flat, thin, ventral edge slightly convex, dorsal edge straight, distal edge slanting, without specific articular structure (flat stereom), proximal edge tapered.

Oral shield

Internally proximal half thickened, demarcated from distal half by horizontal ridge, distal half thinner. Madreporite (specimen of 11.9 mm dd) with constricted and flatter distal portion on inner side, separated from proximal half by horizontal ridge, one large hole in distal part, two large irregular openings in proximal part, hydropore in one distal lateral edge. Madreporite from smaller specimen (9 mm dd) similar, but with 2 smaller openings in proximal part.

Radial shield

Rectangular, three times as long as wide, no specific articular structures (flat stereom).

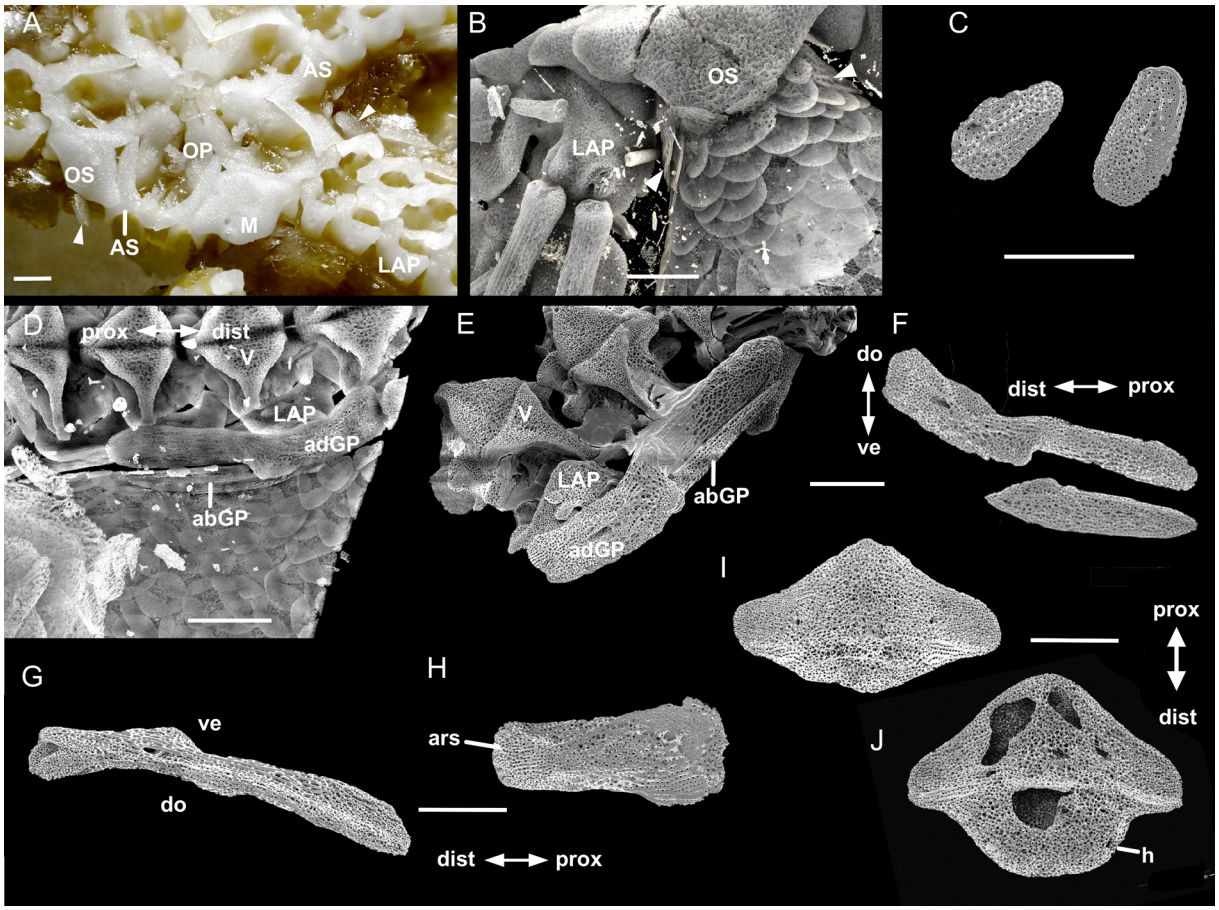

Fig. 11. Ophioscolecidae Lütken, 1869, *Ophiolycus purpureus* (Düben & Koren, 1846), SEM, unless otherwise noted. **A**. Mouth parts in situ (bleached, arrowheads mark oGPs), digital photo. **B**. oGP in situ (arrowheads), micro-CT. **C**. Oral GP. **D**. adGP and abGP in situ, micro-CT. **E**. adGP and abGP in situ. **F**. adGP and abGP, dissociated, adradial aspect. **G**. adGP, dorsal aspect. **H**. Radial shield, inner aspect. **I**. Oral shield, inner aspect. **J**. Madreporite, inner aspect. Scale bars: 0.5 mm.

Family Ophiohelidae Perrier, 1893

Genus ***Ophiomyces*** Lyman, 1869
Fig. 12

Type species

Ophiomyces frutectosus Lyman, 1869.

Examined species

Ophiomyces delata Koehler, 1904, *O. frutectosus*.

Oral GP

Not examined, not identified in situ. Considered absent.

Adradial GP

Flat, thin, blade-like, ventral edge convex, dorsal edge straight, articular structure at distal end as embossed oval patch with finer stereom.

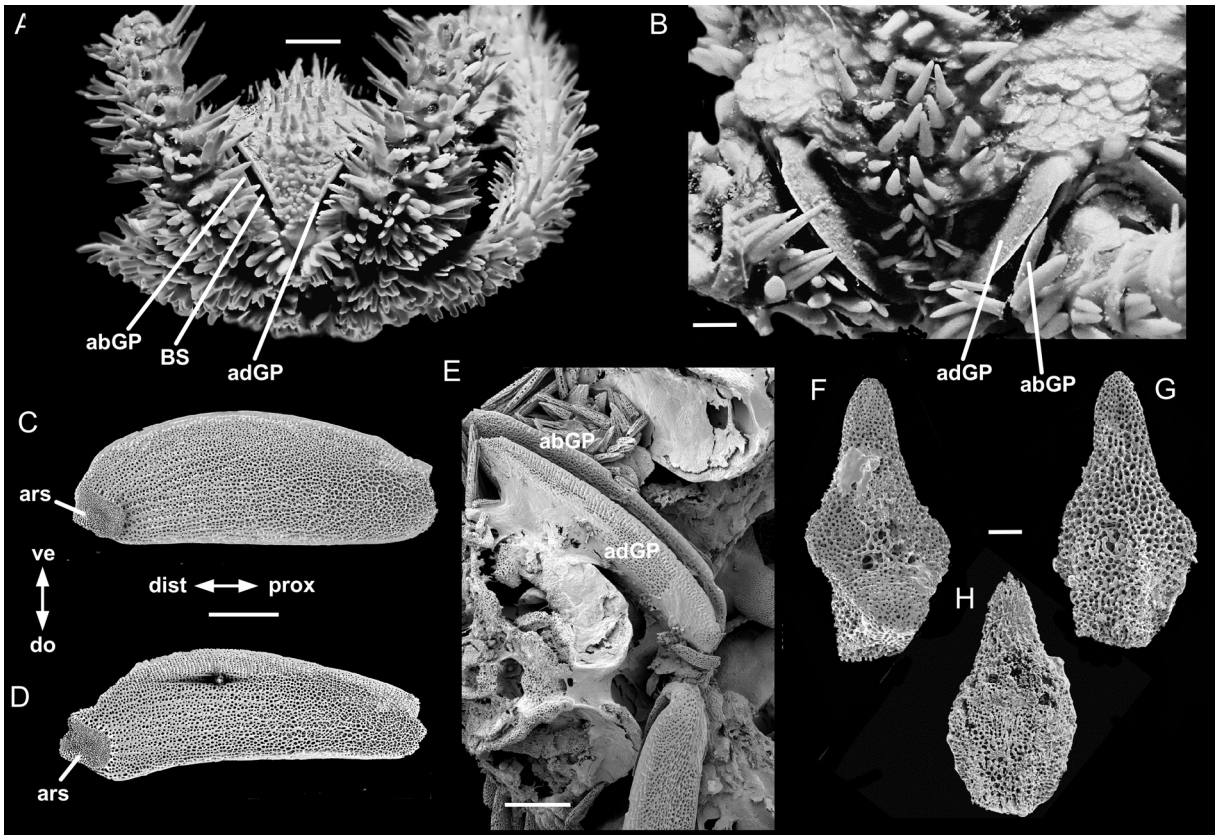

Fig. 12. Ophiohelidae Perrier, 1893. **A–B**. *Ophiomyces frutectosus* Lyman, 1869, digital photos. **A**. Lateral view. **B**. Detail of genital plates in situ. **C–H**. *Ophiomyces delata* Koehler, 1904, SEM. **C**. adGP, abradial aspect. **D**. abGP, adradial aspect. **E**. Genital plates in situ. **F**. Oral shield, external aspect. **G**. Oral shield, inner aspect. **H**. Madreporite, inner aspect. Scale bars: A–B = 1 mm; C–E = 0.5 mm; F–H = 0.1 mm.

Abradial GP

Similar to adGP, articular patch depressed. When both GP are articulated, they are parallel, leaving a narrow slit between them.

Oral shields

Minute, elongated drop-shaped, with thickened rectangular distal end, depressed center of OS with coarse, porous stereom in external and internal views. Madreporite similar, with several small pores in middle part.

Radial shield

Absent.

Remarks

Matsumoto (1915, 1917) considered the abradial genital plate (his "genital scale") and the radial shield in *Ophiomyces* to be absent (Table 1). Lyman (1882) considered the radial shield to be absent, but both genital plates to be present (Table 1), and the present study confirms his interpretation. They both described the adradial genital plate as curved over the top of the arm. Instead, both genital plates are flat and straight, and in the intact disc they may be upright or diagonal across the arm base (Fig. 12E). Oral GPs were not found after dissociating the skeleton and may be absent, since the adGP and abGP extend the full length from oral shield to disc edge, with the genital slit opening between them. Conditions in *Ophiotholia spathifer* (Lyman, 1879) are the same as in *Ophiomyces*.

Order Ophiacanthida O'Hara, Hugall, Thuy, Stöhr & Martynov, 2017
Suborder Ophiodermatina Ljungman, 1867
Superfamily Ophiodermatoidea Ljungman, 1867
Family Ophiodermatidae Ljungman, 1867

Genus ***Ophioderma*** Müller & Troschel, 1840
Fig. 13

Type species

Asterias longicauda Bruzelius, 1805.

Examined species

Ophioderma longicaudum, *O. zibrowii* Stöhr, Weber, Boissin & Chenuil, 2020, *O. africanum* Stöhr, Weber, Boissin & Chenuil, 2020 (Stöhr *et al.* 2020).

Oral GP

Comma-shaped, ventrally flat, dorsal keel on distal part, three times as long as greatest width, half as long as proximal genital slit, curved along slit, with rounded proximal end and pointed distal end, longitudinal row of about six small pores. Pair distally at a wide angle from each other, proximally close but separated. Proximal part covered by oral shield. (Only examined in *O. longicaudum*).

Adradial GP

Rod with bulbous distal end, flatter proximal to bulbous part, tapering proximalwards, ventral edge convex, dorsal edge straight. Bulbous end composed of a domed condyle and a flat condylar process, adradial one surrounded by a circular groove. In situ, this groove and a corresponding groove and condyle on adradial inner surface of radial shield connected by muscle fibres. A large hole near base of adradial condyle.

Abradial GP

Trapezoid, with straight distal and dorsal edges, ventral and proximal edges angling upwards. Adradial surface with conspicuous pore in distal part, abradial surface with shallow longitudinal groove. Articulating with adradial GP on its abradial side, at proximal border of abradial condyle.

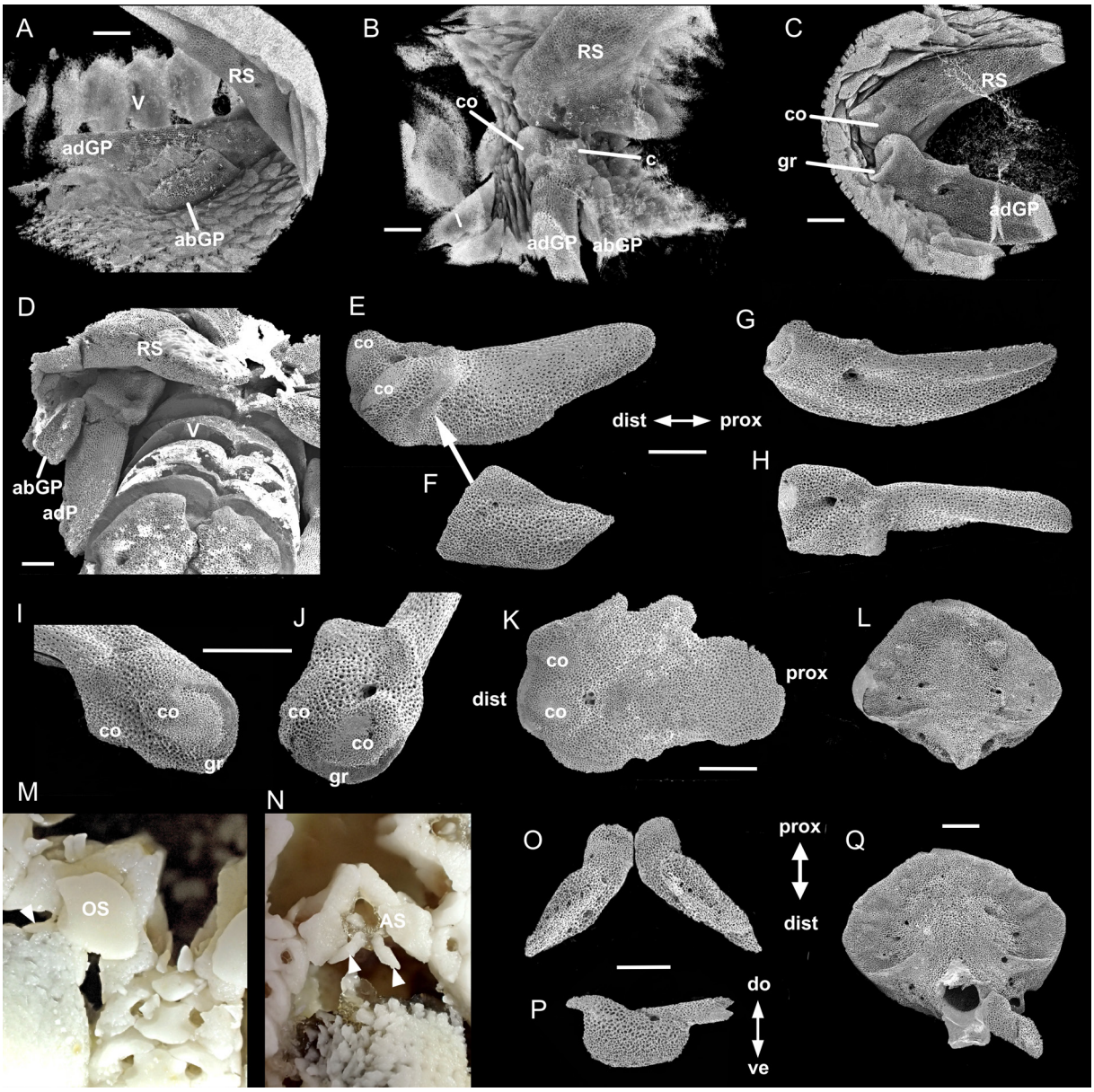

Fig. 13. Ophiodermatidae, Ljungman, 1867, *Ophioderma longicaudum* (Bruzelius, 1805), SEM, unless otherwise noted. **A–C**. adGP and abGP in situ, in various orientations, micro-CT. **D**. adGP and abGP in situ. **E**. adGP, abradial aspect. **F**. abGP, arrow points to corresponding articular structure on adGP. **G**. adGP, adradial aspect. **H**. adGP, dorsal view. **I–J**. adGP, distal aspect. **K**. Radial shield, inner side. **L**. Oral shield, inner side. **M**. Jaw (arrowhead marks oGP), bleached, digital photo. **N**. Jaw with oral shield removed, oGP exposed (arrowheads), bleached, digital photo. **O**. Pair of oGP, ventral aspect. **P**. oGP, lateral aspect. **Q**. Madreporite, inner side. Scale bars: 0.5 mm.

Oral shields

Rounded triangular, with groove in distal edge. Inner surface with scattered small pores, lateral edges in distal half depressed, distal part raised as a ridge with straight-edged wide median process. Madreporite inner surface with rough stereom on raised middle part, denser stereom on flat outer edge and with 2–3 low spurs, distally a thickened spur to either side of a large hole that opens to one side in a smaller hole (hydropore), bordered distally by rectangular process. Externally madreporite with deep, round depression in distal half, groove in distal process, hydropore in one side.

Radial shield

With two large, low condyles of denser stereom occupying most of inner distal surface of shield, proximal to and between them a large opening and proximal to that a round, slightly depressed patch of smaller pore stereom. Adradial condyle bordered by a groove.

Remarks

Matsumoto (1917) stated: "In *Ophioderma*, the genital plate and scales of the same side of a radius are soldered together at the middle, so that the genital slit is divided into two secondary pores, an inner and an outer." (Table 1). He probably referred to the disc scales, not the "genital scale" (= abradial GP), because there is only a single short "genital scale" at either side of an arm. It is unclear what he meant by "soldering", but GPs and disc scales fall apart in bleach, suggesting no hard parts are fused, and in the 3D reconstructions, there is a gap between vertebrae and adGP. The body wall forms a wide bridge across the genital slit, dividing it into a proximal and a distal opening. The abradial GP is less than half as long as the adradial GP and supports only the distal genital opening; the proximal one is supported abradially by the oral GP. The three species closely related to *O. longicaudum* for which ossicle data are available are all highly similar in the examined structures.

Family Ophiomyxidae Ljungman, 1867

Genus ***Ophiomyxa*** Müller & Troschel, 1840
Fig. 14A–Q

Type species

Ophiura pentagona Lamarck, 1816.

Examined species

Ophiomyxa pentagona, *O. serpentaria* Lyman, 1883.

Oral GP

Elongated, three and a half times as long as greatest width, bar-like, flat, proximal end thickened, straight edge.

Adradial GP

Bar-like, proximal half flat, distal half thicker, end round, curving dorsalwards to meet RS, distal edge flat. In middle of ventral edge, a short process, to which abGP attaches.

Abradial GP

About half as long as adGP, flat, thin blade, straight, distal end slightly thicker, dorsalwards curved, edge slanting, proximal end rounded. Adradial surface in distal part with one to several conspicuous pores.

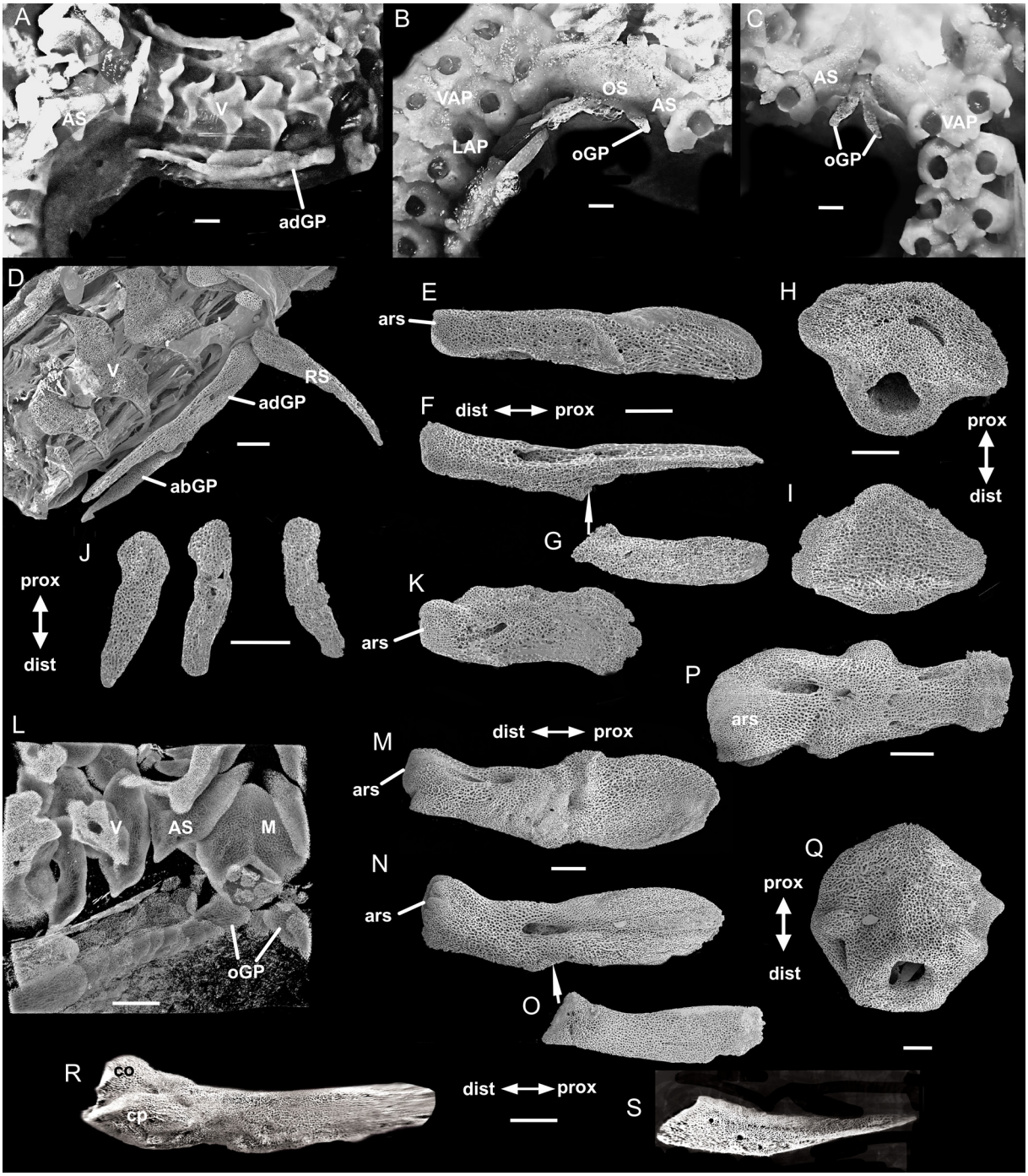

Fig. 14. Ophiomyxidae Ljungman, 1867, SEM, unless otherwise noted. **A–K**. *Ophiomyxa serpentaria* Lyman, 1883. **A–C**. Digital photos. **A**. Arm, dorsal view. **B**. Arm and mouth section. **C**. Arm and mouth section with oral shield removed. **D**. Arm with genital plates attached. **E**. adGP, adradial aspect. **F**. adGP, abradio-ventral aspect. **G**. abGP, arrow connects articular structures. **H**. Madreporite, inner aspect. **I**. Oral shield, inner aspect. **J**. oGPs. **K**. Radial shield, inner aspect. **L–Q**. *Ophiomyxa pentagona* (Lamarck, 1816). **L**. oGPs, view from inside disc, micro-CT. **M**. adGP, adradial aspect. **N**. adGP, abradial aspect. **O**. abGP, arrow connects articular structures. **P**. Radial shield, inner aspect. **Q**. Madreporite, inner aspect. **R–S**. *Ophiarachna incrassata* (Lamarck, 1816). **R**. adGP, abradial aspect. **S**. abGP. Scale bars: A–Q = 0.5 mm; R–S = 1 mm.

Oral shields

Rounded triangular, distal edge convex and thicker than thin main part. Madreporite distally inflated, inner side with large distal opening, a spur to either side, smaller hole in one laterodistal edge.

Radial shield

Rectangular to bar-like, distal end wider than proximal end, on distal inner side a patch of denser stereom as articular structure, no condyle.

Remarks

The abGP of *Ophiarachna incrassata* (Lamarck, 1816) (Fig. 14S) somewhat resembles the hockey-stick shape of the abGP of *Ophiochiton* (Fig. 24C) or a longer version of the abGP of *Ophioderma* (Fig. 13F). Its adGP (Fig. 14R) has a condyle and a condylar process (or two condyles), unlike that of *Ophiomyxa*, but resembling that of *Ophioderma* (Fig. 13E, G–H). No material was available to examine other angles of *O. incrassata* (nor any other congeneric species).

Superfamily Ophiocomoidea Ljungman, 1867
Family Ophiocomidae Ljungman, 1867

Genus ***Ophiocoma*** L. Agassiz, 1836
Fig. 15

Type species

Ophiura echinata Lamarck, 1816.

Examined species

Ophiocoma echinata, *O. erinaceus* Müller & Troschel, 1842, *O. schoenleinii* Müller & Troschel, 1842 (compared to *Breviturma krohi* (Stöhr, Boissin & Hoareau, 2013)), *O. scolopendrina* (Lamarck, 1816), *B. dentata* (Müller & Troschel, 1842) and *B. doederleini* (De Loriol, 1899)).

Oral GP

Flat, open right angle (short L-shaped), one end slightly convex attaching to distal edge of OS, the other concave and attaching to inside of OS, rounded angle outwards. (Only examined in *O. scolopendrina*.)

Adradial GP

Bar-like long, flat for most of its length, with longitudinal ridge on adradial surface, distal end somewhat thicker, articular structures consist of a lateral bar to which abGP attaches, one large condyle, bordered by a spiral-shaped groove and high stereom edge. A large hole at base of condyle, a bulbous process proximal to condyle on dorsal edge.

Abradial GP

Strongly curved, boomerang-shaped, flat, dorsal edge thickened into ridge abradially, distal end widened, concave with oval depression, articulating just proximal to distal end of adGP. Abradial surface with one to several conspicuous pores near distal edge. Longitudinal groove in abradial surface.

Oral shields

Inner side with two small flat middle spurs, two larger flat laterodistal spurs, and a round centrodistal depression to which oral GPs attach. Madreporite inner side with large round central hole, smaller round distal hole, offset to one side a large oval hydropore, visible externally.

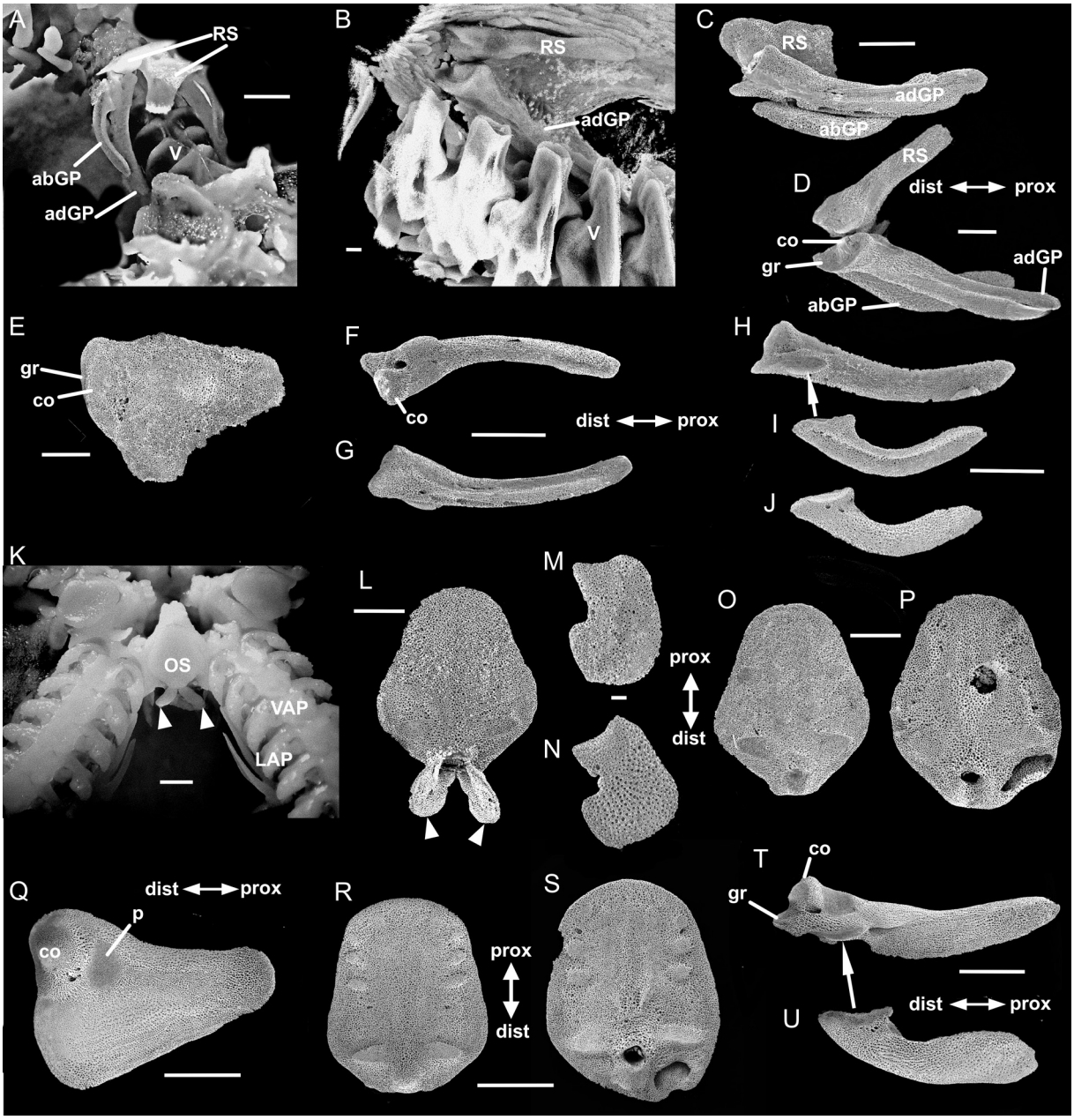

Fig. 15. Ophiocomidae Ljungman, 1867, SEM, unless otherwise noted. **A–P**. *Ophiocoma scolopendrina* (Lamarck, 1816). **A**. Genital plates in situ, dorsal view, digital photo. **B**. Genital plates in situ, distal ends, adradial view, micro-CT. **C–D**. adGP, abGP and RS articulating, adradial aspect. **E**. Radial shield, inner aspect. **F**. adGP, ventro-adradial aspect. **G**. adGP, abradial aspect. **H**. adGP, abradial aspect. **I**. abGP, abradial aspect, arrow connects articular structures. **J**. abGP, adradial aspect. **K**. Ventral arms and mouth (arrowheads mark oGP), digital photo. **L**. Oral shield with oGP attached (arrowheads). **M**. oGP, abradial aspect. **N**. oGP, adradial aspect. **O**. Oral shield, inner aspect. **P**. Madreporite, inner aspect. **Q–U**. *Ophiocoma erinaceus* Müller & Troschel, 1842. **Q**. Radial shield, inner aspect. **R**. Oral shield, inner aspect. **S**. Madreporite, inner aspect. **T**. adGP, abradial aspect. **U**. abGP, adradial aspect. Scale bars: A–B, E, K–L, O–P = 0.5 mm; C–D, F–J, Q–U = 1 mm; M–N = 0.1 mm.

Radial shield

Single low condyle bordered by a short dorso-distal groove.

Remarks

All examined species in the closely related genera *Ophiocoma* and *Breviturma* Stöhr, Boissin & Hoareau, 2013 are similar in the observed characteristics, but some variation exists. The radial shields have a thicker condyle and an obvious patch of finer stereom proximal to it in *O. erinaceus*, *O. schoenleini* and *B. krohi*. These are less well expressed and more similar to those of *O. scolopendrina* in *B. doederleini* and *B. dentata*. The oral shield has three lateral spurs in *O. erinaceus*, and all are more embossed than in *O. scolopendrina* (not examined in other species). The articular structures on the adGP are more strongly expressed in *O. erinaceus* and the *Breviturma* species than in *O. scolopendrina*.

Suborder Ophiacanthina O'Hara, Hugall, Thuy, Stöhr & Martynov, 2017
Family Ophiacanthidae Ljungman, 1867

Genus ***Ophiacantha*** Müller & Troschel, 1842
Fig. 16

Type species

Asterias bidentata Bruzelius, 1805.

Examined species

Ophiacantha bidentata, *O. abyssicola* G.O. Sars, 1872.

Oral GP

Pair close together, overlapping ventral disc scales. Rounded triangular or rectangular with median fold. Attached to distal point of oral shield with thickened edge. Large pore in inner side.

Adradial GP

Bar-like, with slightly widened distal end, articular structures as single dorso-distal condyle, bordered by curved groove with low protruding ventral stereom edge. Abradially a process and patches of denser stereom, where abGP attaches. Dorsal part of condyle meets flat surface of underside of RS.

Abradial GP

Thin, flat, curved scale, abradial edge strongly convex, adradial edge concave, with tapered, rounded proximal end, wider, slanting straight distal edge with flat or slightly domed articular surface. Adradial surface in distal part with conspicuous pore.

Oral shields

Hexagonal, wing-like, twice as wide as long, inner surface domed in centre, distal third of inner side thickened. Madreporite larger, wing-like with rounded lateral edges, strongly convex distal lobe, inner side flat on 'wings', thickened in centre and on lobe, which has a large hole, opening into a smaller hole (hydropore) in one latero-distal edge.

Radial shield

Narrow bar-like, distal end fan-shaped widened, small pore in distal part, straight distal edge, no specific articular structure.

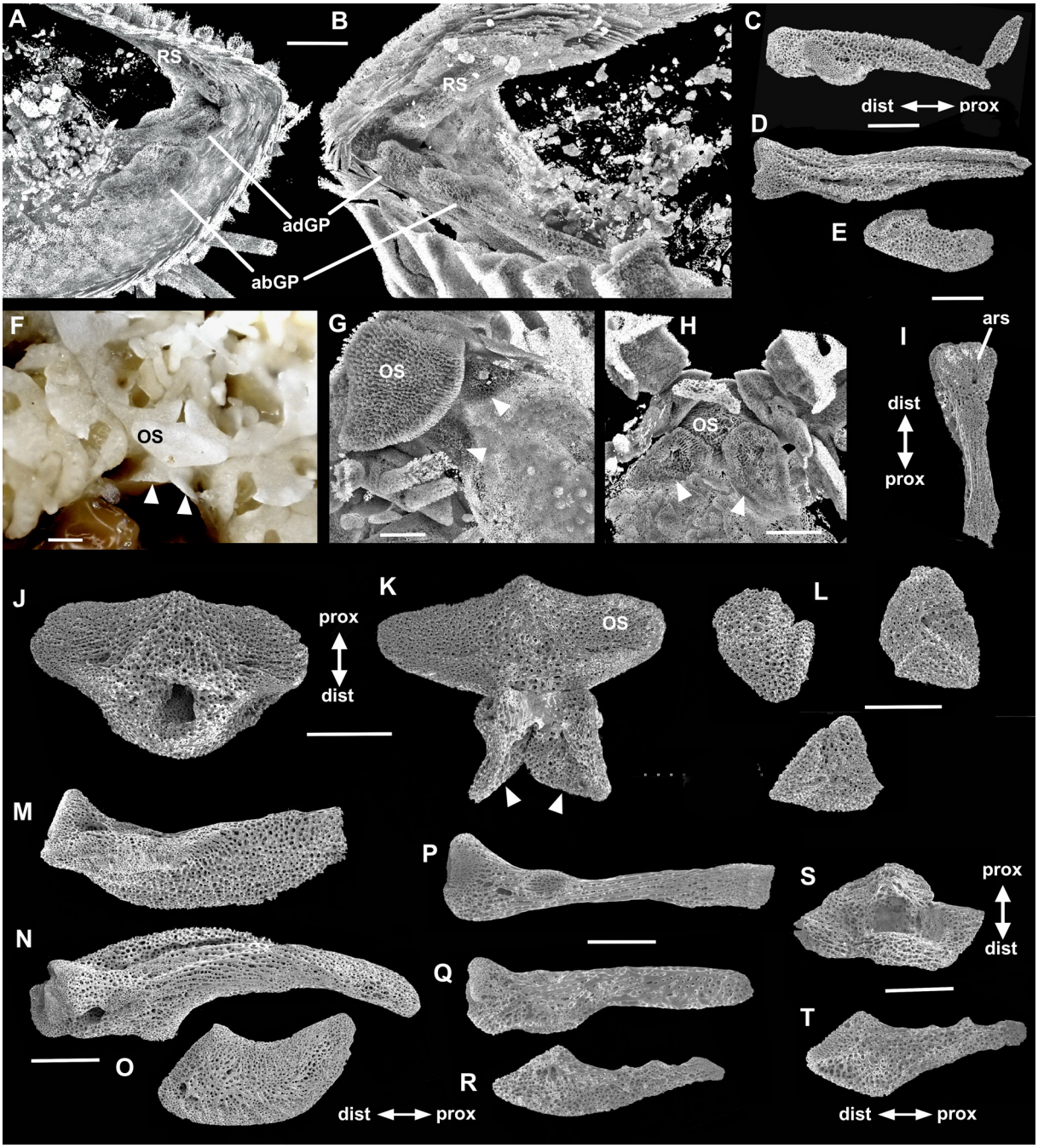

Fig. 16. Ophiacanthidae Ljungman, 1867. SEM, unless otherwise noted. **A–L**. *Ophiacantha bidentata* (Bruzelius, 1805) (11.5 mm dd). **A–B**. Genital plates and radial shield in situ, micro-CT. **C**. adGP, abradial aspect. **D**. adGP, adradial aspect. **E**. abGP. **F**. Oral shield and oGP, in situ, bleached specimen, digital photo. **G**. Madreporite and oGP in situ, external aspect, micro-CT. **H**. Madreporite and oGP in situ, internal aspect, micro-CT. **I**. Radial shield, internal aspect. **J**. Madreporite, internal disto-lateral aspect. **K**. Oral shield and oGP (arrowheads), internal aspect. **L**. oGP, various aspects. **M–O**. *O. bidentata* (13 mm dd). **M**. adGP, adradial aspect. **N**. adGP, abradial aspect. **O**. abGP. **P–T**. *O. abyssicola* G.O. Sars, 1872. **P**. adGP, adradial aspect. **Q**. adGP, abradial aspect. **R**. abGP. **S**. Madreporite. **T**. Radial shield, internal aspect. Scale bars: 0.5 mm.

Remarks

Two specimens of *O. bidentata* from Svalbard were analysed; the smaller one (11.5 mm dd) was dissected for this project and had narrower abGPs, a shorter but wider madreporite and slightly different adGPs (Fig. 16A–L) than the larger one (13 mm dd, Fig. 16M–O), of which images existed prior to this project. It is unclear whether these differences are due to the small size difference or whether this is variation between individuals in this morphologically variable species (evidenced by the fact that it has been synonymized with five other nominal species (Stöhr *et al.* 2022)). Since there is no geographic difference between these two specimens, it seems unlikely that these differences indicate different species. There is also some variation within the genus *Ophiacantha*. A specimen of *O. abyssicola* of similar size (13 mm dd) had narrower adGPs, smaller, less curved, more tapered abGPs, RSs with a triangular distal end with embossed part, and a madreporite with a large central hole.

Family Ophiocamacidae O'Hara, Stöhr, Hugall, Thuy & Martynov, 2018

Genus ***Ophiocamax*** Lyman, 1878
Fig. 17

Type species

Ophiocamax vitrea Lyman, 1878.

Examined species

Ophiocamax vitrea.

Oral GP

Rounded comma-shaped, externally convex, with many thorns, placed at either side of distal lobe of madreporite.

Adradial GP

Bar-like, straight, distally thickened, proximally tapered to a point. Articular structure with one condyle, bordered by half-circular shallow groove. Proximal to condyle a depression and a pore.

Abradial GP

Flat, strong, curved blade-like, as long as adGP, but wider, distal end curved towards adGP, convex abradial edge thicker, proximal end thinner. Articular structure a concave depression with thickened rim. Distal half of ventral edge with pointed thorns.

Oral shields

Proximally wing-like triangular, large distal lobe, creating a spearhead shape, folded along horizontal midline. Madreporite with large hole in midline of inner side.

Radial shield

Large condyle on distal radial corner, bordered by dorso-distal groove.

Remarks

Ophiocamax vitrea is the only species among the here examined Ophiacanthida in which the hole in the madreporite is not near the distal edge. It is unknown whether this is true for other species of *Ophiocamax*. The strong fold in the middle of the madreporite may have led to the displacement of the hole, but more species need to be studied.

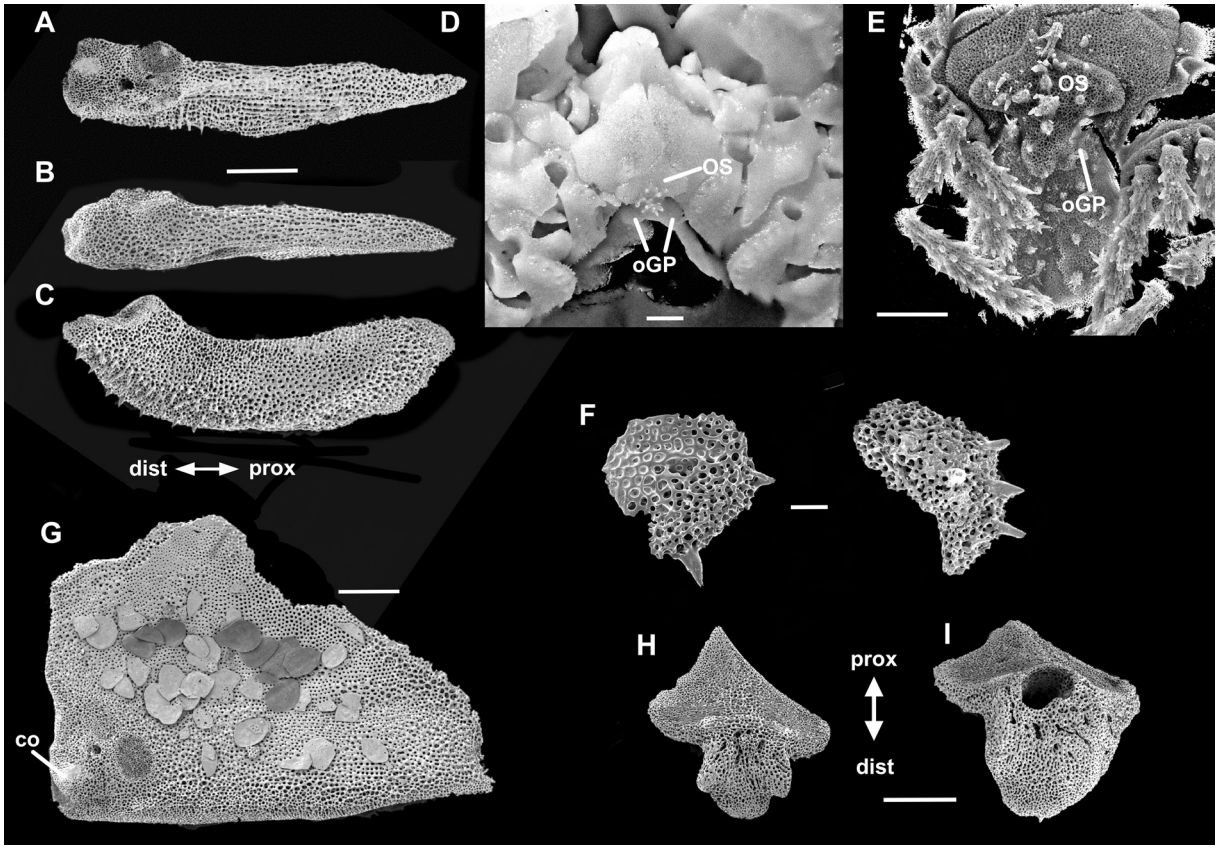

Fig. 17. Ophiocamacidae O'Hara, Stöhr, Hugall, Thuy & Martynov, 2018. *Ophiocamax vitrea* Lyman, 1878, SEM, unless otherwise noted. **A**. Adradial genital plate, dorsal aspect. **B**. Adradial genital plate, lateral aspect. **C**. Abradial genital plate. **D**. Oral genital plates in situ, digital photo. **E**. Oral shield and genital plates, micro-CT. **F**. Oral genital plates. **G**. Radial shield, internal aspect. **H**. Oral shield, internal aspect. **I**. Madreporite, internal aspect. Scale bars: A–E, G = 0.5 mm; F, H–I = 0.1 mm.

Family Ophiotomidae Paterson, 1985

Genus ***Ophiocomina*** Koehler in Mortensen, 1920
Fig. 18

Type species

Asterias nigra Abildgaard in O.F. Müller, 1789.

Examined species

Ophiocomina nigra.

Oral GP

Rounded rectangular with finger-like proximal lobe, thin. Articulates with oral shield with lobe at distolateral spurs, pair of oGP close together.

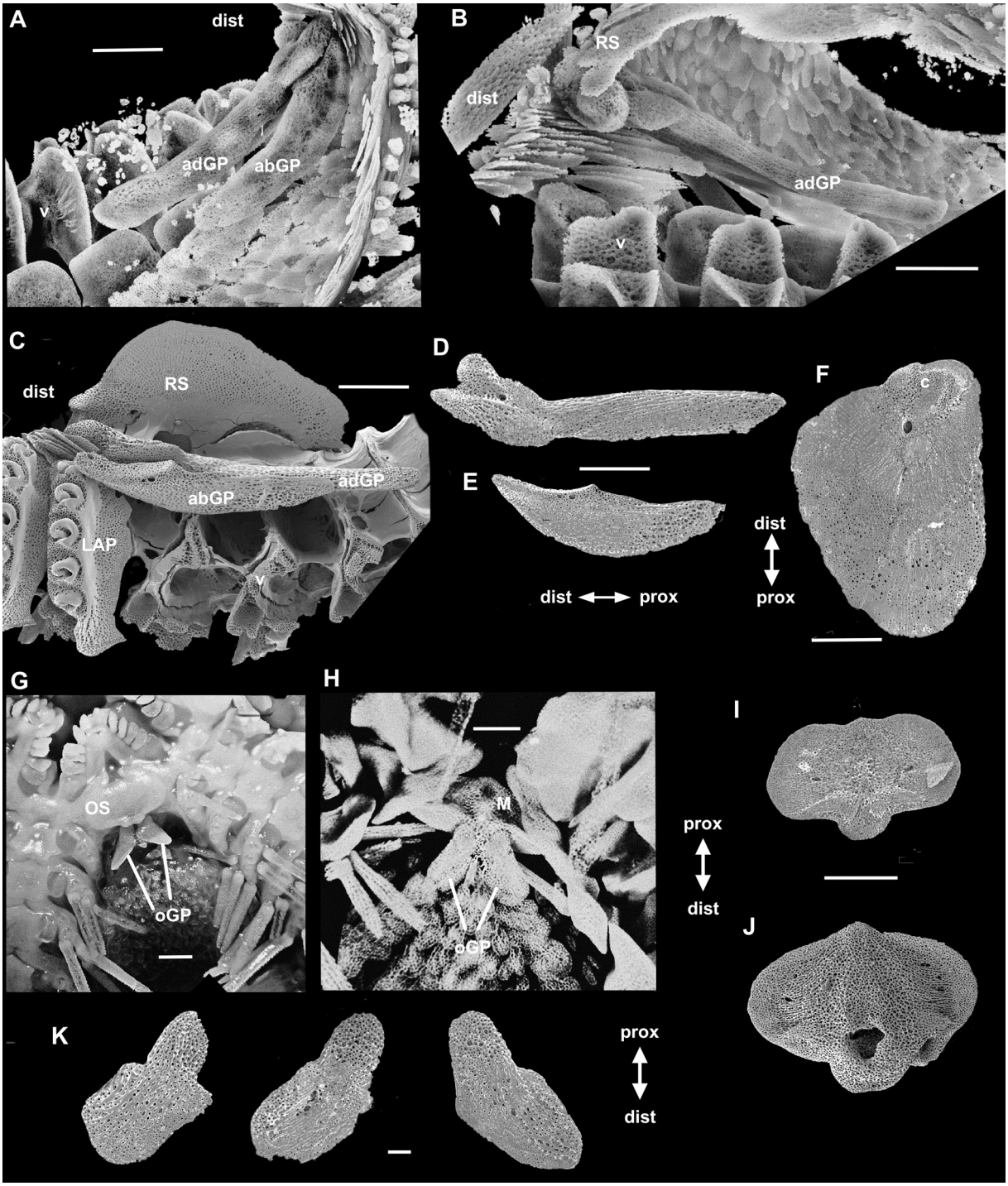

Fig. 18. Ophiotomidae Paterson, 1985. *Ophiocomina nigra* (Abildgaard in O.F. Müller, 1789), SEM, unless otherwise noted. **A–B**. abGP and adGP in situ (micro-CT). **C**. adGP and abGP at arm. **D**. adGP abradial aspect. **E**. abGP, lateral aspect. **F**. Radial shield, inner aspect. **G**. Oral GP in situ, bleached specimen, digital photo. **H**. oGPs at madreporite, inside disc view, micro-CT. **I**. Oral shield, internal aspect. **J**. Madreporite, inner aspect. **K**. Oral GPs. Scale bars: A–J = 0.5 mm; K = 0.1 mm.

Adradial GP

Bar-like, distal end widened, curved dorsalwards, articular structures two-pronged condylar processes, adradial one with round dorso-distal condyle bordered by ventral groove, abradial one articulates with abGP.

Abradial GP

Flat scoop-shaped, thin, proximally tapered, ventral edge convex, dorso-proximal half straight, dorso-distal half with concave articular structure. Adradial surface with distal pore.

Oral shield

Inner side flat, two lateral spurs at distal edge. Madreporite inner surface with raised middle part, large distal hole, opening to one side in a smaller hole (hydropore). Flat lateral inner portions with small pores.

Radial shield

Distal edge with one large and one smaller condyle, larger one bordered by dorsal ledge. Proximal to two condyles a conspicuous hole.

Genus ***Ophiocopa*** Lyman, 1883
Fig. 19A–E

Type species

Ophiocopa spatula Lyman, 1883.

Examined species

Ophiocopa spatula.

Oral GP

Not examined in detail, but in situ appears like large round scale, pair widely separated at the oral shield.

Adradial GP

Bar-like, with thin rod and widened distal end with lateral processes and finer meshed patch, single condyle and groove.

Abradial GP

Thin, curved scale, abradially convex, straight articular distal edge. As long as adGP. Conspicuous pores in distal part of adradial surface.

Oral shields

Madreporite inner side with median transverse ridge/two spurs, split in two halves by central opening.

Radial shield

Articular structure a smooth patch, slightly depressed. In centre of distal half, a finer meshed patch.

Genus ***Ophiotreta*** Verrill, 1899
Fig. 19F–I

Type species

Ophiacanha lineolata Lyman, 1883.

Examined species

Ophiotreta valenciennesi (Lyman, 1878).

Oral GP

Not examined, but considered present.

Adradial GP

Bar-like, thicker rod with slightly wider distal end with lateral processes, single condyle and groove.

Abradial GP

Thick curved scale, half as long as adGP, straight distal articular edge of abradial surface with conspicuous pore.

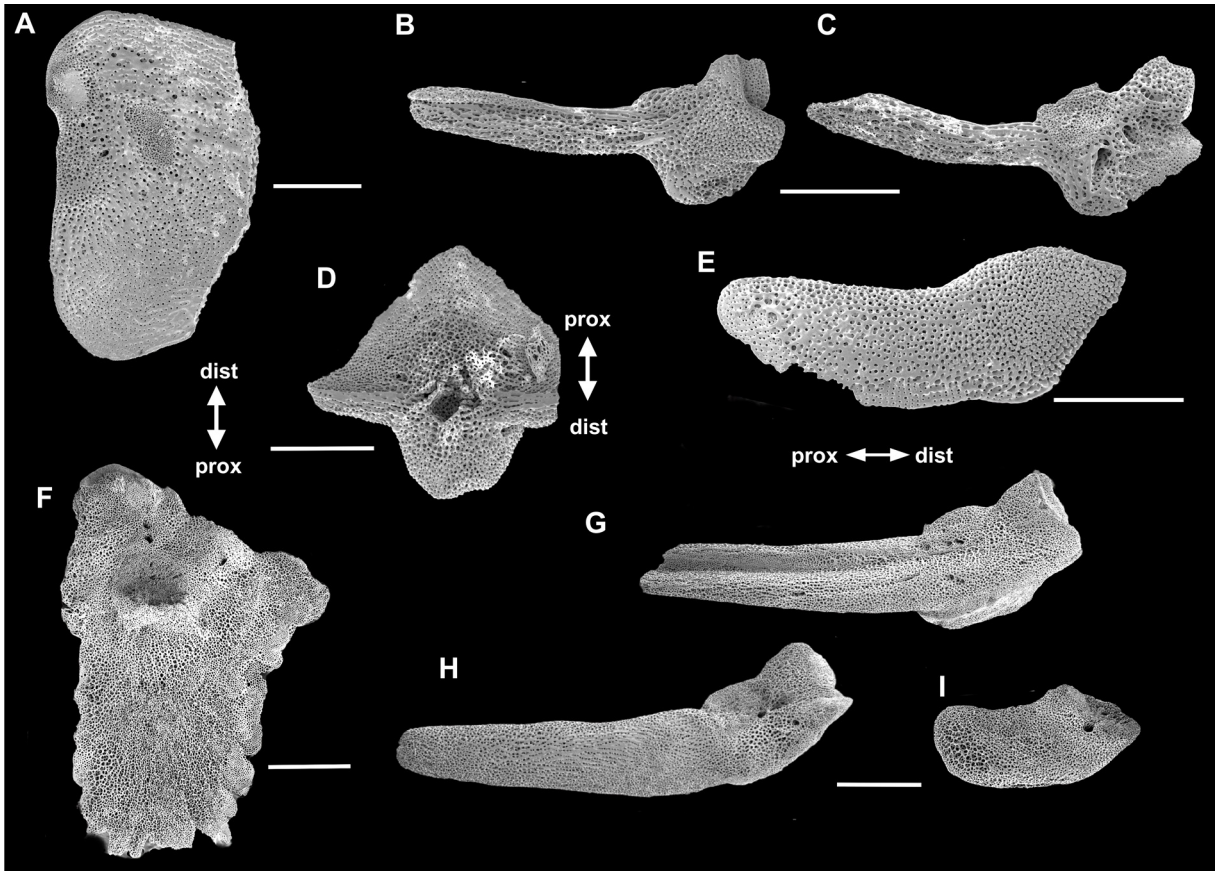

Fig. 19. Ophiotomidae Paterson, 1985, SEM. **A–E**. *Ophiocopa spatula* Lyman, 1883. **A**. Radial shield, inner aspect. **B**. adGP, abradial aspect. **C**. adGP, adradial aspect. **D**. Madreporite, inner aspect. **E**. abGP, abradial aspect. **F–I**. *Ophiotreta valenciennesi* (Lyman, 1878). **F**. Radial shield, inner aspect. **G**. adGP, abradial aspect. **H**. adGP, abradial aspect. **I**. abGP. Scale bars: A–E = 0.5 mm; F–I = 1 mm.

Oral shields

Not examined.

Radial shield

Inner side with distal condyle and curved groove, proximal to this a depression with protruding proximal edge.

Order Amphilepidida O'Hara, Hugall, Thuy, Stöhr & Martynov, 2017
Suborder Ophionereidina O'Hara, Hugall, Thuy, Stöhr & Martynov, 2017
Superfamily Ophiolepidoidea Ljungman, 1867
Family Hemieuryalidae Verrill, 1899

Genus ***Ophiozonella*** Matsumoto, 1915
Fig. 20

Type species

Ophiozona longispina H.L. Clark, 1908.

Examined species

Ophiozonella longispina.

Oral GP

Not examined in detail. Genital slit lined by narrow elongated plates connecting to OS laterodistally, pair widely separated, similar to condition in *Ophiolepis*.

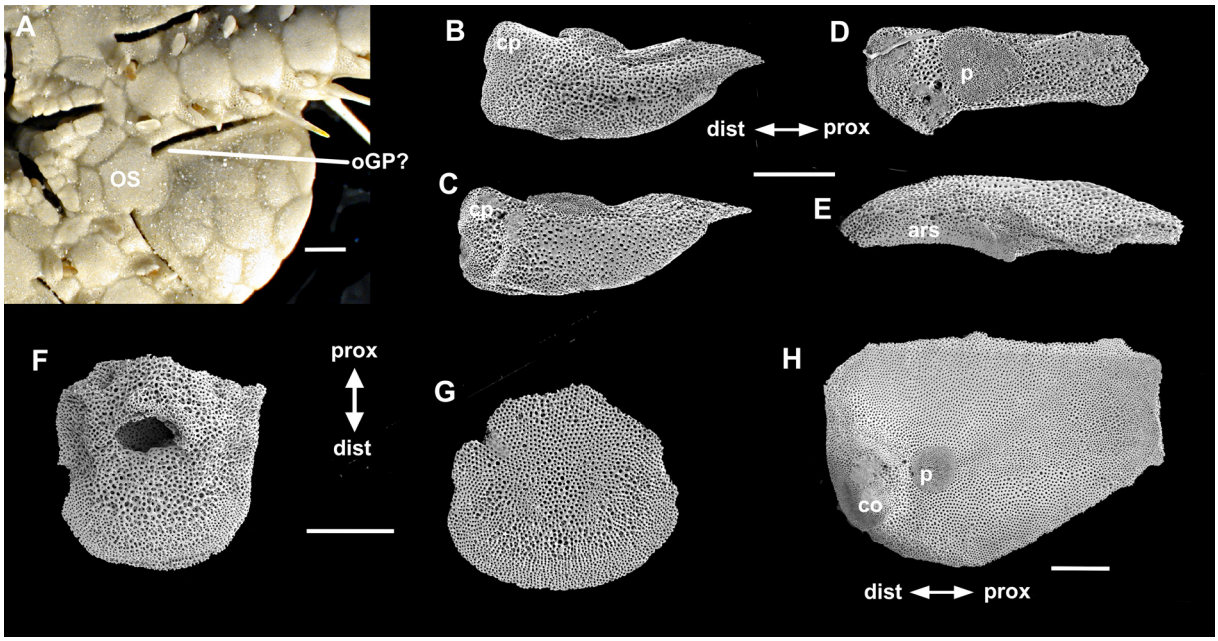

Fig. 20. Hemieuryalidae Verrill, 1899. *Ophiozonella longispina* (H.L. Clark, 1908), SEM, unless otherwise noted. **A**. Section of ventral aspect, digital image. **B**. adGP, abradial aspect. **C**. adGP, adradaial aspect. **D**. adGP, dorsal aspect. **E**. abGP, dorsal aspect. **F**. Madreporite, inner aspect. **G**. Oral shield, inner aspect. **H**. Radial shield, inner aspect. Scale bars: 0.5 mm.

Adradial GP

Comma-shaped, distally wide and thick, proximally tapered to a point, ventral edge convex, dorsal edge concave and with a rough protrusion. Articular structures a distal depression, a condylar process with flat distal surface, bordered by a groove, proximally to this a large round to heart-shaped patch of finer stereom.

Abradial GP

As long as adGP, scoop-shaped with smooth, concave dorso-distal articular structure, accounting for a third to half plate length.

Oral shields

Inner side flat, no remarkable structures. Madreporite inner side with thickened proximal part with large central hole, opening into two proximal small pores.

Radial shield

Articular structures consist of a distal condyle and depression on an embossed part, at distal edge bordered by a narrow ledge. Proximal to depression a round coarse patch.

Remarks

The type species of Hemieuryalidae, *Hemieuryale pustulata* von Martens, 1867, has a short abradial GP with a wider distal half and proximal thinner stalk (Gondim *et al.* 2015), more or less comma-shaped. The articular structures consist of a shallow stereom depression and a curved distal groove, matching similar structures on the radial shield; the abradial GP was not found and may be absent (Gondim *et al.* 2015). The radial shield has similar articular structures as in *O. longispina*. Oral GPs were not known when that study was performed, but oral images of *H. pustulata* in Gondim *et al*. (2015) show that the short proximally positioned genital opening is abradially lined by a large flat scale that connects to the oral shield and this is likely an oral GP. In *Sigsbeia murrhina* Lyman, 1878 and *S. lineata* Lütken & Mortensen, 1899, the genital slits are limited to small round openings near the oral shield (Gondim de Farias 2016) and oral GP are considered absent.

Family Ophiolepididae Ljungman, 1867

Genus ***Ophiolepis*** Müller & Troschel, 1840
Fig. 21A–L

Type species

Ophiolepis superba H.L. Clark, 1915.

Examined species

Ophiolepis variegata Lütken, 1856.

Oral GP

In situ visible as narrow elongated plates latero-distally at OS. Positioned slanted vertically at distal lateral edge of OS. Elongated oval in shape with raised central ridge and slanting sides; ventral edge convex and thickened, dorsal edge straight. Small pore in distal edge.

Adradial GP

Cleaver-shaped, proximal half a thick rod, distal half dorso-adradially with wide blade-like protrusion, single condyle, bordered by deep groove in distal adradial edge. Proximal to condyle a large depression with protruding rim.

Abradial GP

Longer and wider than adGP, rounded scalene triangular, dorsal edge strongly convex and wavy, ventral edge straight, distal end rounded, proximal end tapered to round point, ventral edge thickened into ridge, distally widened. One to two conspicuous pores in distal edge. Attaches broadly to blade-like protrusion on adGP.

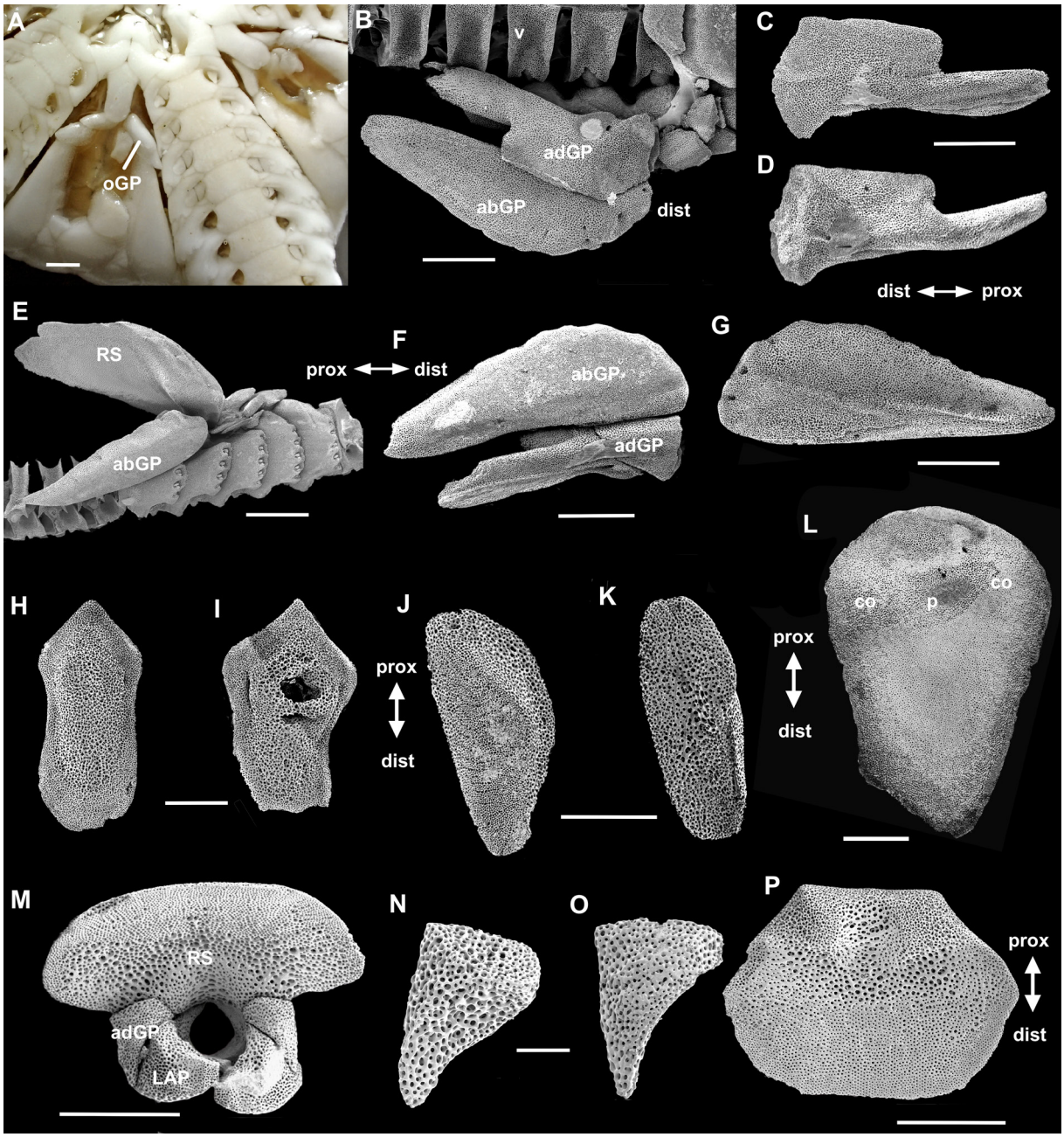

Fig. 21. Ophiolepididae Ljungman, 1867, SEM, unless otherwise noted. **A–L**. *Ophiolepis variegata* Lütken, 1856. **A**. Oral disc, digital image. **B**. Genital plates at arm. **C**. adGP, abradial aspect. **D**. adGP, adradial aspect. **E**. Radial shield and abGP at arm. **F**. abGP and adGP articulated. **G**. abGP, inner aspect. **H**. Oral shield, inner aspect. **I**. Madreporite, inner aspect. **J–K**. Oral GP, uncertain aspects. **L**. Radial shield, inner aspect. **M–P**. *Ophiotypa simplex* Koehler, 1897. **M**. adGP articulated at arm and under fused radial shields (or radial primary plates). **N**. oGP, inner aspect. **O**. oGP, outer aspect. **P**. Radial shields (or radial primary plates), inner aspect. Scale bars: A–G, L–M, P = 1 mm; H–K = 0.5 mm; N–O = 0.2 mm.

Oral shields

Elongated oval with proximal pointed angle, inner side embossed with thin rim. Madreporite similar, with large hole proximo-central in inner side, divided by narrow bridge.

Radial shield

Inner side of distal part embossed with two poorly defined condyles, bordered by short ledge, proximal to embossed part a patch of coarser stereom with finer centre.

Remarks

The protrusion that gives the adGP its cleaver-like shape is present in all species of *Ophiolepis* that have been examined so far, albeit sometimes less pronounced or shorter than in *O. variegata*, and the abGP also has a similar shape in all species (Pineda-Enriquez 2013). The two condyles on the inner RS are more obvious in *O. superba* than in *O. variegata*.

Genus ***Ophiotypa*** Koehler, 1897
Fig. 21M–P

Type species

Ophiotypa simplex Koehler, 1897.

Examined species

Ophiotypa simplex.

Oral GP

Absent.

Adradial GP

Cup-shaped convex, smaller than lateral arm plate to which it attaches. Articular structure a flat distal surface.

Abradial GP

Absent.

Oral shields

Not examined.

Radial shield

Single large plate above each arm base with two flat articular structures separated by a depression.

Remarks

Ophiotypa simplex is the only species in its genus and strongly paedomorphic. Its disc consists of few large plates. Pairs of radial shields appear to have been fused into a single large plate or are replaced by the radial primary plates functioning as radial shields, but individuals with a pair of plates on one or several radii have been observed (unpublished data, Stöhr & Martynov). The ventral disc is covered by the large oral shield, genital slits are not visible and the abGP appears to be absent.

Superfamily Ophionereidoidea Ljungman, 1867
Family Amphilimnidae O'Hara, Stöhr, Hugall, Thuy & Martynov, 2018

Genus ***Amphilimna*** Verrill, 1899
Fig. 22

Type species

Ophiocnida olivacea Lyman, 1869.

Examined species

Amphilimna olivacea.

Oral GP

Large, rectangular, flat, thin, with round, elongated proximal lobe. Almost vertical along proximal abradial bursa edge.

Adradial GP

Bar-like with widened distal end. Articular structures a low condyle, bordered by shallow groove and low edge. Proximal to condyle a rounded abradial process to which the abGP articulates ventrally, a round depression of coarse stereom and a small pore. Proximal part twisted.

Abradial GP

Twisted s-shape, thin, with distal adradial appendix, one third as long as plate, folded proximalwards and fold articulates with adGP, folding around flat extensions of lateral arm plates. Distal edge straight. Large adradial plates (flat and interlocked arm spines) bordering genital slit fold over abGP and under appendix, similar enlarged disc scales fold over the slit edge abradially, on their inner side supported by the abGP.

Oral shields

Flat, on distal part a spur on each side, offsetting distal lobe from proximal part. Madreporite slightly inflated in centre, with large opening between distal lateral spurs, proximal to large hole stereom wider meshed with pores. Externally a single hydropore at distal edge, offset from centre.

Radial shield

Inner side with distal flat condyle, bordered by curved groove. Distal to RS midline a rough round patch.

Remarks

The shape of the abradial GP sets *Amphilimna olivacea* apart from all other here examined species. The peculiar shape matches the specialized lateral arm plates, which are blade-like flat and form the adradial border of the s-shaped genital slit. The genital plates of *A. multispina* Koehler, 1922 are similar to those of *A. olivacea* (Martynov 2010), but their shape is unknown for other species in the genus. Contrary to the original description of *A. olivacea*, no genital plate is exposed to the outside (Lyman 1869), as is evident from the micro-CT reconstruction.

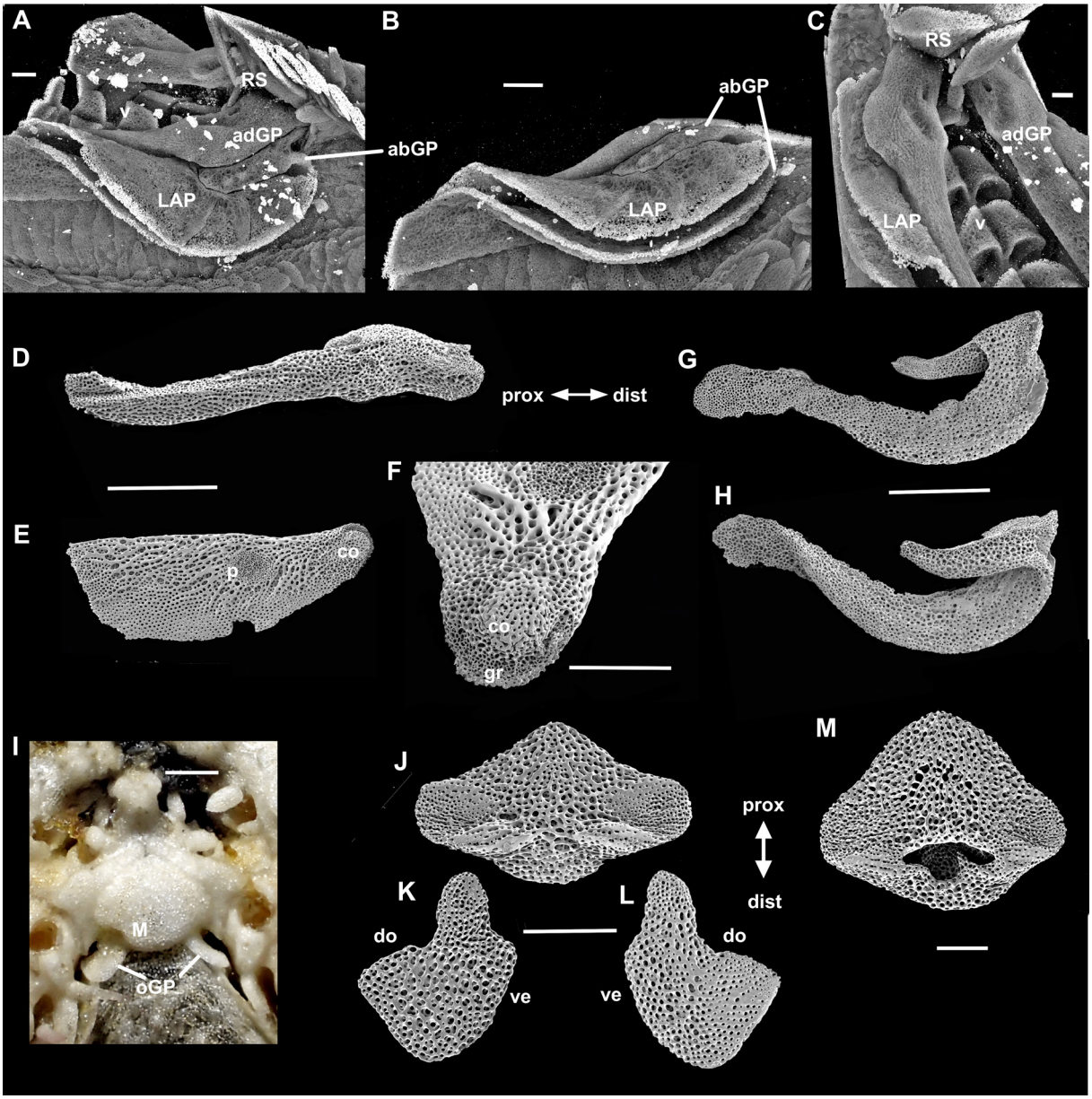

Fig. 22. Amphilimnidae O'Hara, Stöhr, Hugall, Thuy & Martynov, 2018, *Amphilimna olivacea* (Lyman, 1869). A–C = micro-CT; D–H, J–N = SEM; I = digital image. **A**. adGP, abGP, wing-like LAPs in situ. **B**. Detail of A, different angle. **C**. adGP in situ, dorsal aspect. **D**. adGP, adradial aspect. **E**. Radial shield, inner aspect. **F**. RS articular structures. **G**. abGP, abradial aspect. **H**. abGP, adradial aspect. **I**. Jaw in situ, bleached. **J**. Oral shield, inner aspect. **K–L**. oGP inner/outer aspects (unclear which is which). **M**. Madreporite, inner aspect. Scale bars: A–C, F, J–M = 0.2 mm; D–E, G–I = 0.5 mm.

Family Ophionereididae Ljungman,1867

Genus ***Ophionereis*** Lütken, 1859
Fig. 23

Type species

Ophiura reticulata Say, 1825.

Examined species

Ophionereis reticulata, *O. porrecta* Lyman, 1860, *O. degeneri* (A.H. Clark, 1949).

Oral GP

Elongated oval, flat, thin, proximal end under OS, pair not meeting (only examined in *O*. *reticulata*, but externally visible in *O*. *degeneri* and *O*. *porrecta*). On some plates a round lateral process. Beset with small round granules/papillae at abradial edge. Large scales along the genital slit connect to oGP.

Adradial GP

Ophionereis reticulata: weakly cleaver-shaped with wavy abradial edge. Proximal half rod-like with longitudinal groove, distal half widened rectangular, protruding abradial edge wavy, articulates with ventral surface to abGP. Abradial surface with small adradial process with coarser stereom, oval hole in distal part. Distal end curved dorsalwards, dorsally rounded, no distinct condyle, but a groove, distal edge concave. Proximal ends of adGP and abGP crossing. *Ophionereis porrecta*: widened projection smaller, cleaver shape less obvious; distally a condylar process terminating flat. *Ophionereis degeneri*: cleaver shape slightly more pronounced than in *O*. *porrecta*, but not as strong as in *O*. *reticulata*; distal condylar process and groove.

Abradial GP

Ophionereis reticulata: sabre-shaped, as long as adGP, sligthly curved, dorsal edge concave, ventral edge convex, with furrow in abradial side, distal third dorsally flattened concave, articulates to adGP, proximal end crosses adGP. *Ophionereis porrecta*: thin, flat, curved, distally widest with slanting edge, proximally tapered to round point. *Ophionereis degeneri*: similar to *O*. *porrecta*, but articular edge concave.

Oral shields

On inner surface, near distal edge a spur to either side. Madreporite in distal half inflated, with large opening, proximal half thinner (only examined in O. *reticulata*).

Radial shield

Single condyle and coarser round patch at some distance proximal to condyle in all three examined species, condyle more pronounced in *O*. *degeneri* than in the others.

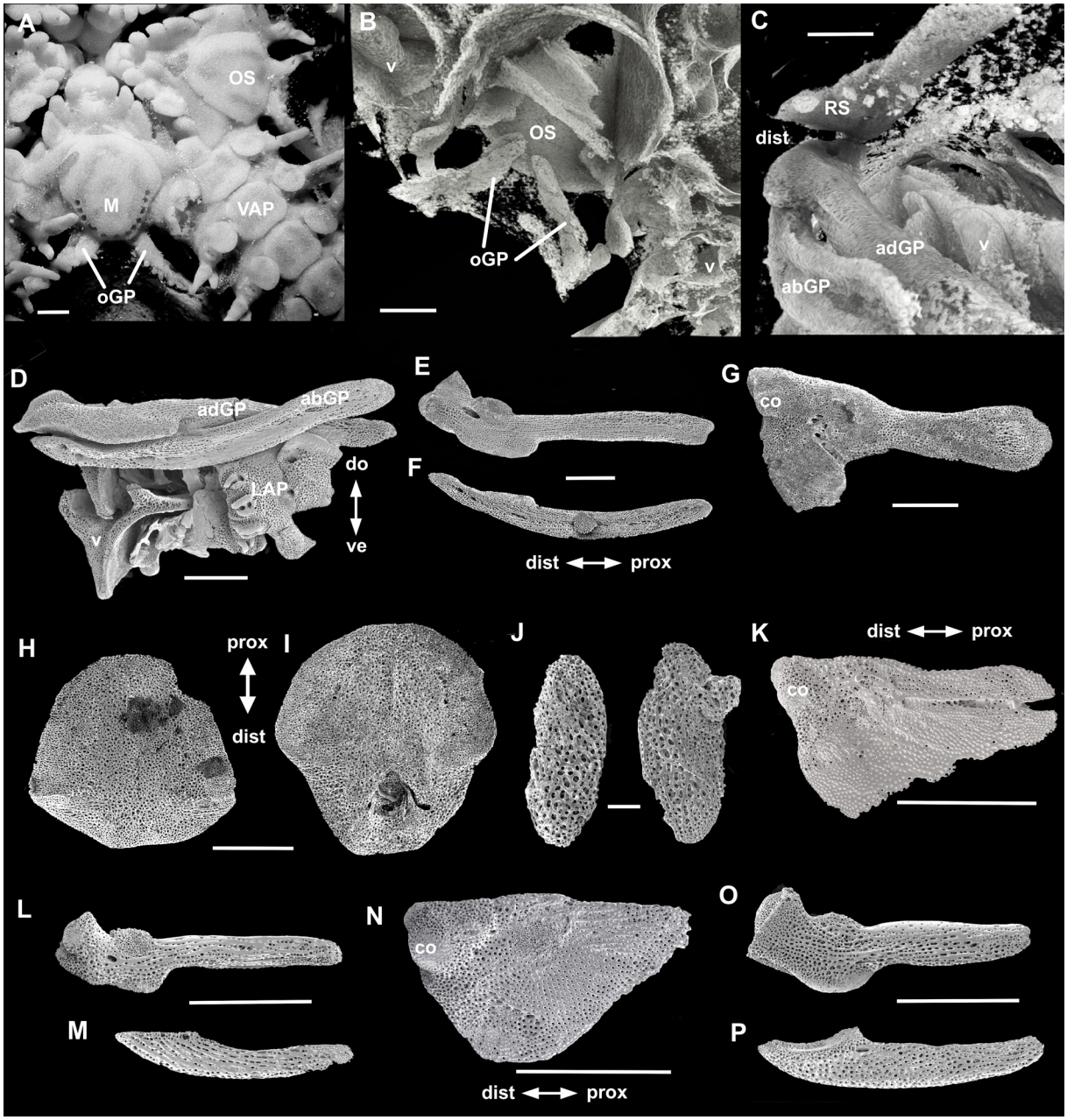

Fig. 23. Ophionereididae Ljungman, 1867, SEM, unless otherwise noted. **A–J**. *Ophionereis reticulata* (Say, 1825). **A**. Oral aspect, digital image. **B–C**. Micro-CT. **B**. Oral shield with oGP, inner view. **C**. abGp, adGB and RS in situ. **D**. abGP and adGP in situ. **E**. adPG, abradial aspect. **F**. abGP. **G**. Radial shield, inner aspect. **H**. Oral shield, inner aspect. **I**. Madreporite, inner aspect. **J**. Oral genital plates, one with round tubercle/process. **K–M**. *Ophionereis porrecta* (Lyman, 1860). **K**. Radial shield, inner aspect. **L**. adGP, abradial aspect. **M**. abGP. **N–P**. *Ophionereis degeneri* (A.H. Clark, 1949). **N**. Radial shield, inner aspect. **O**. adGP, abradial aspect. **P**. abGP. Scale bars: 0.5 mm.

Genus ***Ophiochiton*** Lyman, 1878
Fig. 24A–C

Type species

Ophiochiton fastigatus Lyman, 1878.

Examined species

Ophiochiton fastigatus.

Oral GP

Externally visible as large, round scales, but not examined.

Adradial GP

Weakly cleaver-shaped, flat, blade-like proximal part, distal end depressed with high edges, a large rough patch on adradial surface towards dorsal edge, and a large hole in middle of distal part on adradial surface.

Abradial GP

Hockey-stick-shaped, blade-like, flat, as long as adGP, distal end angled, pointed, distal dorso-adradial edge with depression. Lines abradial edge of genital slit (= part of edge of interradial disc).

Oral shields

Not examined.

Radial shield

Not examined.

Remarks

The available pre-existing images allow only limited assessment of the articular structures of the adradial GP. Martynov (2010) described them as a condyle bordered by a low ridge but without figures, whereas Matsumoto (1917) wrote that the radial shield and adradial GP articulate with two condyles and one pit. The images presented here appear to be the first published SEM images of genital plates of *Ophiochiton*.

Genus ***Ophioplax*** Lyman, 1875
Fig. 24D–J

Type species

Ophioplax ljungmani Lyman, 1875.

Examined species

Ophioplax lamellosa Matsumoto, 1915.

Oral GP

Not examined, in situ obscured by granules, but laterally at oral shield a large scale discernible at either side, considered as oral GP.

Adradial GP

Proximal half bar-like, distally weakly cleaver-shaped with wide dorsal and ventral processes; rounded distal part offset from proximal bar by a kink. Articular structure a prominent round distal condyle, bordered by a deep groove and wide edge. Proximal to condyle on dorsal side of offset part a large patch of finer meshed stereom.

Abradial GP

Sabre-shaped, flat, thin, ventral edge convex, dorsal edge slightly concave, long concave distal articular structure.

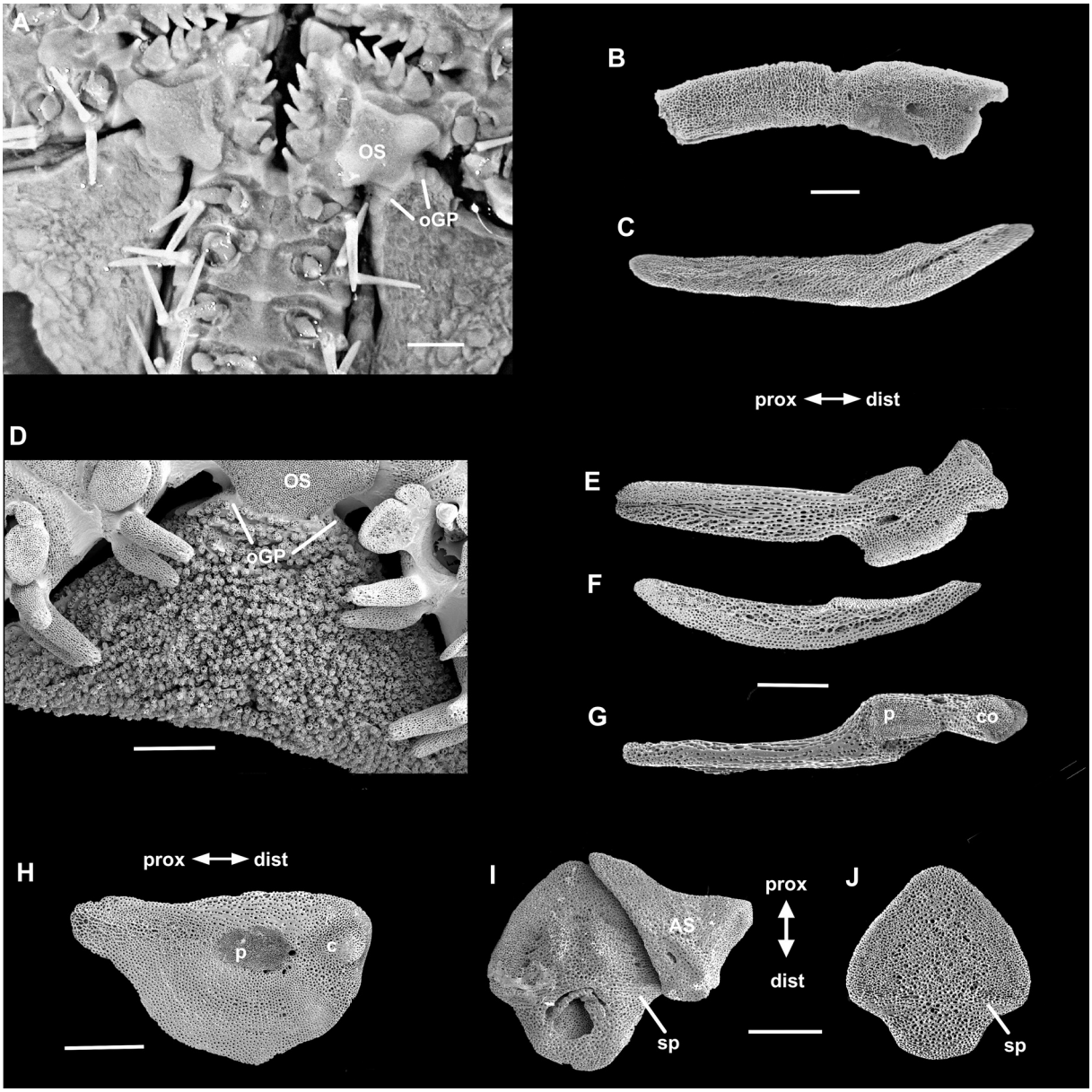

Fig. 24. Ophionereididae Ljungman, 1867, SEM, unless otherwise noted. **A–C**. *Ophiochiton fastigatus* Lyman, 1878. **A**. Ventral disc section, digital photo. **B**. adGP, proximal end broken. **C**. abGP. **D–J**. *Ophioplax lamellosa* Matsumoto, 1915. **D**. Ventral interradius. **E**. adGP, lateral aspect (adradial?). **F**. abGP. **G**. adGP, dorsal aspect. **H**. Radial shield, inner aspect. **I**. Madreporite, inner aspect. **J**. Oral shield, inner aspect. Scale bars: 0.5 mm.

Oral shields

Flat, on distal part a weak spur on each side, offsetting distal lobe from proximal part. Madreporite inner side inflated in middle, two lateral distal spurs, flat proximal margins, large opening in distal lobe.

Radial shield

Low distal condyle near adradial edge, distally bordered by short groove. Proximal to condyle a large oval patch of finer stereom.

Suborder Gnathophiurina Matsumoto, 1915
Superfamily Amphiuroidea Ljungman, 1867
Family Amphiuridae Ljungman, 1867

Genus ***Amphiura*** Forbes, 1843
Fig. 25A–R

Type species

Amphiura chiajei Forbes, 1843.

Examined species

Amphiura chiajei, *A. filiformis* (O.F. Müller, 1776).

Oral GP

Amphiura chiajei: comma-shaped, flat, with oval proximal end, thin, needle-like appendix on inner distal end curved towards proximal end. *Amphiura filiformis*: elongated, curved or straight (in same individual), proximal end thickened, without distal needle-like appendix. Paired plates meet under the oral shield with convex edges towards each other (*A. chiajei*).

Adradial GP

Distal end widened with lateral lobes, long bar-like proximal shank, laterally curved with distal end above arm vertebrae, left and right plate almost meeting. Abradial distal lobe with dense, smooth, flat articular structure meeting abGP, distal end with protruding edge and curved depression with single round condyle meeting condyle on radial shield.

Abradial GP

Sabre-shaped, flat, thin, narrow blade, curved with dorsal edge concave, ventral edge convex, with longitudinal dorsal rim, at dorsal distal end a denser, smooth and slightly concave articular structure matching lobe on adGP, straight distalmost edge also joining distal end of adGP. Proximal end crosses proximal end of adGP. As long as adGP.

Oral shields

Inner side proximal part thickened, distal part thin, flat. Madreporite all over thicker, only margins thin, large opening in distal half, narrow slit in one proximolateral part.

Radial shield

Inner side distal end with large domed condyle, bordered by long narrow dorsal groove, proximal to condyle a large oval patch with finer stereom.

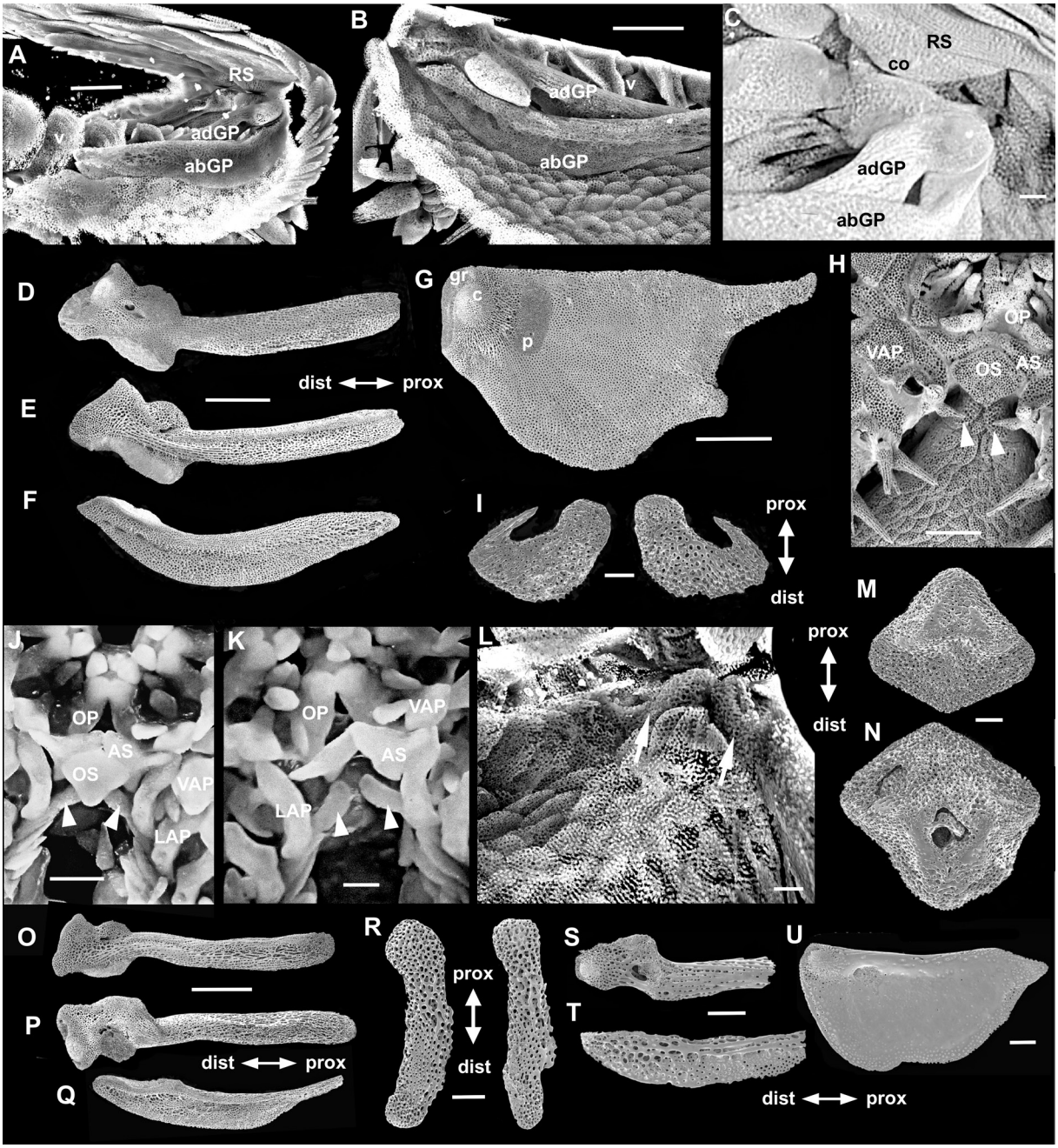

Fig. 25. Amphiuridae Ljungman, 1867, SEM, unless otherwise noted. **A–N**. *Amphiura chiajei* Forbes, 1843. **A–C**. adGP and abGP in situ, micro-CT. **D**. adGP, dorsal aspect. **E**. adGP, ventral aspect. **F**. abGP, lateral aspect. **G**. Radial shield, inner aspect. **H**. Oral section, oGP. **I**. Oral GP. **J–K**. Digital images. **J**. Oral shield section, ventral disc scales removed, oGP. **K**. Oral GP in situ after removal of oral shield. **L**. Oral GP in situ (arrows), inside disc, micro-CT. **M**. Oral shield, inner aspect. **N**. Madreporite, inner aspect. **O–R**. *Amphiura filiformis* (O.F. Müller, 1776). **O**. adGP, dorsal aspect. **P**. adGP, ventral aspect. **Q**. abGP, lateral aspect. **R**. Oral GP. **S–U**. *Amphipholis squamata* (Delle Chiaje, 1828). **S**. adGP, lateral aspect. **T**. abGP lateral aspect. **U**. Radial shield, inner aspect. Arrowheads (H, J–K) mark oGP. Scale bars: A–H, J–L, O–Q = 0.5 mm; I, M–N, R–U = 0.1 mm.

Remarks

Oral GP are visible externally in situ as large scale-like ossicles in *Amphipholis squamata* (Delle Chiaje, 1828), *Amphioplus congensis* (Studer, 1882), *Acrocnida brachiata* (Montagu, 1804) and in *Silax* cf. *abditus* Clark, 1970 (Stöhr & O'Hara 2021: fig. 2e–f). In *A. squamata*, the adradial GP has a single distal lobe that articulates with the abradial GP, a single prominent condyle and a groove (Fig. 25S), similar to *Amphiura*. The abradial GP in *A. squamata* is sabre-like flat with longitudinal rim, not as strongly curved as in *Amphiura*. The oral GP of the two examined species of *Amphiura* differ greatly in shape and more data are needed to understand the variability of these ossicles. Perhaps, the soft, often scale-less ventral disc of *A. filiformis* has led to the evolution of the elongated oral GP for support of the genital slit.

Family Amphilepididae Matsumoto, 1915

Genus ***Amphilepis*** Ljungman, 186
Fig. 26

Type species

Amphiura norvegica Ljungman, 1865.

Examined species

Amphilepis norvegica.

Oral GP

Not identified among small disc scales near oral shields.

Adradial GP

Bar-like, curved, proximal end tailfin-like broadened and pointed or rounded, abradial ventrolateral edge with fin-like process, distal end with adradial condyle, bordered by deep groove on abradial side, proximal to condyle a large round patch of almost imperforate stereom, edges extending disc-like from main plate.

Abradial GP

Thin, flat, half-circular with concave adradial edge, strongly convex abradial edge, straight adradial articular edge to adGP. Part of ventral disc, encircling small genital opening. About ⅔ of length of adGP.

Oral shields

Inner side flat, with horizontal ridge across middle. Madreporite with large oval opening in centre.

Radial shield

Inner side with distal large domed condyle, bordered by curved, wide distal ledge, proximal to condyle an oval, almost imperforate patch.

Superfamily Ophiactoidea Ljungman, 1867
Family Ophiactidae Matsumoto, 1915

Genus ***Ophiactis*** Lütken, 1856
Fig. 27

Type species

Ophiactis krebsii Lütken, 1856 = *Ophilepis savignyi* Müller & Troschel, 1842.

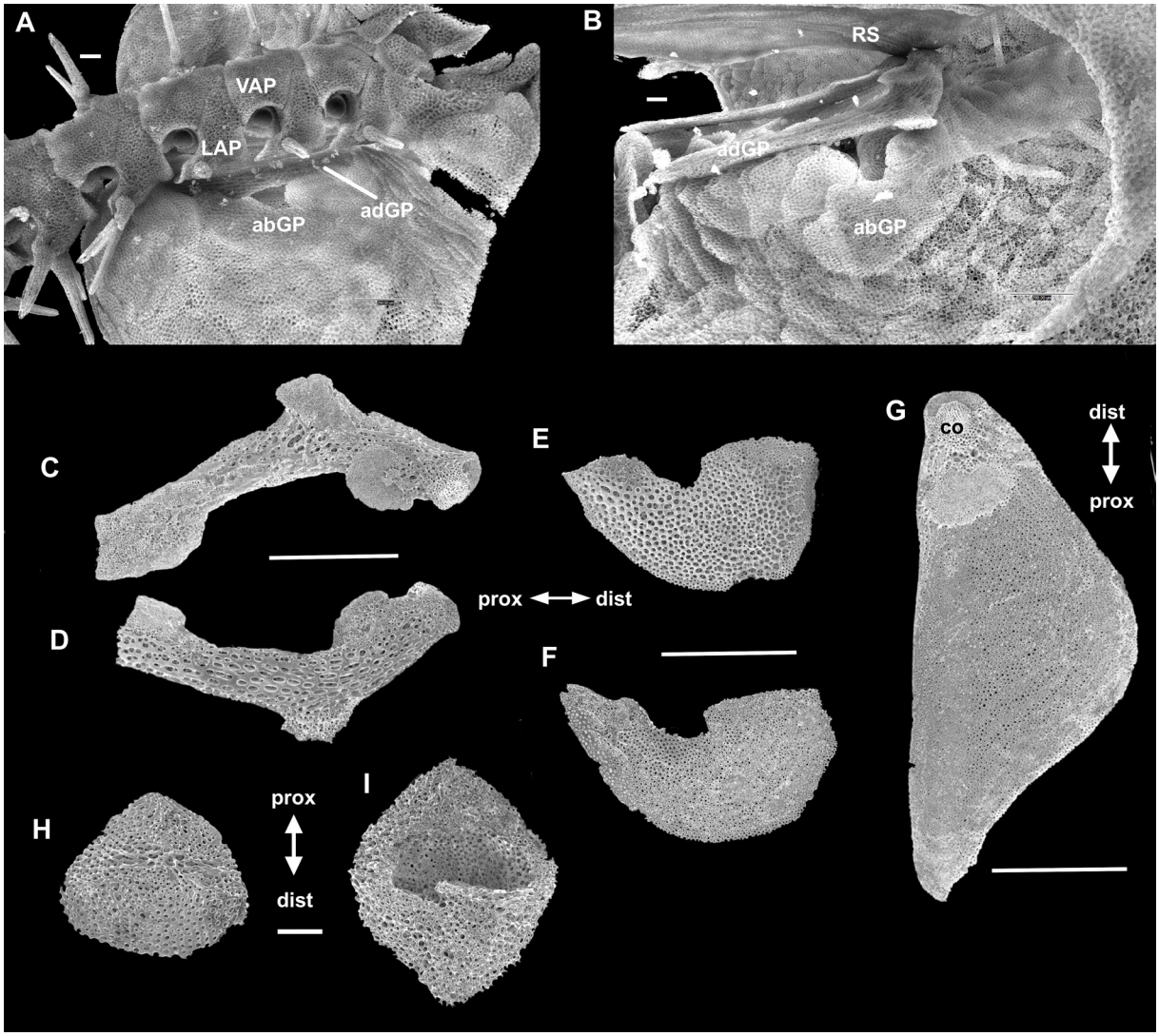

Fig. 26. Amphilepididae Matsumoto, 1915, *Amphilepis norvegica* (Ljungman, 1865), SEM, unless otherwise noted. **A–B**. Micro-CT. **A**. Genital plates in situ, external aspect. **B**. Genital plates in situ, internal aspect. **C**. adGP, ventral aspect. **D**. adGP, dorsal aspect. **E**. abGP, ventral aspect. **F**. abGP, dorsal aspect. **G**. Radial shield, inner aspect. **H**. Oral shield, inner aspect. **I**. Madreporite, inner aspect. Scale bars: A–B, H–I = 0.1 mm; C–G = 0.5 mm.

Examined species

Ophiactis abyssicola (M. Sars, 1861), *O. savignyi*.

Oral GP

Drop-shaped, round with small lobe at one end (unknown if proximal or distal). (Only examined in *O. abyssicola*.)

Adradial GP

Bar-like, with longitudinal dorsal furrow, distally widened, somewhat thicker than proximal shank, single condyle bordered by deep groove, proximal to condyle a protruding patch of finer stereom articulating with abGP, separated from condyle by deep groove, forming wrench-shaped adradial distal end.

Abradial GP

Two thirds as long as adGP, thin, broadly sickle-shaped**,** strongly convex ventral edge, distally twice as wide as proximally, distal edge straight and articulating with adGP.

Oral shields

Distal half of inner side thickened, proximal half flat and thin. Madreporite thick, lateral margins flat, two large openings, one in centre, one offset from centre in proximal half.

Radial shield

Inner side with distal condyle, bordered by curved groove, proximal to condyle a round, rough patch.

Remarks

The presence of oral GPs was also observed externally in *O. macrolepidota* Marktanner-Turneretscher, 1887 and *O. savignyi*. These fissiparous species are not well suited for the examination of dissociated ossicles, because most individuals are a composite of parts in different stages of regeneration, and therefore the ossicles vary considerably in size and shape within an individual.

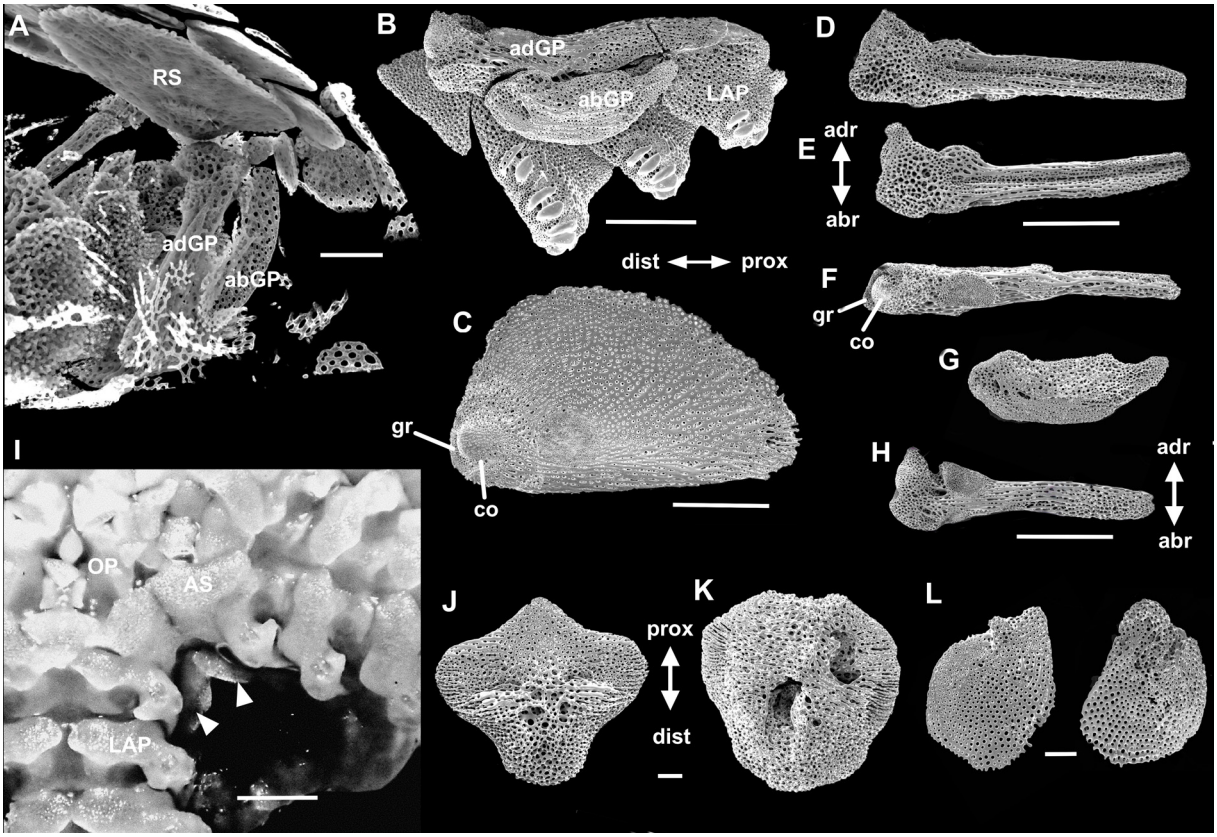

Fig. 27. Ophiactidae Matsumoto, 1915, SEM, unless otherwise noted. **A**. *Ophiactis savignyi* (Müller & Troschel, 1842), genital plates in situ, micro-CT. **B–L**. *Ophiactis abyssicola* (M. Sars, 1861). **B**. adGP and adGP articulated. **C**. Radial shield, internal aspect. **D–E**. adGP, dorsal aspect. **F**. adGP, ventral aspect. **G**. abGP, abradial aspect. **H**. adGP, ventrolateral view (from other, smaller specimen). **I**. oGP in situ (arrowheads, digital image), oral shield removed. **J**. Oral shield, internal aspect. **K**. Madreporite, internal aspect. **L**. oGP. Scale bars: A, J–L = 0.1 mm; B–I= 0.5 mm.

Family Ophiopholidae O'Hara, Stöhr, Hugall, Thuy & Martynov, 2018

Genus ***Ophiopholis*** Müller & Troschel, 1842
Fig. 28

Type species

Asterias aculeata Linnaeus, 1767.

Examined species

Ophiopholis aculeata.

Fig. 28. Ophiopholidae O'Hara, Stöhr, Hugall, Thuy & Martynov, 2018, *Ophiopholis aculeata* (Linnaeus, 1767), SEM, unless otherwise noted. **A**. Genital plates and radial shield in situ, micro-CT. **B–C**. Articulated adGP and abGP. **D**. Radial shield, inner aspect. **E**. adGP, abradial aspect. **F**. abGP. **G**. adGP adradial aspect. **H**. oGP in situ (arrowheads), digital image. **I**. oGP. **J**. Oral shield, inner aspect. **K**. Madreporite, inner aspect. Scale bars: A, H–K = 0.5 mm; B–G = 1 mm.

Oral GP

Flat, oval scale.

Adradial GP

Flat, blade-like for most of its length, distal end bulbous with several depressions and protrusions, curved dorsalwards. Proximal part tapered, ventral edge convex, dorsal edge straight. Distal condyle asymmetrically near arm meets condyle on RS, ridge at lateral abradial depression attaches to abGP. Large oval depression with finer stereom on dorsal side on proximal part of bulb.

Abradial GP

Kidney-shaped to half-circle, strong, half as long as adGP, distal end wider and thicker, with a groove that attaches to a ridge at adGP. Proximal end rounded tapered.

Oral shields

Oral shield inner surface with two weakly expressed spurs on midline. Madreporite inner surface proximally and in centre domed with large hole, opening in hydropore at proximal edge; lateral and distal margins flat and thinner.

Radial shield

Inner surface with large distal condyle, bordered by long, curved groove, proximal to condyle an oval patch of finer stereom.

Family Ophiotrichidae Ljungman, 1867

Genus ***Ophiothrix*** Müller & Troschel, 1840
Fig. 29

Type species

Asterias fragilis Abildgaard in O.F. Müller, 1789.

Examined species

Ophiothrix fragilis.

Oral GP

Oval scale-like, thin, as long as OS, some with notch in proximal part of ventral edge. Pair at acute angle, to either side of distal lobe on OS, half covered by OS. Visible through skin as v-shaped pair of ossicles, supporting proximal end of genital slits.

Adradial GP

Bar-like with bulbous distal end, curved with dorsal edge concave, ventral edge convex. Slanting away from arm, not completely vertical. Large, round, knob-like condyle at distal end bordered by deep groove meets similar condyle on underside of radial shield. Proximal to condyle several other protrusions and fine meshed stereom patches.

Abradial GP

Half-circle to kidney-shaped, dorsal edge concave in middle, straight in proximal half, dorso-distal end with concave articular groove, ventral edge strongly convex. Articulated with adradial GP by elongated depression. Almost dorsoventrally horizontal, only slightly downward slanting. Dorsal surface with radiating striations, ventral surface without.

Oral shields

Oral shield with distal lobe, to which at either side an oral GP attaches. Madreporite bulging in centre, with large central opening.

Radial shield

Large distal condyle, bordered by curved groove, proximal to condyle a kidney-shaped patch of smooth, finer meshed stereom.

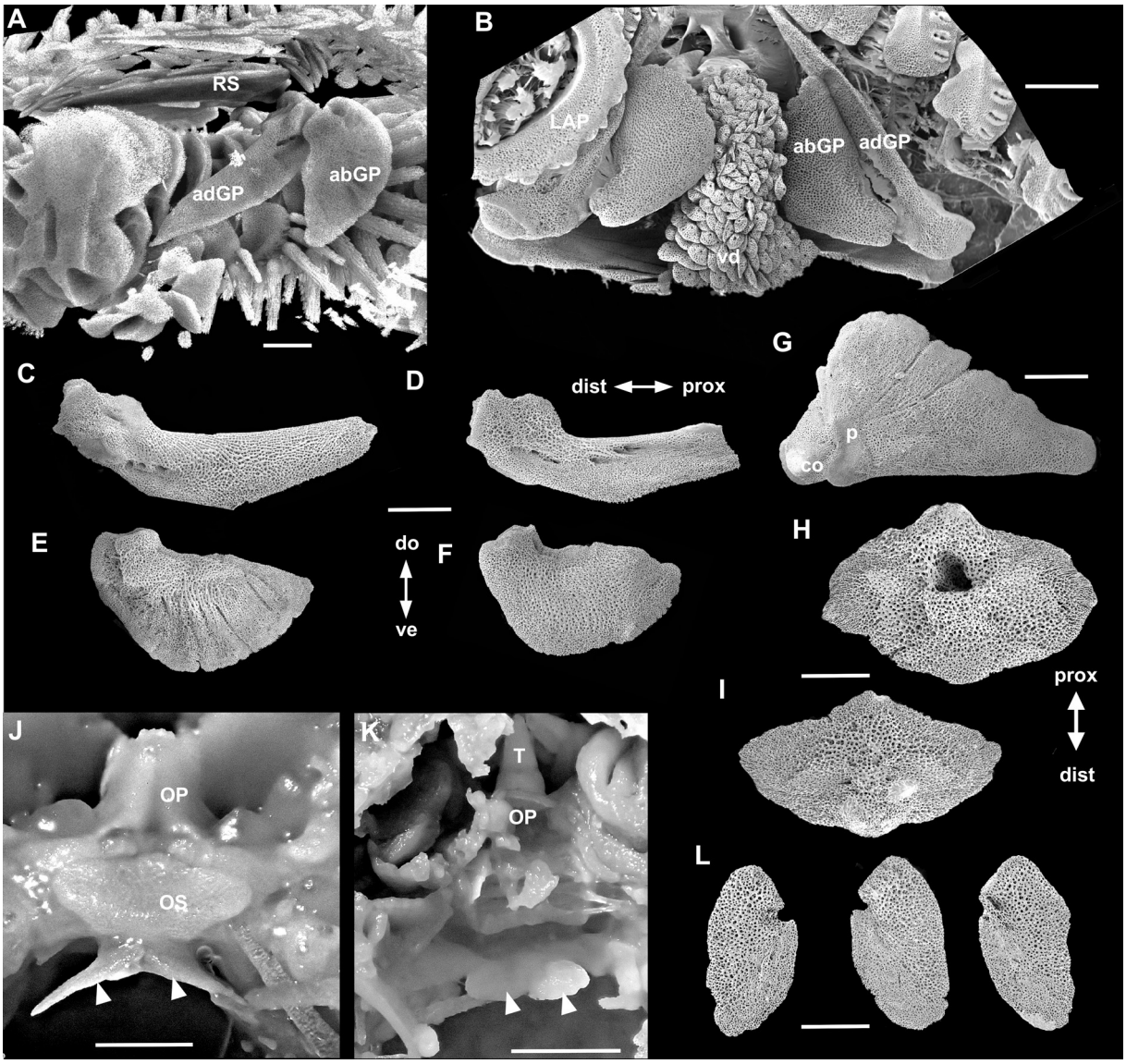

Fig. 29. Ophiotrichidae Ljungman, 1867, *Ophiothrix fragilis* (Abildgaard in O.F. Müller, 1789), SEM, unless otherwise noted. **A**. Genital plates and radial shield inside disc, micro-CT. **B**. Genital plates in situ, ventral aspect. **C**. adGP, abradial aspect. **D**. adGP, adradial aspect. **E**. abGP, abradial aspect. **F**. abGP, adradial aspect. **G**. Radial shield, internal aspect. **H**. Madreporite, internal aspect. **I**. Oral shield, internal aspect. **J**. oGP (arrowheads) in situ, ventral aspect, digital image. **K**. Same, internal dorsal aspect. **L**. oGP. Scale bars: A–G, J–K = 1 mm; H–I, L = 0.5 mm.

Remarks

In *Ophiothrix*, the oral GP are more obvious than in most other here examined genera, strong and large plates, in contrast to the small, thin scales covering the soft ventral disc.

Family Ophiothamnidae O'Hara, Stöhr, Hugall, Thuy & Martynov, 2018

Genus ***Histampica*** A.M. Clark, 1970
Fig. 30

Type species

Amphiactis umbonata Matsumoto, 1915.

Examined species

Histampica duplicata (Lyman, 1875).

Oral GP

Oval scales, widely separated under OS, not visible externally.

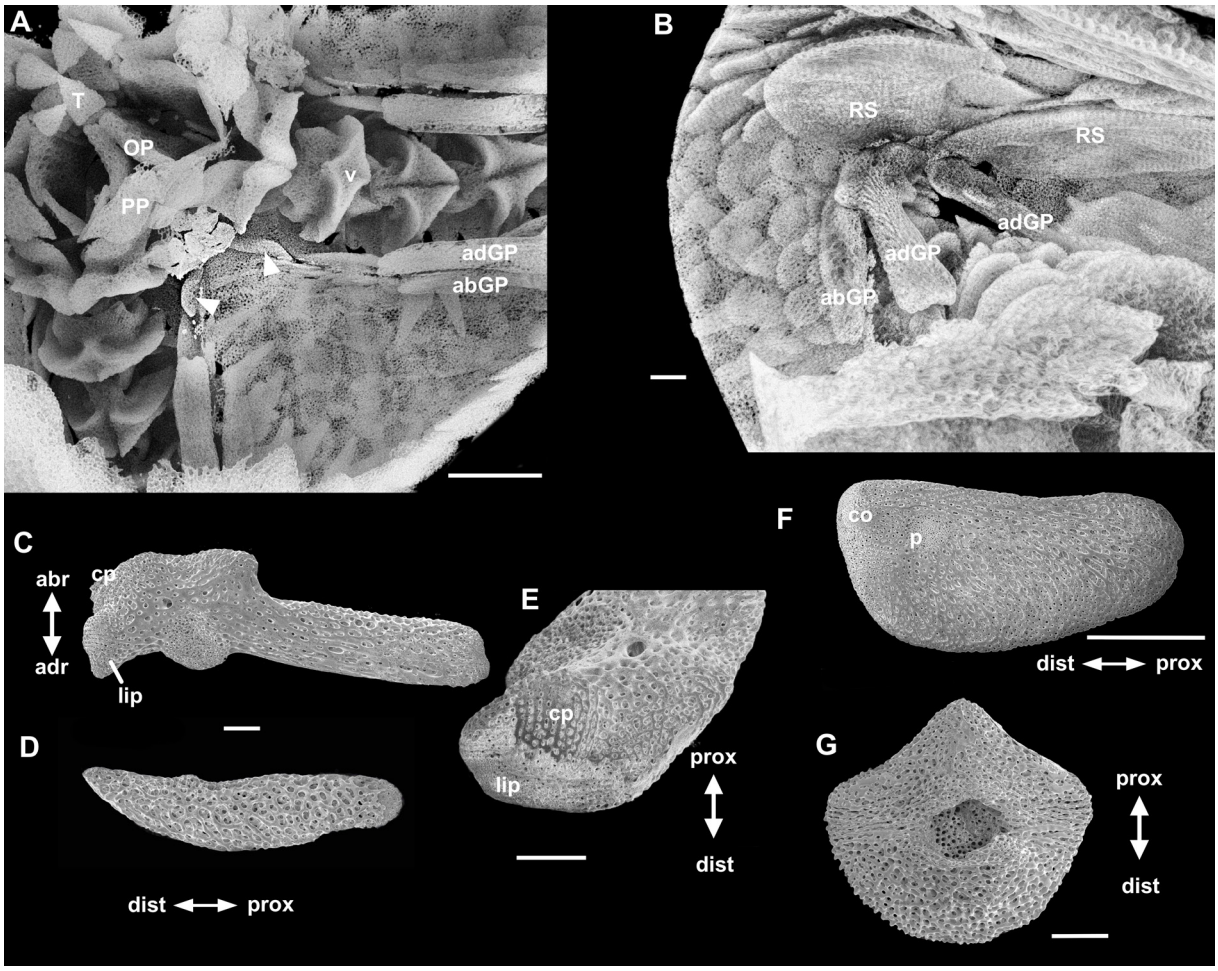

Fig. 30. Ophiothamnidae O'Hara, Stöhr, Hugall, Thuy & Martynov, 2018, *Histampica duplicata* (Lyman, 1875). **A–B**. Micro CT, all others SEM. **A**. oGP (arrowheads) in situ, internal dorsal aspect. **B**. Genital plates in situ. **C**. adGP. **D**. abGP. **E**. adGP, distal end. **F**. Radial shield, internal aspect. **G**. Madreporite, internal aspect. Scale bars: A, F = 0.5 mm; B–E, G = 0.1 mm.

Adradial GP

Bar-like narrow, flat shaft, distal end with condylar process and lip-like extension adradialwards, both connecting to condyles on RS. Proximal to condylar process on abradial edge a lateral process with flat surface, at adradial edge a larger flat process articulating with abGP. Distal adradial end somewhat wrench-shaped.

Abradial GP

Thin, flat, blade-like, abradial edge convex, adradial edge straight, distal end pointed. Articular structure a weakly offset distal part of adradial edge.

Oral shields

No special structures. Madreporite domed in centre with large opening.

Radial shield

Inner side with two low distal condyles, proximal to them a patch of finer stereom, no groove or ledge.

Suborder Ophiopsilina Matsumoto, 1915
Superfamily Ophiopsiloidea Matsumoto, 1915
Family Ophiopsilidae Matsumoto, 1915

Genus ***Ophiopsila*** Forbes, 1843
Fig. 31

Type species

Ophiopsila aranea Forbes, 1843.

Examined species

Ophiopsila guineensis Koehler, 1914.

Oral GP

Flat, elongated, bar-like. V-shaped pair distally at oral shield, meeting row of similar scales continuing to abGP along abradial edge of genital slit.

Adradial GP

Long, rod-like shaft, distally inflated. Single condyle bordered by shallow groove. As long as five arm segments.

Abradial GP

Sabre-shaped, flat. Distal edge straight with simple articular surface. Shorter than adGP.

Oral shields

Oral shield inner side with two knob-like median spurs and proximally thickened. Madreporite externally with two lateral rows of multiple hydropores, inner side thickened, with large opening in distal part, spurs less expressed than in OS.

Radial shield

Inner side with large distal condyle, bordered by groove, proximal to condyle a round patch of denser stereom.

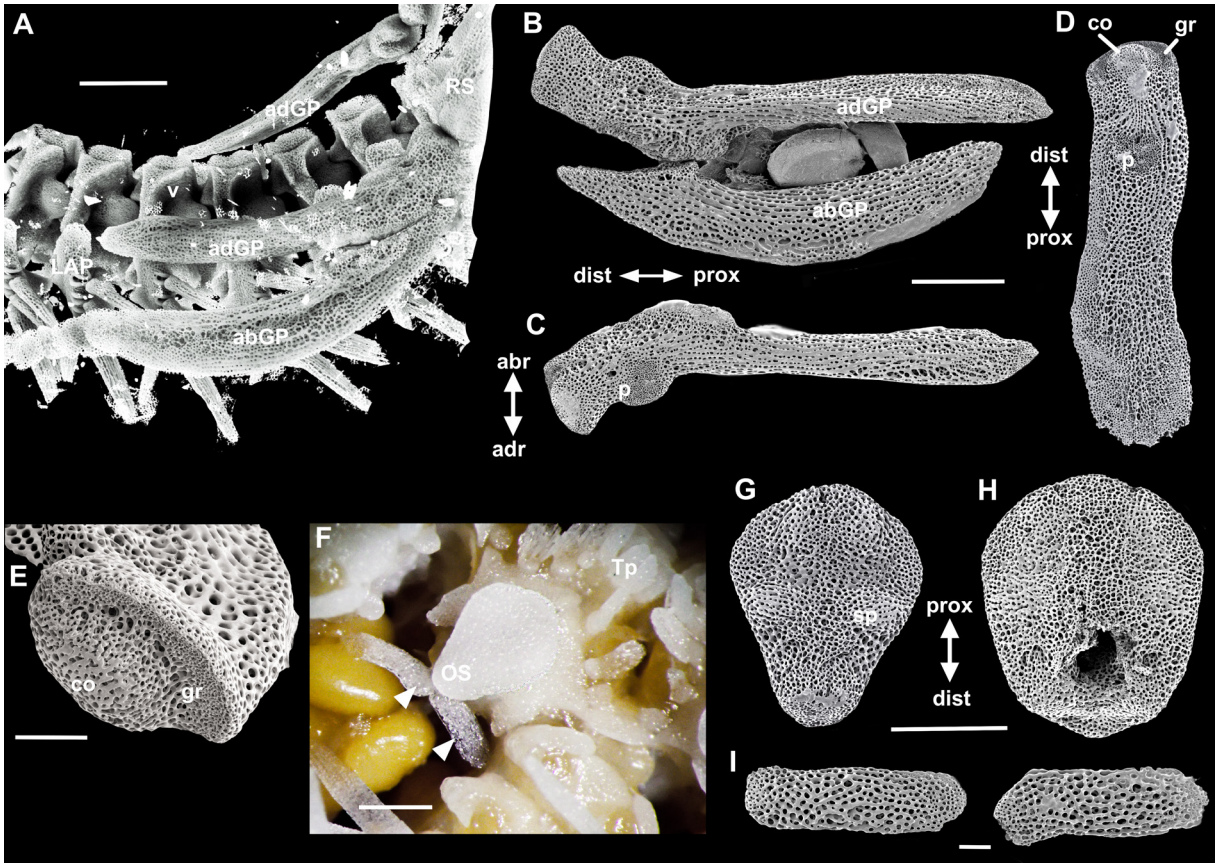

Fig. 31. Ophiopsilidae Matsumoto, 1915, *Ophiopsila guineensis* Koehler, 1914, SEM, unless otherwise noted. **A**. Genital plates in situ, micro-CT. **B**. Articulated adGP and abGP. **C**. adGP, adradial aspect. **D**. Radial shield, inner aspect. **E**. adGP, articular structures. **F**. oGP in situ, bleached, digital image. **G**. Oral shield, inner aspect. **H**. Madreporite, inner aspect. **I**. oGP. Scale bars: A–D, F–H = 0.5 mm; E, I = 0.1 mm.

Order Amphilepidida O'Hara, Hugall, Thuy, Stöhr & Martynov, 2017
Family incertae sedis

Genus ***Ophiopus*** Ljungman, 1867
Fig. 32A–E

Type species

Ophiopus arcticus Ljungman, 1867.

Examined species

Ophiopus arcticus.

Oral GP

Absent.

Adradial GP

Wrench-shaped adradio-dorsal distal end, single flat distal condyle bordered by groove, separated from round process by deep incision, process finer meshed on adradial side. Proximal half bar-like, with longitudinal groove in abradial surface. On abradial side a longitudinal groove.

Abradial GP

Absent.

Oral shields

Inner side in distal half laterally thinner with smoother, finer porous stereom. Madreporite inner side with large centrodistal opening.

Radial shield

Articular structure a low condyle and groove, large round patch of finer stereom proximal to condyle.

Remarks

Ophiopus arcticus lacks genital slits, which may explain the absence of oral GP and abradial GP.

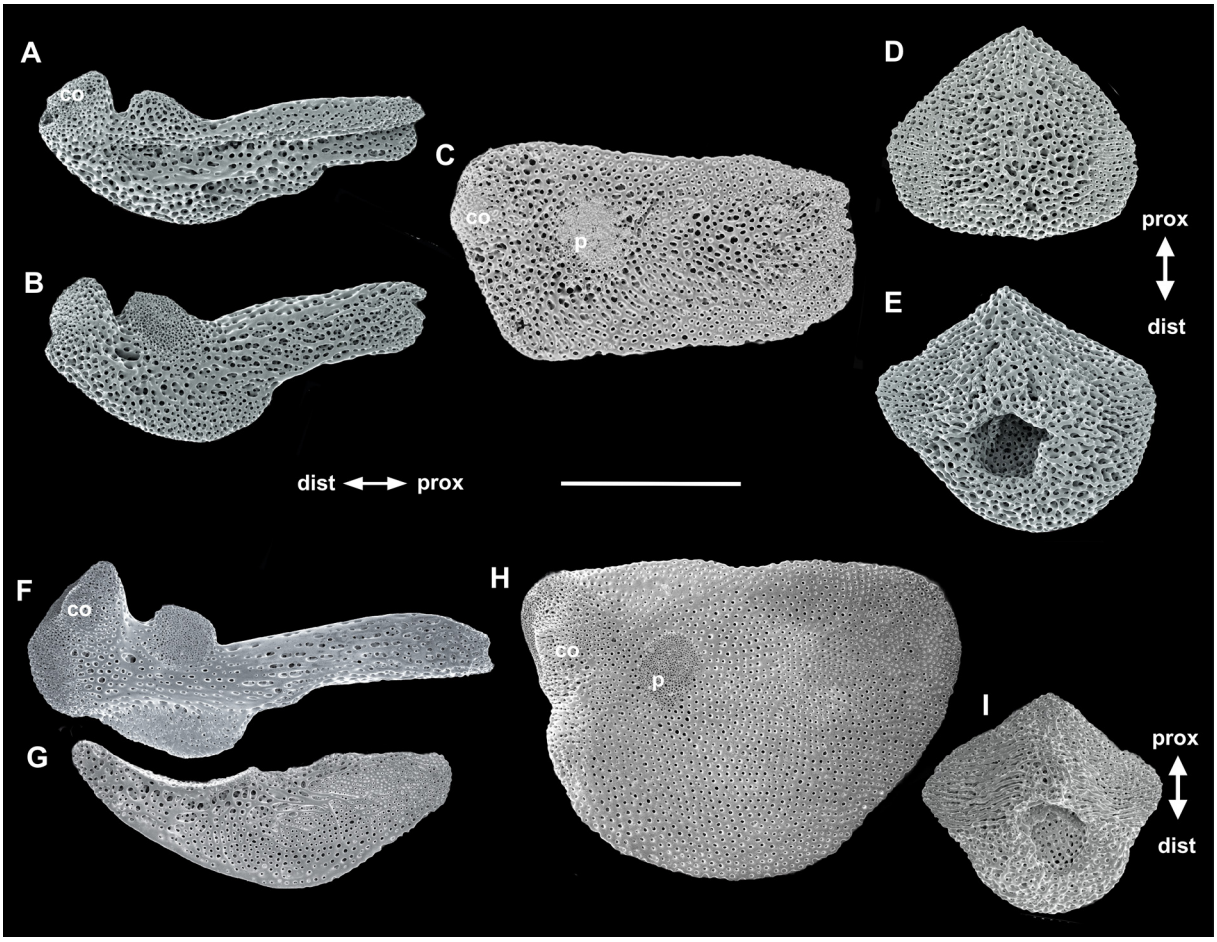

Fig. 32. Amphilepidida O'Hara, Hugall, Thuy, Stöhr & Martynov, 2017, family incertae sedis, SEM images. **A–E**. *Ophiopus arcticus* Ljungman, 1867. **A**. adGP, abradial aspect. **B**. adGP, adradial aspect. **C**. Radial shield, inner aspect. **D**. Oral shield, inner aspect. **E**. Madreporite, inner aspect. **F–I**. *Ophienigma spinilimbatum* Stöhr & Segonzac, 2005. **F**. adGP, adradial aspect. **G**. abGP. **H**. Radial shield, inner aspect. **I**. Madreporite, inner aspect. Scale bar: A–I = 0.5 mm.

Genus ***Ophienigma*** Stöhr & Segonzac, 2005
Fig. 32F–I

Type species

Ophienigma spinilimbatum Stöhr & Segonzac, 2005.

Examined species

Ophienigma spinilimbatum.

Oral GP

Not examined.

Adradial GP

Wrench-shaped adradio-dorsal distal end (condyle separated from process by deep incision), single condyle bordered by shallow groove.

Abradial GP

Sickle-shaped, flat, distally with concave articular structure, almost as long as adGP.

Oral shields

Madreporite with large centrodistal opening.

Radial shield

Single condyle and shallow groove. Patch of finer meshed stereom proximal to condyle.

Remarks

The genital plates and madreporites of *Ophienigma spinilimbatum* and *Ophiopus arcticus* show great similarity, which suggests that they are most likely closely related. The wrench shape of the adradial GP is also shared with *Ophiactis*.

Order Ophioleucida O'Hara, Hugall, Thuy, Stöhr & Martynov, 2017
Family Ophiernidae O'Hara, Stöhr, Hugall, Thuy & Martynov, 2018

Genus ***Ophiernus*** Lyman, 1878
Fig. 33

Type species

Ophiernus vallincola Lyman, 1878.

Examined species

Ophiernus vallincola.

Oral GP

Not recognized among disc scales, may be absent.

Adradial GP

Long, narrow, bar-like, distal end slightly wider, with triangular process at ventro-abradial edge, ending in single condyle and curved groove with high edge.

Abradial GP

Blade-like flat, straight, articular structure slightly concave part on dorso-distal edge. More than half as long as adGP.

Oral shields

Coarse inner side, middle slightly thicker, madreporite with lateral pore in central part.

Radial shield

Articular structure with several minute spurs in middle of distal edge. No obvious muscle attachment patch on inner side.

Remarks

The ventral disc of *O. vallincola* is covered by delicate thin scales, embedded in thick skin. The oral shields distally overlay several scales, but none of them appeared to articulate with the oral shield. Oral genital plates may thus be reduced and are considered absent for now. External examination of species of *Ophioleuce* Koehler, 1904 suggests that oGP may be present in the shape of thin, elongated scales at the proximal end of the genital slit, abutting the oral shield distolaterally, but this needs to be verified when material for maceration is available.

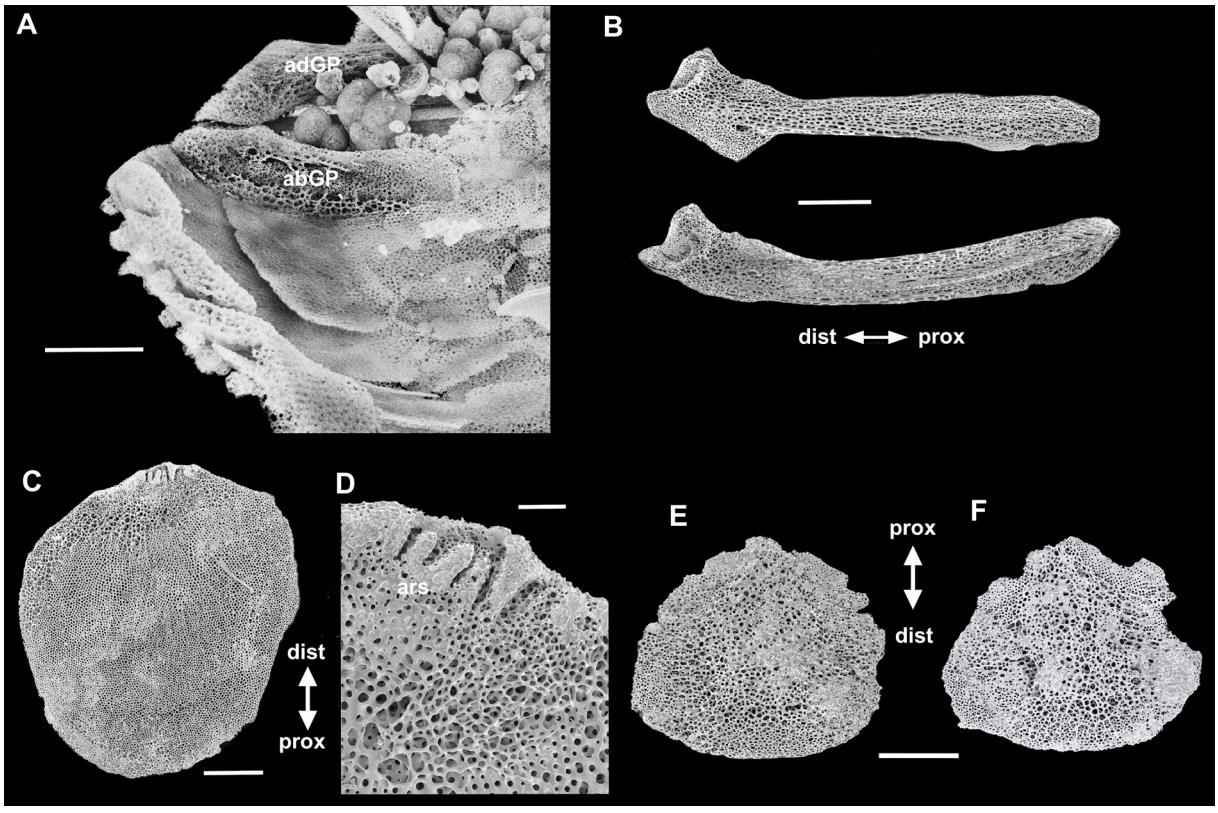

Fig. 33. Ophiernidae O'Hara, Stöhr, Hugall, Thuy & Martynov, 2018, *Ophiernus vallincola* Lyman, 1878, SEM, unless otherwise noted. **A**. Genital plates in situ, adGP distally cut off during scan, micro-CT. **B**. adGP, lateral aspects. **C**. Radial shield, inner aspect. **D**. Same, close-up of articular structures. **E**. Oral shield, inner aspect. **F**. Madreporite, inner aspect. Scale bars: A–C, E–F = 0.5 mm; D = 0.1 mm.

Family Ophioleucidae Matsumoto, 1915

Genus ***Ophiopallas*** Koehler, 1904
Fig. 34

Type species

Ophiopallas paradoxa Koehler, 1904.

Examined species

Ophiopallas paradoxa.

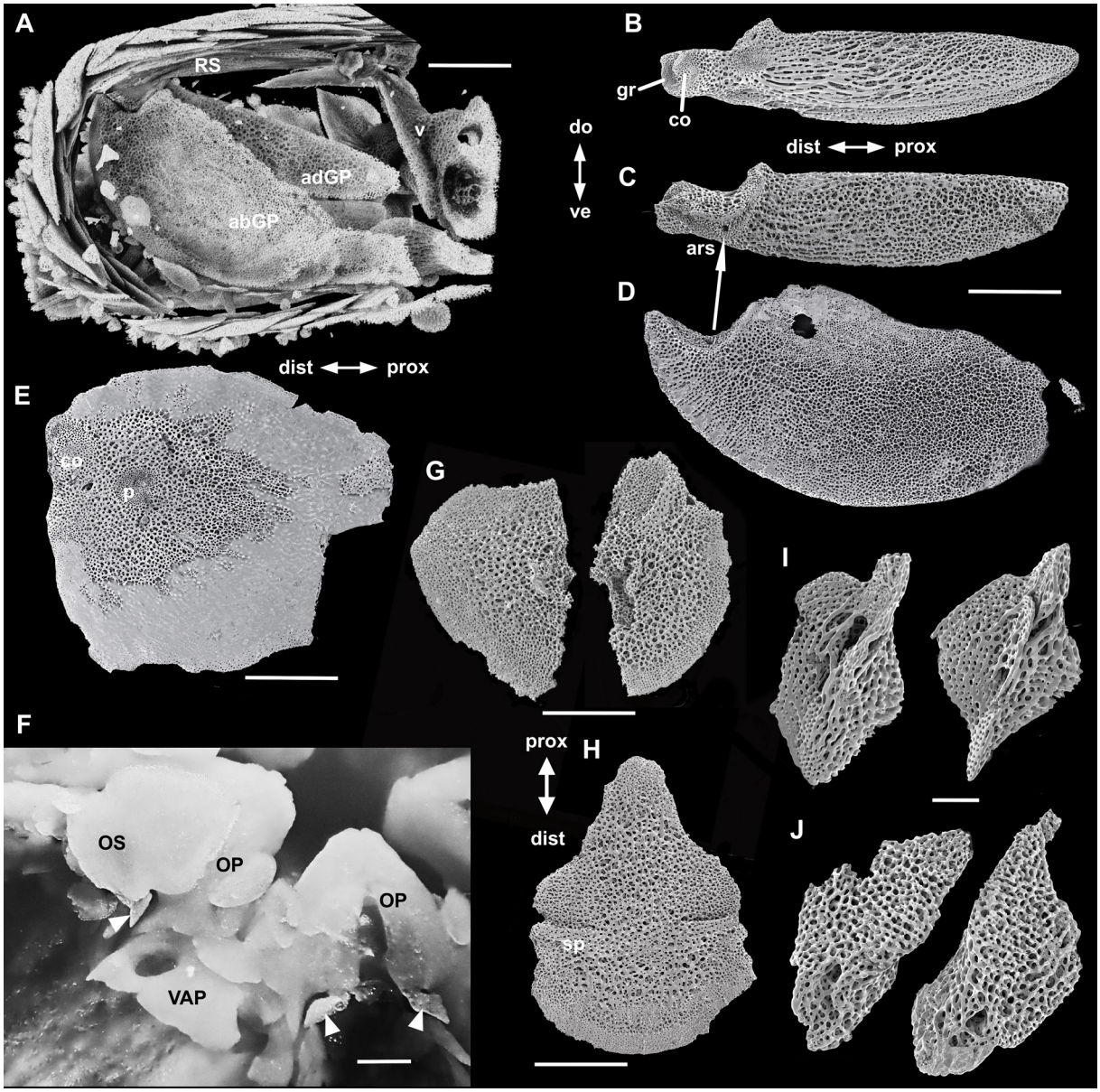

Fig. 34. Ophioleucidae Matsumoto, 1915, *Ophiopallas paradoxa* Koehler, 1904*,* SEM, unless otherwise noted. **A**. Genital plates in situ, micro-CT. **B**. adGP, adradial aspect. **C**. adGP, abradial aspect. **D**. abGP, arrow connects articular structures to adGP. **E**. Radial shield, internal aspect. **F**. Oral GP (arrowheads) in situ, digital image. **G**. Madreporite, internal aspect (broken during bleaching). **H**. Oral shield, internal aspect. **I**. oGP, abradial aspect. **J**. oGP, adradial aspect. Scale bars: A–H = 0.5 mm; I–J = 0.01 mm.

Oral GP

Minute, at laterodistal edges of OS, also connected to adoral shield, adradial surface flat, abradial side with longitudinal median keel-like ridge.

Adradial GP

Blade-like, ventrally convex, dorsally straight edge, pointed proximal end, scoop-shaped distal end, terminating in curved groove and single condyle, on adradial side proximal to articular structures a finer stereom patch, on abradial distal end sickle-shaped ridge articulating with abGP.

Abradial GP

Wide flat blade, as long as adGP, twice as wide, distal articular structure as concave notch.

Oral shields

Flat, with horizontal spurs dividing OS in proximal and distal halves. Madreporite flat, with central large opening.

Radial shield

Single low condyle bordered by short distal groove. Proximal to condyle a round, finely porous patch on a larger, coarsely meshed area.

Early ontogeny (Fig. 35)

Ophiura sarsii: genital plates are present at a disc diameter of under 1 mm, at 1.12 mm dd the adGP is conical with flat distal end, the abGP is rounded triangular, both are larger and more defined at 1.4 mm dd. In juveniles of about 3 mm dd, both GPs are equal in length.

Ophiomusa lymani: at 2.4 mm dd, the adGP is elongated flat and weakly s-curved; the abGP is a flat round scale.

Amphiophiura convexa (Lyman, 1878): at 3.2 mm dd, the adGP is conical with a wide, flat distal surface; the cup-shaped abGP is about the same size as the adGP.

Amphipholis squamata: genital plates are present at a disc diameter less than 1 mm, at 1.12 mm dd the adGP is curved, flat, distally thicker and widened, specific articular structures cannot be identified.

Remarks

Oral GPs have not been identified in small juveniles.

Information from fossils (Fig. 36)

Aganaster gregarius (Meek & Worthen, 1869) (Ophiurina incertae sedis), Early Carboniferous: adGP cleaver-shaped, long, bar-like proximal part with widened distal third, distal abradial edge broadened and flat. abGP absent or perhaps fused to adGP. Articular structures with one or two condyles. RS inner side, abGP and oGP unknown.

Aplocoma agassizi (von Münster, 1839) (Ophiacanthida incertae sedis), Late Triassic: adGP long club-like, distal end curving dorsalwards. abGP blade-like flat, almost as long as adGP, inserting at distal end of adGP. Articular structures with at least one low condyle and a groove. RS with two condyles, larger distally bordered by curved groove, a muscle attachment patch of denser stereom proximal to condyle. Oral GP unknown.

Palaeocoma milleri (Phillips, 1829) (Ophiopyrgidae?), Middle Triassic to Early Jurassic: adGP club-shaped with long, rod-like proximal part, inflated distal part angling dorsalwards. Articular structures possibly with one or two condyles, and a patch or process proximal to inflated end. abGP cup-shaped, exposed distally, bearing large, flat, rectangular papillae forming an arm comb.

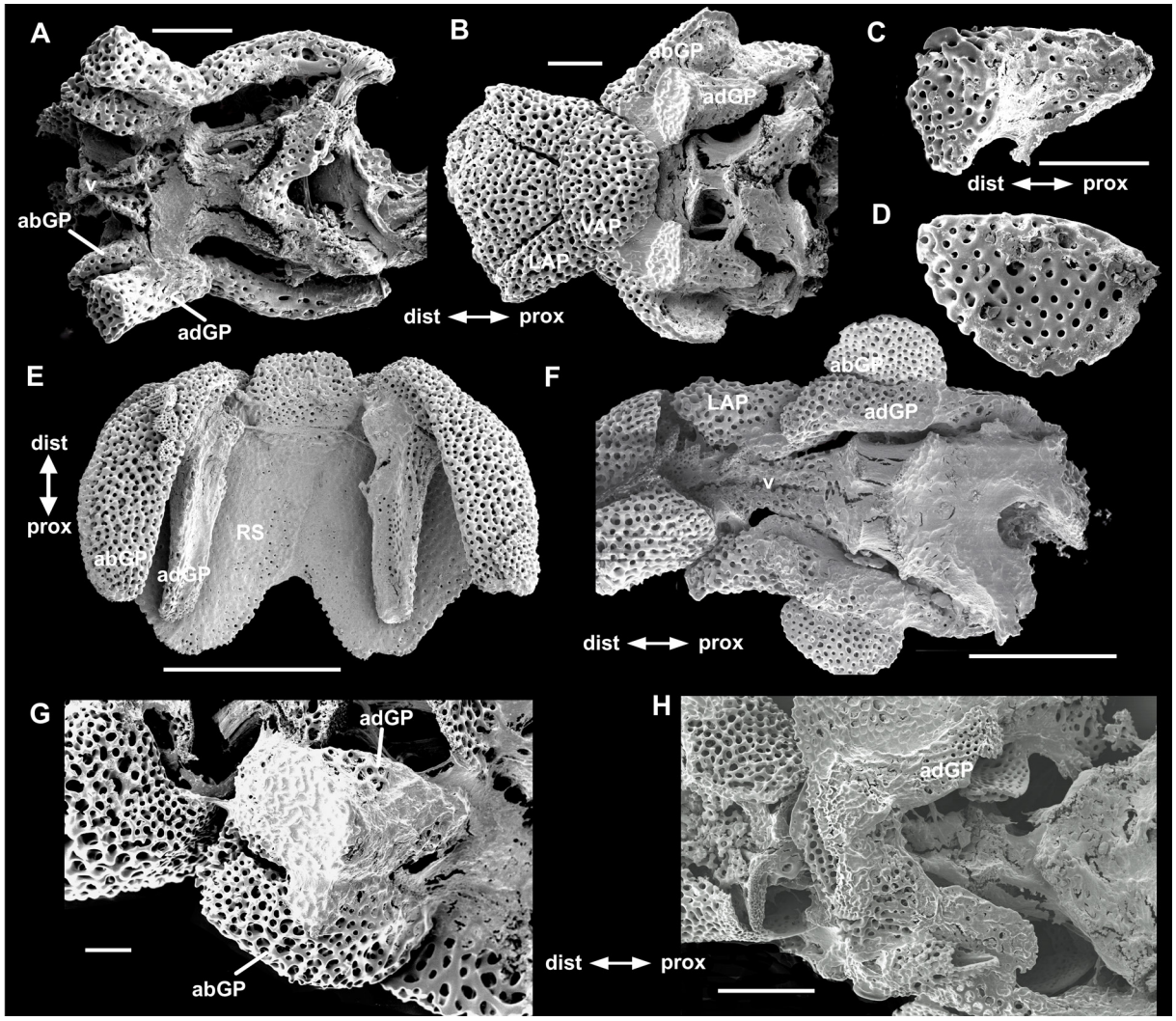

Fig. 35. Genital plates in early developmental stages (postlarvae) of brittle stars. SEM images. **A–E**. *Ophiura sarsii* Lütken, 1855. **A**. 1.12 mm dd, genital plates in situ. **B**. 1.4 mm dd, genital plates in situ. **C**. adGP at 1.4 mm dd. **D**. abGP at 1.4 mm dd. **E**. 3 mm dd, adGP, abGP and RS articulated. **F**. *Ophiomusa lymani* (Wyville-Thomson, 1873), 2.4 mm dd, genital plates in situ. **G**. *Amphiophiura convexa* (Lyman, 1878), 3.2 mm dd, genital plates in situ. **H**. *Amphipholis squamata* (Delle Chiaje, 1828), 1. 2 mm dd, genital plates in situ. Scale bars: A–D, G–H = 0.1 mm; E–F = 0.5 mm.

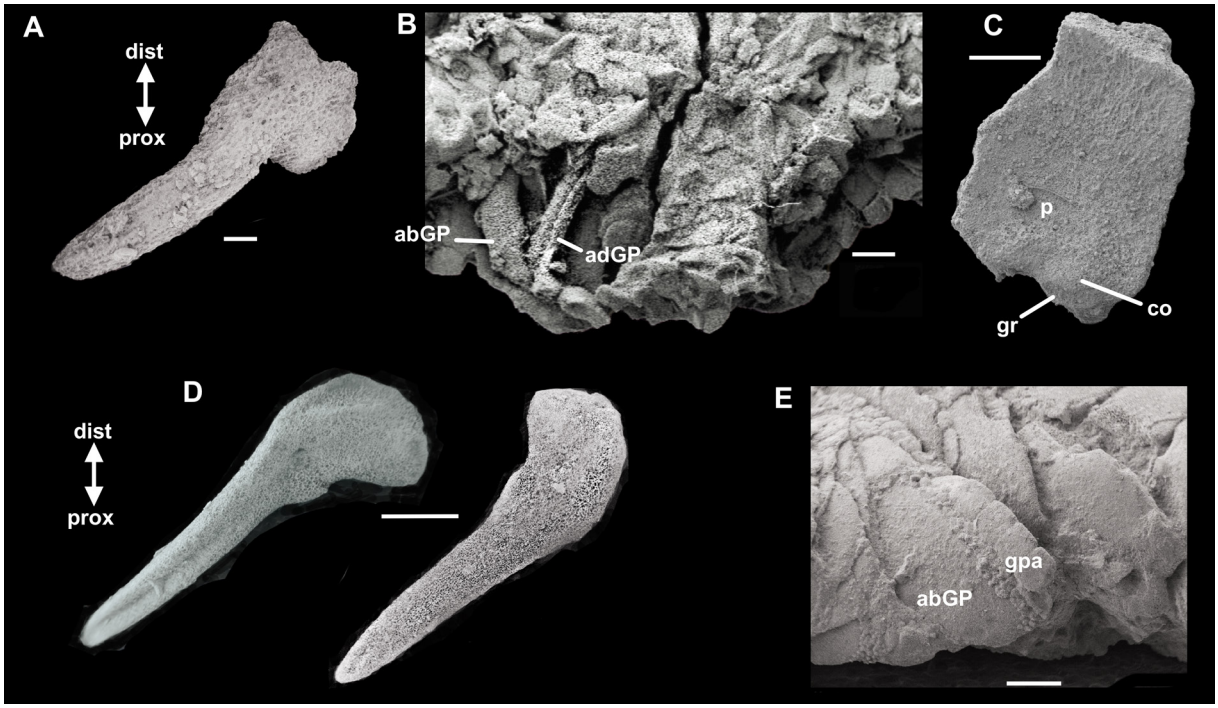

Fig. 36. Genital plates in fossil brittle stars. SEM images. **A**. *Aganaster gregarious* (Meek & Worthen, 1869), adGP. **B–C**. *Aplocoma agassizi* (von Münster, 1839). **B**. adGP and abGP in situ. **C**. Radial shield, internal aspect. **D–E**. *Palaeocoma milleri* (Phillips, 1829). **D**. adGP, different aspects. **E**. Section of ventral disc, showing abGP and genital papillae. Scale bars: A = 0.1 mm; B–C, E = 0.5 mm; D = 1 mm.

Key characteristics of genital plates, madreporites and radial shields

Euryophiurida

- oral GP absent

Ophiurida

- adGP long, bar-like, distally bulbous with two condyles (except *Astrophiura*)
- madreporite inner side with large central opening (not confirmed in *Astrophiura*)

Ophiuridae

- abGP shorter than adGP, cup-like
- RS with two low condyles, one groove

Ophiopyrgidae, Ophiomusaidae

- abGP as long as adGP
- RS with single low condyle, one groove

Astrophiuridae

- adGP flat, condyles reduced
- abGP unknown, may be absent
- RS inner side unknown

Euryalida

Asteronychidae, Gorgonocephalidae

- RS with overlapping scales, easily fragmenting, flat articular structures

Gorgonocephalidae
- adGP bar-like, with bulbous distal end, articular structures large and flat
- abGP articulates proximal to bulbous part or may be fused to adGP
- madreporite inner side a meshwork of lamellae and pores

Asteronychidae
- adGP and abGP fused together, single flat articular structure
- madreporite with two inner openings

Euryalidae
- adGP bar-like, distally inflated, flat articular structures
- abGP elongated half-circle, distally thicker, flat articular structures
- RS without scales, easily fragmenting, bar-like, curved, dorsodistally spatulate, ventrally round and thick, flat articular structures
- madreporite inner side with large openings or network structure

Ophintegrida
- oral GP present (sometimes secondarily lost)

Ophioscolecida
- abGP thin, flat, straight blade-like

Ophioscolecidae
- oral GP oval, thin
- adGP bar-like, with simple flat articular structures
- RS (when present) with simple flat articular structure
- madreporite with large asymmetrical distal opening

Ophiohelidae
- oral GP absent
- adGP thin, flat, straight, blade-like, articular structure weakly domed
- RS absent
- madreporite with small central opening

Ophiacanthida
- madreporite inner side with large opening near distal edge (except in Ophiocamacidae)

Ophiodermatoidea
- oral GP comma-shaped
- abGP half as long as adGP

Ophiodermatidae
- adGP club-like with two condyles
- abGP rectangular, attached to distal bulb of adGP
- RS with two large, low condyles, rough patch in middle

Ophiomyxidae
- adGP bar-like, proximally flattened, no condyles
- abGP blade-like flat, thin, attached at middle of adGP
- RS articular structure a distal, denser stereom patch

Ophiocomoidea/Ophiocomidae
- oral GP flat, short L-shaped
- adGP bar-like, flat, single condyle with spiral groove

- abGP boomerang-shaped
- RS with single low condyle and groove, middle denser stereom patch
- madreporite with additional distolateral wide opening

Ophiacanthina
- oral GP rectangular
- adGP bar-like, distally thickened

Ophiacanthidae
- oral GP with folded edge
- adGP bar-like, distally weakly inflated, with single condyle
- abGP kidney-shaped, thin, half as long as adGP
- RS without articular structures

Ophiocamacidae
- oral GP strongly curved
- adGP bar-like, distally weakly inflated, with single condyle
- abGP blade-like flat
- RS with single condyle and groove
- madreporite inner side with central opening

Ophiotomidae
- oral GP with lobe
- adGP bar-like, distally widened, with two condylar processes
- abGP sickle-shaped

Ophioleucida
- central opening in inner madreporite

Ophiernidae
- adGP bar-like, distal triangular lateral process, single condyle, groove
- abGP flat blade-like, concave articular structure
- RS articular structure as minute spurs

Ophioleucidae
- adGP bar-like, distally scoop-shaped, condyle and curved groove, several stereom patches
- abGP wide blade-like, articular structure concave notch
- RS with low condyle, groove, round rough patch

Amphilepidida
- madreporite inner side with single large opening in varying positions

Incertae sedis (*Ophiopus*, *Ophienigma*)
- oral GP unknown
- adGP wrench-shaped
- abGP sickle-shaped, low condyle
- centro-distal opening in inner madreporite

Ophionereidina
Ophiolepidoidea
- central opening in inner madreporite (unknown in *Hemieuryale*)

Hemieuryalidae
- oral GP possibly large, flat scale (but not examined)
- adGP comma-shaped, articular structures as depression and ledge
- abGP scoop-shaped, articular structure concave (minute or missing in *Hemieuryale*)
- RS articular structures depression, narrow ledge and rough patch

Ophiolepididae
- oral GP oval pyramid-shaped
- adGP cleaver-shaped, articular structures as low condyle and ledge
- abGP rounded scalene triangular, wider than adGP
- RS articular structures embossed distal end, ledge, coarse patch

Ophionereidoidea
- distal opening in inner madreporite

Amphilimnidae
- oral GP rectangular, thin
- adGP bar-like, distal end widened
- abGP twisted s-shaped with proximalwards directed distal appendix
- RS articular structures single flat condyle and groove

Ophionereididae
- oral GP oval, thin
- adGP more or less cleaver-shaped, distal edge widened abradially, distal low condyle
- abGP bar-like, as long as adGP, articular structure straight or concave edge (with distal angle 'hockey-stick shape' in *Ophiochiton*)
- RS with single low condyle

Gnathophiurina
Amphiuroidea
- centro-distal opening in inner madreporite

Amphiuridae
- oral GP rounded comma-shaped or elongated curved, with or without pointed appendix
- adGP distally lobed, with bar-like shank, single condyle and groove
- abGP long sabre-like, thin, with adradial longitudinal rim
- RS with single condyle, curved groove and narrow ledge, oval patch proximal to condyle

Amphilepididae
- oral GP not identified, possibly absent
- adGP bar-like, lateral protrusions, single condyle and groove
- abGP half-circular, thin
- RS with large condyle, wide ledge, smooth patch proximal to condyle

Ophiactoidea
- central opening in inner madreporite

Ophiactidae
- oral GP drop-shaped
- adGP wrench-like, distally wider, but flat, single condyle and groove
- abGP half as long as adGP, sickle-shaped, articular structure a straight distal edge
- RS with condyle and ledge, smooth patch proximal to condyle

Ophiopholidae
- oral GP thin, oval
- adGP bar-like, bulbous distal end, two condyles, lateral ridge
- abGP kidney-shaped, articular structure a groove
- RS with large condyle, long curved groove

Ophiotrichidae
- oral GP thin, oval, distal notch
- adGP bar-like bulbous, domed condyle and ledge
- abGP half-circle, articular structure concave distal edge
- RS with large condyle, curved groove

Ophiothamnidae
- oral GP unknown
- adGP bar-like with bulbous end, condylar process
- abGP thin, flat, blade-like
- RS with low condyle, no groove or ledge

Ophiopsilina
- distal opening in inner madreporite

Ophiopsilidae
- oral GP elongated, narrow, thin
- adGP with single condyle and shallow groove
- abGP sabre-like, simple articular surface

Phylogeny

On the phylogenetic tree (Fig. 37), the modern Ophiuroidea were divided into two large clades, corresponding to Euryophiurida and Ophintegrida (Fig. 38) with 96% support, but *Ophiomusa lymani* was placed outside as an ancient sister group and Euryophiurida was split into two major clades. Within the Ophiurida, *Amphiophiura* and *Ophiopyrgus* formed a clade, and its sister clade contained *Ophiura*, *Ophiocten* and *Ophiopleura*. The relationship of these groups to Euryalida was not resolved and *Palaeocoma milleri* was placed outside of these clades. The Ophintegrida were divided into two major clades (99% support), clade B and Clade C, largely corresponding to Ophiacanthida and Amphilepidida, but with some weakly supported branches. *Ophiernus* was placed outside all other members of clade B. Ophiohelidae and Ophioleucidae were suggested as sister taxa with 96% support, nested inside major Clade D. The relationships between the remaining families currently classified in Ophiacanthida were not fully resolved, and Ophioscolecidae was placed in the same cluster as Ophiotomidae, Ophiocamacidae and Ophiacanthidae. Ophiocomidae formed a well-resolved clade, sister to Ophiodermatidae, with *Ophiarachna* in a weakly supported sister position to *Ophiocoma*. Ophiomyxidae grouped with these, but with low support (54%). In major clade C (Amphilepidida), Ophiolepididae and Hemieuryalidae formed well-supported sister clades. Ophionereididae formed a clade, but the inclusion of *Ophiochiton* had weak support (55%). Amphilepididae and Ophiopsilidae were suggested as close relatives of Amphiuridae. *Ophienigma* and *Ophiopus* formed sister taxa within Ophiactoidea. The genera *Astrophiura* and *Ophiotypa* were left out of the final analysis, because including them resulted in improbable relationships (e.g., *Astrophiura* in Euryalida).

In a test run with all 66 species, but with all characters of the genital plates left out (134 characters remaining), the phylogenetic tree assumed a comb shape (Fig. 39), in which the major clades as well

as most orders and families were no longer recovered. Posterior probabilities were considerably lower than in the analysis of the full matrix. This suggested a strong phylogenetic signal in the genital plates.

Discussion

Form and function

Previous authors (Table 1) considered mainly the articular structures of the adradial and abradial genital plates and the radial shield, rarely mentioning other details. The present study shows that additional phylogenetically informative characters can be found when the overall shape of the plates is included,

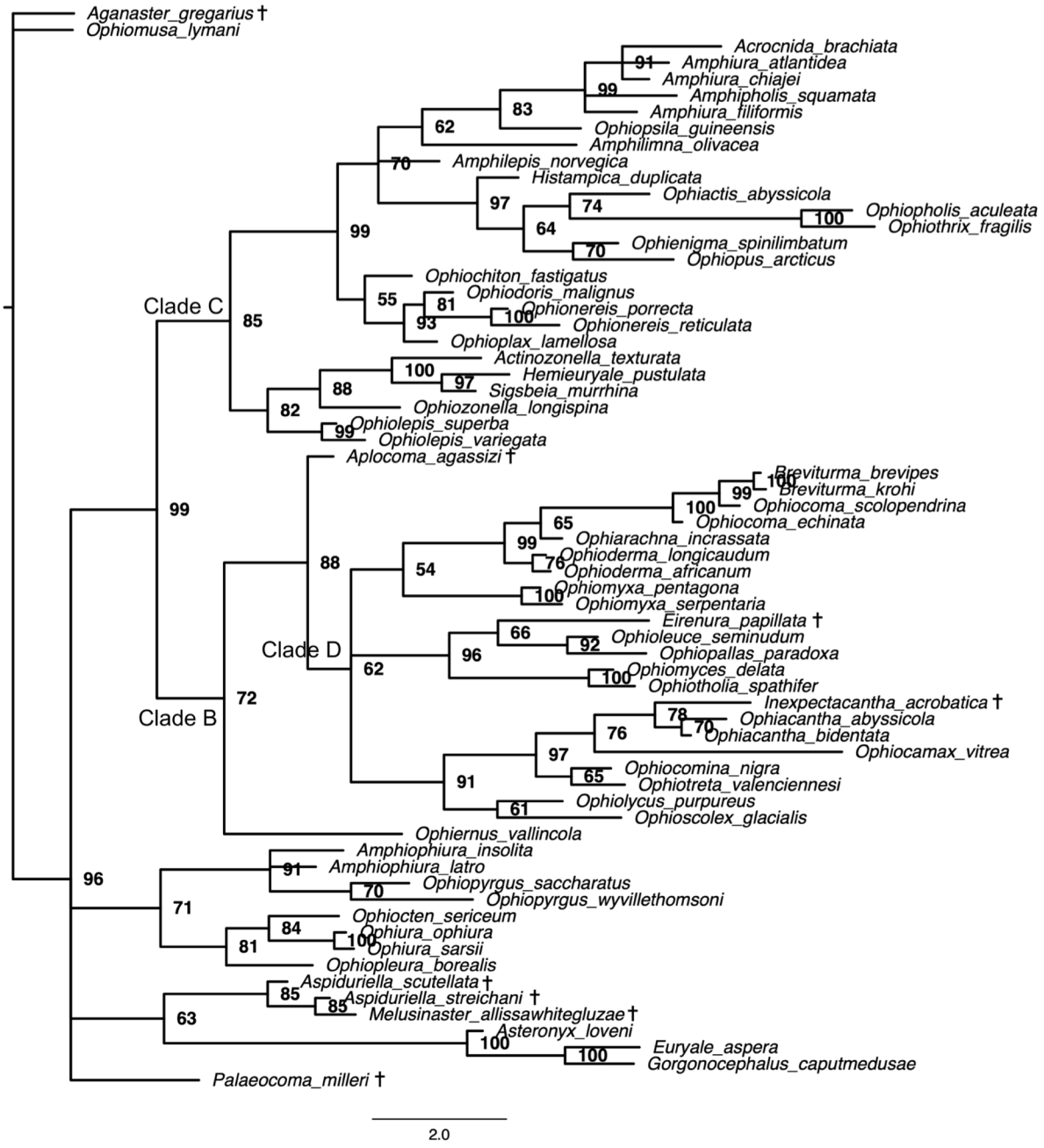

Fig. 37. Bayesian phylogenetic tree, inferred from the morphological character matrix revised in this study. Numbers at nodes represent posterior probabilities. Extinct species are marked with a cross.

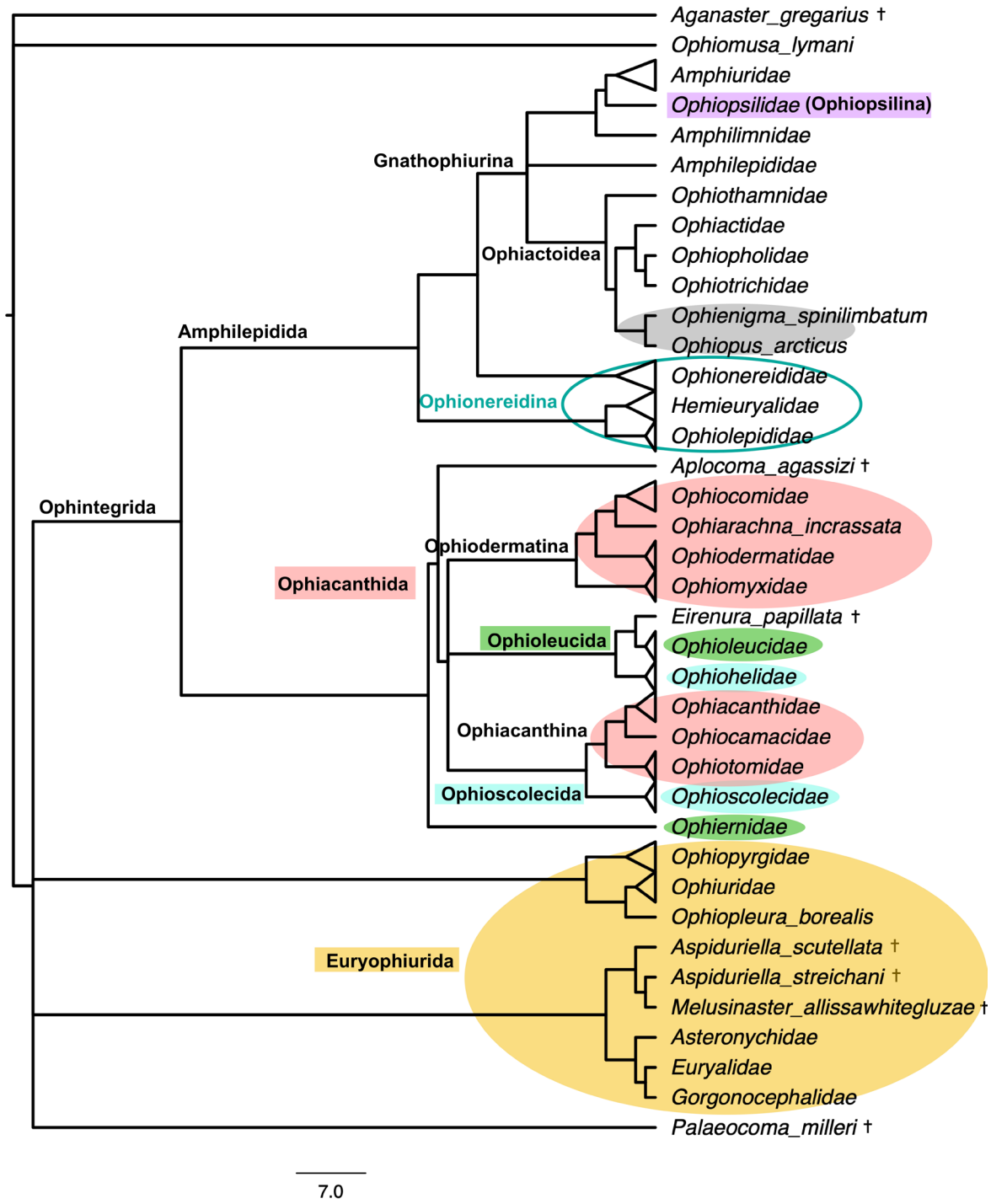

Fig. 38. Same tree as in Fig. 37, clades collapsed into families. Coloured ellipses mark clades that are paraphyletic, compared to the molecular phylogeny in O'Hara *et al*. (2017). Ophiopsilina Matsumoto, 1915 is nested inside Gnathophiurina Matsumoto, 1915, instead of being a sister clade. Ophioleucida Matsumoto, 1915 is in Ophiacanthida O'Hara, Hugall, Thuy, Stöhr & Martynov, 2017 instead of being a sister clade to Amphilepidida O'Hara, Hugall, Thuy, Stöhr & Martynov, 2017. Ophioscolecida O'Hara, Hugall, Thuy, Stöhr & Martynov, 2017 may be a sister clade to Ophiacanthida, but the relationships in this group of clades are unclear. *Ophienigma* Stöhr & Segonzac, 2005 and *Ophiopus* Ljungman, 1867 may constitute a new family. The relationships of Ophiomusaidae O'Hara, Stöhr, Hugall, Thuy & Martynov, 2018 could not be resolved.

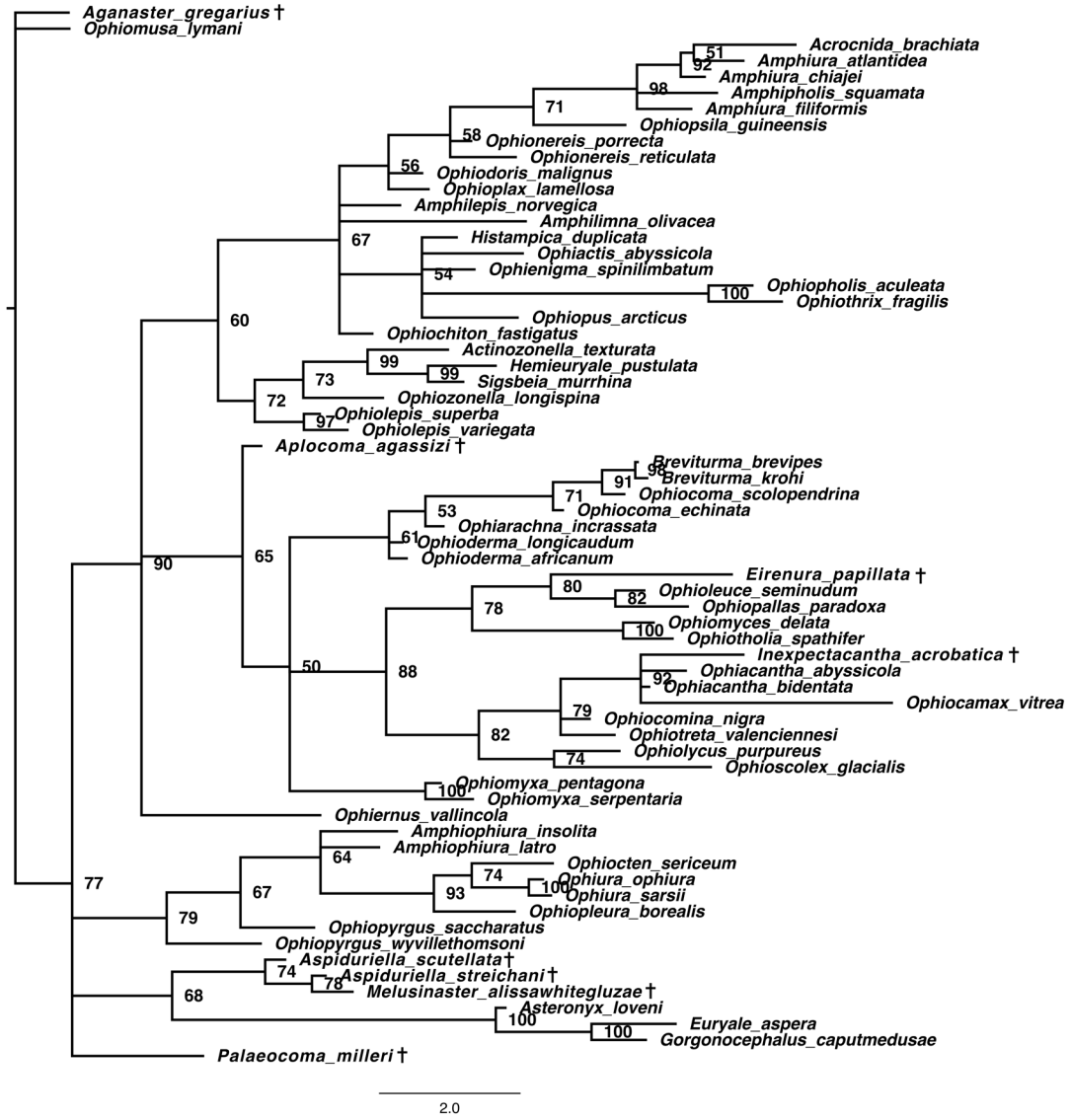

Fig. 39. Bayesian phylogenetic tree, inferred from the same matrix as in figure 37, but with all genital plate characters removed. Numbers at nodes represent posterior probabilities. Extinct species are marked with a cross. The overall structure is more comb-shaped, and most clades are no longer recovered.

and the combination of the plates is also important, e.g., both *Ophiolepis* and *Ophionereis* have similar cleaver-shaped adradial GPs, but they are orientated differently and their abradial GPs differ in shape. Several taxonomic groups have sabre-like abradial GPs, but differ in the adradial GP and/or the oral GP. Matsumoto (1915, 1917) mentioned the presence of scales (here named oral genital plates) at the distal edge of the oral shield in particular in *Ophiothrix*, Amphilepididae, Amphiuridae and generally in Gnathophiurida (Table 1). They are most obvious in *Ophiothrix*/*Macrophiothrix*, but this study shows for the first time that they occur in most other groups as well. They appear to be absent in the Euryophiurida, but present in most here examined Ophintegrida and may be a synapomorphy of the latter, probably secondarily lost in some species.

The observations made in the present study differ somewhat from previous accounts (Table 1). Martynov (2010) described a weakly defined condyle in Ophiacanthidae and the abradial GP as similar in size or slightly smaller than the adradial GP. This was not confirmed here. The articular structures on the radial shield and adradial GP are flat, not domed, which concurs with Matsumoto's (1915, 1917) assessment, whereas the description of Lyman (1882) of the adradial GP as thick and "club-headed" is too unspecific to evaluate. The abradial GP is half as long as the adradial GP in the family type species, *Ophiacantha bidentata*, but about two thirds as long in *Ophiacantha abyssicola*. Likewise, concurring with Matsumoto (1915, 1917), species of *Ophiomyxa* do not possess condyles, contrary to Martynov's (2010) claim that they have a well-defined condyle. It is unclear what his statement of the adGP and abGP being small relates to. The adradial GP of *Ophiomyxa* is at least three arm segments long and the abradial GP is half as long as the adradial GP, attached at a process in the middle of the adGP and indeed presenting the appearance of a "lobster-claw", as Lyman (1882) remarked. Interestingly, the genital plates in *Ophiolycus* are more similar to those of *Ophiomyxa* than to those of *Ophioscolex* (Figs 10–11, 14). In Ophionereididae, Matsumoto (1915, 1917) recorded two condyles, whereas Martynov (2010) mentioned a single condyle, which concurs with the present study. Lyman (1882) believed that the abradial GP in *Ophionereis* continued to the oral shield, which was not confirmed here. Instead, between the abGP and oral GP a connecting row of disc scales was found. Matsumoto (1915, 1917) recorded two condyles in *Ophiopsila*, but the present study found only a single condyle each on the adGP and radial shield. He described the abradial GP as long, narrow and bar-like, which was here refined to sabre-shaped. Some of these differences between historical and modern descriptions can probably be explained by differences in the definition of the observed structures. In the days of Lyman (1882), microscopes may not have had sufficient optical resolution to allow detailed observations, but his illustrations are still remarkably detailed and accurate. For instance, *Asteronyx* was here described as having a flat articular structure on a condylar process on the adradial GP, interpreted by Martynov (2010) as a condyle (summarily described for all Euryalida), but strangely Matsumoto (1915, 1917) mentioned a transverse ridge. In this study, the adGP and abGP in *Asteronyx* were found to be firmly fused together, a condition not mentioned by either of the previous authors (Table 1). Martynov also interpreted the flat articular structures in *Gorgonocephalus* and *Euryale* as condyles, in contrast to Matsumoto (1915, 1917) and the present study. In Hemieuryalidae, the adGP and abGP were described as "soldered" by both Lyman (1882) and Matsumoto (1915, 1917), which may be correct, since Gondim *et al*. (2015) observed only a single genital plate, but this should be verified.

As Lyman (1882) described for *Gorgonocephalus*, radial shields and adradial genital plates work together to expand and contract the disc vertically in a behaviour known as disc pumping, which serves to flush water in and out of the genital slits for respiration (Hainey & Emlet 2020). Previous studies (Table 1) did not observe the mechanics of the joints, and we still know little about this. In *Gorgonocephalus* and *Asteronyx*, the present study found matching patches of stereom at the distal ends of both radial shields and adradial GPs, but the plates seem to connect only at the proximal patch in the animals used for micro-CT, leaving a gap distally. Presumably, expanding and contracting muscle fibres that attach at these patches can move the plates upwards and downwards to expand and contract the disc, thereby changing the place of closest connection between the plates. For many of the species studied here, the 3D-reconstructions from the micro-CT scans showed that the dorsal distal surface of the adradial GP meets the ventral distal surface of the radial shield, whereas muscles connect both plates at their distalmost lateral surfaces, where the condyles and grooves are placed. In species with many protrusions and depressions on the adradial GP, only few of these meet corresponding structures on associated plates (radial shields, abradial GP). In contrast to the joints between arm vertebrae (LeClair 1996; Clark *et al.* 2018), the articulations between radial shields and adradial genital plates are not fitting interlocking structures, and a condyle often meets a condyle, not a depression like in a ball and socket joint. Most of these structures are presumably muscle attachment sites, which should be studied further to better understand the mechanics between genital plates and radial shields. Conversely, the joint between

adradial and abradial genital plate usually consists of corresponding structures, where protrusions meet depressions, and it is unknown how much movement is possible between them.

The inner side of the madreporites was studied here for the first time and taxon specific differences were observed, in contrast to their external characters that were not found to be phylogenetically informative (Ezhova *et al.* 2016). Usually, a large opening is present, but it may be proximal (Amphilepidida), distal (Ophiacanthida) or central (Ophiuridae) and some taxa have evolved unique structures (Euryalida, *Ophiomyces*). However, a larger number of species and genera from each family should be examined to confirm these observations. The oral shields usually lack specific articular structures, and it is often not obvious exactly where they connect to the oral genital plates. There is a considerable variety of shape and size in the oral GPs between the species studied here, which provides taxonomic information. The abradial and oral GPs support the abradial bursal wall, and perhaps the abradial GPs facilitate the opening and closing of the genital slit, but no functional studies have been performed yet. Interestingly, during bleach treatment the oral GPs would remain attached to the oral shield for some time after the disc scales had detached, as can be seen in some of the digital images presented here (Figs 22A, 25K, 27I, 34F). This observation suggests that there is a firmer bond by connective tissue between oral shields and oral GPs, possibly supporting the hypothesis of a genital slit stabilizing function. It doesn't seem likely that the oral GPs are moveable, because there are rarely any articular structures and probably no muscles attached. In some species, abradial GP and oral GP meet or are part of a row of scales; in others, the oral GP is widely separated from the abradial GP. Species that lack bursae are either small enough for oxygen to diffuse through the tissues or possess other compensating adaptations, such as the presence of haemoglobin in the body fluid and Simroth appendages in *Hemipholis elongata* (Say, 1825) (Christensen & Colacino 2000). Among the species examined here, *Ophiopus arcticus* and *Ophiotypa simplex* completely lack genital slits, and they possess only adradial GPs that articulate with the radial shields, which could be an indication of a different primary function of these two ossicles than support of the genital slit or respiration. They may provide structure and stability to the disc, which may be deduced from species that lack radial shields such as *Ophiomyces*, where both genital plates are of identical shape and support the genital slit, whereas the disc is soft and dorsally high conical. The absence of abradial and oral GPs in *O. arcticus* and *O. simplex* may suggest that these are related to the genital slit and have no function without it. In contrast, loss of the radial shields (e.g., *Ophioscolex glacialis*, *Ophiomyces*, *Ophiotholia*) does not lead to a loss of the adradial GP, suggesting that it has another function besides expansion and contraction of the disc. The absence of oral GPs in Euryophiurida is here considered a plesiomorphy, but it is unknown whether their ancestor possessed these. In Euryalida, genital slits are often small openings that may not need additional support, apart from the often large abradial GPs. Ophiurida generally have strong disc scales that may serve to support the genital slit, and in some Ophiopyrgidae, Ophiomusaidae and Ophiosphalmidae, the abradial GP is strong and part of the ventral disc, not covered by scales.

The early ontogeny of the radial plates, oral shields and madreporites has been observed in a wide range of species by studying postmetamorphic juveniles (Schoener 1967, 1969; Sumida *et al.* 1998; Stöhr 2005), but the development of the genital plates has so far rarely been examined (Hendler 1978), and no morphological characters on these have been documented in a juvenile stage. The adradial and abradial genital plates are discernible in animals with a disc diameter less than 1 mm (this study; Hendler 1978) and can be assumed to begin to develop much earlier. Likewise, in studies of presumably paedomorphic ophiuroid species, genital plates have not been treated yet (Vadon 1988; Stöhr & Martynov 2016). The juvenile or paedomorphic condition may provide clues to the evolution of these structures. Oral shields and madreporites have been suggested to be homologous to disc scales, since they first appear at the dorso-distal disc edge and migrate to the mouth during development (Ludwig 1888; Stöhr 2005). The madreporite appears earlier in ontogeny than the other oral shields, e.g., in *Ophiopleura borealis* and other species (Stöhr 2005).

Phylogeny

The inferred tree was similar to the tree in Thuy & Stöhr (2016), suggesting the same major clades that correspond to the superorders Euryophiurida (although with unresolved common origin) and Ophintegrida, and it recognizes the orders Euryalida, Ophiurida, and Amphilepidida, but the Ophiacanthida (Fig. 38) were either split in two separate clades or included the Ophioleucida. In addition, Ophioleucida was paraphyletic for *Ophiernus* compared to the molecular hypothesis (O'Hara *et al.* 2017; Christodoulou *et al.* 2019). The order Ophioscolecida was placed as sister taxon to the suborder Ophiacanthina. The outlier position of Ophiomusaidae was already observed in the original phylogeny of Thuy & Stöhr (2016) and is most likely caused by the unique morphology of the genus *Ophiomusa*. This was recently remedied by the inclusion of additional fossils (Thuy *et al.* 2021), which were not available for this study. However, the fossil data are highly incomplete (relying heavily on lateral arm plates) and introduce a large amount of missing data that can affect the accuracy of Bayesian phylogenetic inference (King 2019). Complete datasets from additional extant species of *Ophiomusa* and *Ophiosphalma* may be needed to reliably recover their position on the tree. Likewise, test runs that included taxa with a strongly modified morphology and many missing structures (*Astrophiura*, *Ophiotypa*) resulted in poorly resolved trees, probably in part caused by the large number of missing characters and superficial similarity to unrelated taxa (e.g., *Astrophiura* was inferred as sister clade to Euryalida, but with low support). The analysis seems to be biased towards the characters for which data are present for all species, which can potentially result in false support for some clades.

Compared to the current classification, Ophiopyrgidae were paraphyletic on the tree, because *Ophiopleura borealis* differs morphologically from *Amphiophiura* and *Ophiopyrgus*, particularly in the genital plates, the thickened skin on the disc (although this character was omitted here) and the long radial shields. In general, morphologically heterogeneous families that include species with multiple losses of morphological features (e.g., Ophiomyxidae, Ophiopyrgidae, Hemieuryalidae) are difficult to recover in a purely morphological phylogenetic inference. For Hemieuryalidae, the addition of more species succeeded in recovering the clade. A key synapomorphy for the superfamily Ophiolepidoidea (Hemieuryalidae + Ophiolepididae) was the presence of accessory dorsal arm plates on at least the most proximal arm segments (newly added character).

Amphilimnidae was placed in the suborder Gnathophiurina, close to Amphilepididae and Amphiuridae, whereas the current classification (O'Hara *et al.* 2018) includes it in the superfamily Ophionereidoidea. Its specialised genital plates and wing-like proximal lateral arm plates lack similarity with those of any other taxon. Likewise, Ophiopsilidae (suborder Ophiopsilina) was suggested as sister taxon to Amphiuridae, a position that it has maintained through several attempts at refining the matrix (Thuy & Stöhr 2016; Thuy *et al.* 2021, 2023). Adding characters of genital plates has not changed the phylogenetic inference for these taxa and it is unclear whether the reason may be unrecognized homoplasy, insufficient character evaluation or the results are accurate and the molecular tree needs to be revised. *Ophiopsila* and *Amphiura* share similar abradial and adradial GPs, and although the oral genital plate of *A. chiajei* is quite different, the oral GP of *A. filiformis* is similar to that of *Ophiopsila*. Neither has the refinement of the oral characters based on Hendler's (2018) work changed the position of Ophiopsilidae on the tree; on the contrary, prior probability has increased from originally 56% (Thuy & Stöhr 2016) to 83% in support of it being the sister taxon of Amphiuridae. Still, its inclusion in Amphilepidida is closer to the current classification than its previous placement in Ophiocomidae (order Ophiacanthida) on account of its numerous tooth papillae (Smith *et al.* 1995), a character that is homoplasious and should probably be refined to describe the shape of the tooth papillae instead, or with a more precise separation of the number of papillae (in the dataset revised here, the number of tooth papillae is scored as "2" or ">2"). Interestingly, the genera *Ophienigma* and *Ophiopus*, which are currently undecided in the classification below order level, formed sister clades. They share with *Ophiactis* the wrench-shaped adradial genital plate and sickle-shaped abradial genital plate, as well as several characters of the oral papillae and arm

plates. The split between these and the other Ophiactoidea (except Ophiothamnidae) on the tree inferred here has low support (64%) and they may eventually be found to belong in Ophiactidae.

There were a few surprising changes to the tree compared to previous analyses (Thuy & Stöhr 2016; Thuy *et al.* 2021, 2023). The refinement of the characters of genital plates and oral papillae showed that the fossil *Palaeocoma milleri* (Phillips, 1829) possesses a mixture of characters shared with widely separate modern taxa. Its oral papillae include a large Lyman's ossicle in line with the other oral papillae, similar to Amphilepidida and Ophiacanthida (Hendler 2018), as well as a large, square, scale-like papilla next to it that may be the primary adoral shield spine. Next to this, a smaller square papilla may be the secondary adoral shield spine. There appear to be tooth papillae, which are absent in Amphilepidida, but present in Ophiacanthida and Ophiurida (Hendler 2018), and the dental plate has a cluster of sockets at least ventrally, similar to Ophiurida. The cup-shaped, exposed abradial genital plate, beset with large block-like papillae, forms an arm comb typical of Ophiuridae, but the dense cover of small granules on the dorsal and ventral disc is more similar to some Ophiacanthida (e.g., *Ophioderma*, *Ophiocoma*). Hence, after revised scoring for these characters, *P. milleri* is not a close relative of Ophiopyrgidae as the tree in Thuy *et al*. (2021) suggested. In the original tree of Thuy & Stöhr (2016), *P. milleri* appeared to support the Euryophiurida, and removing it from the analysis still has a detrimental effect on the tree, but that first matrix was heavily biased on lateral arm plate characters (42 of 130 characters), and oral papillae and genital plates were scored with a few broadly defined characters. In the here revised matrix, 46 of the in total 153 characters pertain to lateral arm plates. Three of these were incorporated from the matrix in Thuy *et al*. (2021), because they are considered to be synapomorphies of *Ophiomusa* (LAP-G-6) and *Palaeocoma* (LAP-I-7, LAP-I-8), within the set of species explored here. Removing them did indeed affect the tree and so these were kept, but there is still less bias towards lateral arm plates.

The extinct species *Eirenura papillata* Thuy, 2011 had previously been suggested as the sister species of Ophiohelidae with 71% support (Thuy & Stöhr 2016) and recently with 98% support (Thuy *et al.* 2021). The disc granules, oral papillae and inner radial shield of *Eirenura* are all more similar to Ophioleucidae than to Ophiohelidae, and in this study it formed a sister clade to Ophioleucidae, albeit with low support (66%). The Ophiohelidae has consistently been inferred as a sister taxon of Ophioleucidae with 89–98% support by morphological phylogenetic inference; however, Ophiohelidae is currently considered a member of the order Ophioscolecida, which was here a paraphyletic group, suggested as sister taxon to Ophiacanthina with 91% support. Also problematic were the genera *Ophiarachna* and *Ophiomyxa*, both currently placed in Ophiomyxidae, in the superfamily Ophiodermatoidea, but here *Ophiarachna* holds an intermediate position between Ophiodermatoidea and Ophiocomoidea, and Ophiomyxidae are included with low support (54%). Small modifications in character assessment caused the genus *Ophiomyxa* to move around on the tree, probably due to its reduced skeleton, which has few shared features with *Ophiarachna*. The dataset on *Ophiarachna* is still incomplete, because no material was available, but the adradial GP has similarities with *Ophiomyxa*. However, its densely granulated disc and the condition of the oral papillae are more similar to conditions in *Ophioderma* and *Ophiocoma*. In the original analysis (Thuy & Stöhr 2016), *Ophiomyxa* was the sister taxon to a group containing *Ophioderma*, *Ophiarachna* and *Ophiocoma*, but *Ophiarachna* was suggested as sister to *Ophiocoma*. Refining and adding characters to the matrix has not had the expected effect on these clades, leaving them essentially in the same positions.

Further improvement of this family level morphological dataset should focus on identifying and removing characters that vary at the species level and are homoplasious at the family level (e.g., "thickened skin" was here removed, numbers of arm spines were deemed unsuitable, the expression of disc scalation may need to be reviewed). Presumably paedomorphic species that lack a large number of characters compared to their (genetically) close relatives have a confusing effect on a purely

morphological analysis, as trials with *Ophiotypa* and *Astrophiura* have shown, and should be omitted. Likewise, the inclusion of fossils is becoming increasingly difficult, when only a limited number of their skeletal parts are known. Thuy & Stöhr (2016) demonstrated that the lateral arm plates alone can deliver reasonably well supported phylogenies, but the case of *P. milleri* points to limits in this approach. The clades Ophiactoidea, Euryalida, Ophiocomidae, Ophiodermatidae, Amphiuridae, Hemieuryalidae and Ophiacanthidae are in remarkable congruence with the molecular phylogeny (O'Hara *et al.* 2017; Christodoulou *et al.* 2019), as are the major lineages Euryophiurida, Ophintegrida, and Amphilepidida, suggesting that the character selection and scoring are working well. Hence, the persistent issues with recovering some of the clades or their position on the tree as proposed by molecular studies (O'Hara *et al.* 2017; Christodoulou *et al.* 2019) could suggest that the molecular data need to be re-analysed with different methods or evolutionary models.

Early evolution of genital plates, radial and oral shields

Abradial and adradial genital plates, radial shields and oral shields are part of the modern ophiuroid bauplan and are believed to have evolved in the Devonian (Thuy *et al.* 2022), about 400 Ma. These four types of ossicles were present in the Late Devonian ophiuroids *Stephanoura belgica* Ubaghs, 1941 and *Ophiaulax decheni* (Dewalque, 1881) according to Ubaghs (1941). The oral genital plates have not yet been documented in fossils. Whereas the abradial and adradial genital plates usually have a characteristic shape that makes them easy to identify in assemblages of microfossils (and dissociated extant specimens), the oral genital plates are minute and often resemble disc scales, which makes them difficult to impossible to recognize. Complete fossil ophiuroids are rare, but those that are available should be examined for oral genital plates. Lyman (1882) considered radial shields to be homologous to disc scales, an idea supported by Ubaghs (1941) and by ontogenetic observations in extant species, which have shown that radial shields are absent in the smallest postlarvae and develop slowly together with regular disc scales (Sumida *et al.* 1998; Stöhr 2005). In *S. belgica*, the radial shields are positioned above the arms, similar to modern ophiuroids, but in *O. decheni*, they are in the shape of marginal plates bordering the disc edge.

The homologies of the genital plates remain unclear. In *S. belgica*, the adradial genital plate was club-like, with a rod-like proximal part as long as two arm segments and a bulbous distal end. The drawings in Ubaghs (1941) suggest one or two round condyles and a depression, possibly a groove surrounding the condyle(s). The abradial genital plate of *S. belgica* was thin, narrow, flat, possibly sabre-shaped, almost as long as the adradial plate and attached abradially to its distal end. The available information on *Ophiaulax decheni* is less detailed, the abradial genital plate is unknown and the adradial plate is similar to that of *S. belgica*, with a rod-like proximal part and swollen distal end, but no details on condyles or other structures are known (Ubaghs 1941). The club-like shape of the adradial genital plate appears to be the plesiomorphic condition, from which other shapes evolved in modern species. Since genital plates, radial and oral shields are well developed in these Late Devonian species, they must have first evolved earlier. Stürtz (1890) mentioned oral shields and marginal disc plates (radial shields?) in the Early Devonian *Ophiurina lymani* Stürtz, 1890, which suggests that these ossicles evolved before that period in time. It is possible that the adradial GP evolved earlier than the abradial GP, but simultaneously with the radial shield, as adradial GP and radial shield seem to form a functional unit, and in extant species, they develop together. In *Amphiophiura*, the abradial GP is strikingly similar to lateral arm plates in its exposed distal part, and the presence of papillae is similar to arm spines on lateral plates. Whether this indicates homology between these plates needs to be investigated further, and the presence of lateral arm plates at all arm segments inside the disc and beyond in addition to abradial GPs (e.g., in *Ophiura*) may contradict this idea. Adradial GPs have been found in all examined species, including those that lack radial shields (*Ophioscolex glacialis*, *Ophiomyces* spp.), which may suggest that they fulfil a vital function in the animal, whereas abradial GPs apparently can be reduced without negative consequences (*Ophiopus arcticus*). Conversely, the presence of dissociated abradial GPs most likely

indicates the presence of genital slits in an extinct species, which may be a useful signal when no whole-body fossil exists. More data are needed to better understand the evolution of the ophiuroid inner disc skeleton and its function.

Microfossils of ophiuroids predominantly consist of lateral arm plates, because each animal possesses a large number of these in every arm. Thuy & Stöhr (2011) showed that lateral arm plate morphology is specific at various taxonomic levels, which provided the foundation for better identification and classification of these microfossils. Genital plates are rare in microfossils (and fossil oral GP are unknown), since each animal possesses only ten of each type of genital plate. Previously, only the articular structures had been analysed for taxonomic purposes and these are rarely clearly visible in fossils. The present study also takes the overall shape of the plates into account, which can improve the usefulness of genital plates in fossil material. However, the cleaver-like adradial GP in *Aganaster gregarius* is here considered to be a case of convergent evolution between Palaeozoic and modern ophiuroids, not supporting the previous idea of it being a member of the family Ophiolepididae (Thuy & Stöhr 2016). It is currently not assigned to a family (Stöhr *et al.* 2022) and belongs to an extinct sister group of the extant Ophiuroidea according to a recent analysis (Thuy *et al.* 2022). *Aplocoma agassizii* appears to lack the cleaver-like shape of the adGP of *Ophiolepis*, but it remains unclear whether this is a synapomorphy of the family or the genus, because among the two other extant genera of Ophiolepididae, in the strongly paedomorphic *Ophiotypa* development may terminate before this character is formed, and for *Ophioteichus* H.L. Clark, 1938, the morphology of the genital plates is unknown. The GPs of *P. milleri* are more similar to those of Ophiuridae than of the here examined species of Ophiopyrgidae. It seems that the genital plates in these fossils are not in accord with other characters, or their classification may need to be re-evaluated.

Limitations of the study

Time-consuming preparation methods and costly instruments limit the number of specimens that can be analysed for internal structures. Whereas external examinations can be performed efficiently on hundreds of specimens with a dissecting microscope to assess intraspecific variation and interspecific differences, the internal skeleton is often known from only a single or few specimens of the same species. Therefore, the effects of size or ontogenetic stage and individual variation are mostly unknown, but should be explored further, as is suggested by the observations from the few species for which this study includes more than a single specimen (e.g., *Ophiacantha bidentata*). Likewise, possible differences between geographically separated populations of the same species and effects of ecological factors on skeleton formation are still incompletely known (Dubois 2014).

Words are insufficient to accurately describe the shape of the here studied ossicles, which hampers the consistent evaluation of characters for phylogenetic inference. Further studies should explore the possibilities of geometric morphometrics applied to three-dimensional images gained from micro-CT reconstructions, as was done with vertebrae by Goharimanesh *et al*. (2022). Shape differences between species can be calculated as distances between landmarks using size independent methods, and these can be used for phylogenetic analysis (David & Laurin 1996; Polly *et al.* 2013), which could reduce the degree of subjectivity in the data and improve reproducibility.

Caveats with the here explored methods of examination are: SEM is highly destructive, requiring surplus material that can be sacrificed, orientating the ossicles in the desired positions on the stubs under the dissecting microscope can be extremely difficult and to a degree subject to chance, and stopping the dissociation process at the right moment to achieve pieces with plates still attached to each other but free of soft tissue was rarely successful. The XRM micro-CT used converts X-rays to visible light and offers several lenses with different magnifications, but for some specimens the optimal magnification was not available, and focusing on the target area has proven difficult, leading to failure in some experiments.

The three-dimensional reconstructions can be rotated and digitally sliced, which allows the examination of the in situ positions of the plates from various angles. This greatly improves the understanding of these structures, but cannot adequately be presented on two-dimensional figures (see supporting files on Zenodo). Digital photography does not have the same resolution as the other two methods, but can document the in situ position of the ossicles. All three techniques compliment each other, and used together they provide more complete information than any one of them alone.

Acknowledgments

I want to thank my collaborators from previous projects, Ben Thuy and Alexander Martynov, who contributed to the image bank used here. Data acquisition by XRM micro-CT was supported by a grant to the Stockholm University Brain Imaging Centre (SU FV-5.1.2-1035- 15) and by a time grant (SUBIC20VTXRAY4) to the author. Many thanks to Tunhe Zhou for assistance with XRM image acquistion. The SEM examinations performed for this study were supported by a grant from Riksmusei Vänner. Previously acquired SEM images were supported by Riksmusei Vänner and Längmanska Kulturfonden. I'm very grateful to the reviewer for taking the time to carefully review such a large manuscript and provide helpful comments.

References

Brazeau M.D. 2011. Problematic character coding methods in morphology and their effects. *Biological Journal of the Linnean Society* 104: 489–498. https://doi.org/10.1111/j.1095-8312.2011.01755.x

Byrne M. 1994. Ophiuroidea. *In*: Harrison F.W. & Chia F.-S. (eds) *Echinodermata*. *Microscopic Anatomy of Invertebrates*: 247–343. Wiley-Liss, New York.

Christensen A.B. & Colacino J.M. 2000. Respiration in the burrowing brittlestar, *Hemipholis elongata* Say (Echinodermata, Ophiuroidea): a study of the effects of environmental variables on oxygen uptake. *Comparative Biochemistry and Physiology Part A: Molecular & Integrative Physiology* 127: 201–213. https://doi.org/10.1016/S1095-6433(00)00254-3

Christodoulou M., O'Hara T.D., Hugall A.F. & Arbizu P.M. 2019. Dark ophiuroid biodiversity in a prospective abyssal mine field. *Current Biology* 29 (22): 3909–3912.e3. https://doi.org/10.1016/j.cub.2019.09.012

Clark E.G., Hutchinson J.R., Darroch S.A.F., Mongiardino Koch N., Brady T.R., Smith S.A. & Briggs D.E.G. 2018. Integrating morphology and in vivo skeletal mobility with digital models to infer function in brittle star arms. *Journal of Anatomy* 233: 696–714. https://doi.org/10.1111/joa.12887

David B. & Laurin B. 1996. Morphometrics and cladistics: measuring phylogeny in the sea urchin *Echinocardium*. *Evolution* 50: 348–359. https://doi.org/10.1111/j.1558-5646.1996.tb04498.x

Dubois P. 2014. The skeleton of postmetamorphic echinoderms in a changing world. *The Biological Bulletin* 226: 223–236. https://doi.org/10.1086/BBLv226n3p223

Ezhova O.V., Malakhov V.V. & Martynov A.V. 2016. Madreporites of Ophiuroidea: are they phylogenetically informative? *Zoomorphology* 135: 333–350. https://doi.org/10.1007/s00435-016-0315-x

Goharimanesh M., Stöhr S., Mirshamsi O., Ghassemzadeh F. & Adriaens D. 2021. Interactive identification key to all brittle star families (Echinodermata; Ophiuroidea) leads to revised morphological descriptions. *European Journal of Taxonomy* 766: 1–63. https://doi.org/10.5852/ejt.2021.766.1483

Goharimanesh M., Ghassemzadeh F., De Kegel B., Van Hoorebeke L., Stöhr S., Mirshamsi O. & Adriaens D. 2022. The evolutionary relationship between arm vertebrae shape and ecological lifestyle in brittle stars (Echinodermata: Ophiuroidea). *Journal of Anatomy* 240: 1034–1047. https://doi.org/10.1111/joa.13617

Gondim A.I., Dias T.L.P., Christoffersen M.L. & Stöhr S. 2015. Redescription of *Hemieuryale pustulata* von Martens, 1867 (Echinodermata, Ophiuroidea) based on Brazilian specimens, with notes on systematics and habitat association. *Zootaxa* 3925 (3): 341–360. https://doi.org/10.11646/zootaxa.3925.3.2

Gondim de Farias A.I. 2016. *Sistemática da família Hemieuryalidae Verrill, 1899 (Echinodermata, Ophiuroidea, Ophiurida)*. PhD thesis. Universidade Federal da Paraíba, João Pessoa, Paraiba.

Hainey M.A.H. & Emlet R.B. 2020. *Gorgonocephalus eucnemis* (Echinodermata: Ophiuroidea) and bursal ventilation. *The Biological Bulletin* 238 (3): 193–205. https://doi.org/10.1086/709575

Hendler G. 1978. Development of *Amphioplus abditus* (Verrill) (Echinodermata: Ophiuroidea). II. Description and discussion of ophiuroid skeletal ontogeny and homologies. *Biological Bulletin* 154: 79–95. https://doi.org/10.2307/1540776

Hendler G. 2018. Armed to the teeth: a new paradigm for the buccal skeleton of brittle stars (Echinodermata: Ophiuroidea). *Contributions in Science* 526: 189–311. https://doi.org/10.5962/p.324539

Hoggett A.K. 1991. The genus *Macrophiothrix* (Ophiuroidea: Ophiotrichidae) in Australian waters. *Invertebrate Taxonomy* 4: 1077–1146. https://doi.org/10.1071/it9901077

Huelsenbeck J.P. & Ronquist F. 2001. MRBAYES: Bayesian inference of phylogenetic trees. *Bioinformatics* 17: 754–755. https://doi.org/10.1093/bioinformatics/17.8.754

King B. 2019. Which morphological characters are influential in a Bayesian phylogenetic analysis? Examples from the earliest osteichthyans. *Biology Letters* 15: e20190288. https://doi.org/10.1098/rsbl.2019.0288

Kokorin A.I., Mirantsev G.V. & Rozhnov S.V. 2014. General features of echinoderm skeleton formation. *Paleontological Journal* 48: 1532–1539. https://doi.org/10.1134/S0031030114140056

Landschoff J. & Griffiths C. 2015. Three-dimensional visualisation of brooding behaviour in two distantly related brittle stars from South African waters. *African Journal of Marine Science* 37: 533–541. https://doi.org/10.2989/1814232X.2015.1095801

LeClair E.E. 1996. Arm joint articulations in the ophiuran brittlestars (Echinodermata: Ophiuroidea): a morphometric analysis of ontogenetic, serial, and interspecific variation. *Journal of Zoology* 240: 245–275. https://doi.org/10.1111/j.1469-7998.1996.tb05283.x

Lewis P.O. 2001. A likelihood approach to estimating phylogeny from discrete morphological character data. *Systematic Biology* 50: 913–925. https://doi.org/10.1080/106351501753462876

Limaye A. 2012. Drishti: a volume exploration and presentation tool. *Proceedings of SPIE, Developments in X-Ray Tomography VIII, 85060X*: 1–9. Society of Photo-Optical Instrumentation Engineers, San Diego, CA. https://doi.org/10.1117/12.935640

Ludwig H. 1888. *Ophiopteron elegans*, eine neue, wahrscheinlich schwimmende Ophiuridenform. *Zeitschrift für wissenschaftliche Zoologie* 47: 459–464.

Lyman T. 1869. Preliminary report on the Ophiuridae and Astrophytidae dredged in deep water between Cuba and Florida Reef. *Bulletin of the Museum of Comparative Zoology* 1: 309–354.

Lyman T. 1874. Ophiuridae and Astrophytidae, new and old. *Bulletin of the Museum of Comparative Zoology* 3: 221–272.

Lyman T. 1882. Report on the Ophiuroidea. *In*: Thomson C.W. & Murray J. (eds) *Report of the Scientific Results of the Voyage of H.M.S. Challenger 1873–76. Zoology V*: 1–386.

Martynov A.V. 2010. Reassessment of the classification of the Ophiuroidea (Echinodermata), based on morphological characters. I. General character evaluation and delineation of the families Ophiomyxidae and Ophiacanthidae. *Zootaxa* 2697 (1): 1–154. https://doi.org/10.11646/zootaxa.2697.1.1

Matsumoto H. 1915. A new classification of the Ophiuroidea: with descriptions of new genera and species. *Proceedings of the Academy of Natural Sciences* 67: 43–92.

Matsumoto H. 1917. A monograph of Japanese Ophiuroidea, arranged according to a new classification. *Journal of the College of Science, Imperial University, Tokyo* 38: 1–408.

Murakami S. 1963. The dental and oral plates of Ophiuroidea. *Transactions of the Royal Society of New Zealand, Zoology* 4: 1–48.

O'Hara T.D., Hugall A.F., Thuy B., Stöhr S. & Martynov A.V. 2017. Restructuring higher taxonomy using broad-scale phylogenomics: the living Ophiuroidea. *Molecular Phylogenetics and Evolution* 107: 415–430. https://doi.org/10.1016/j.ympev.2016.12.006

O'Hara T.D., Stöhr S., Hugall A.F., Thuy B. & Martynov A. 2018. Morphological diagnoses of higher taxa in Ophiuroidea (Echinodermata) in support of a new classification. *European Journal of Taxonomy* 416: 1–35. https://doi.org/10.5852/ejt.2018.416

O'Hara T.D., Thuy B. & Hugall A.F. 2021. Relict from the Jurassic: new family of brittle-stars from a New Caledonian seamount. *Proceedings of the Royal Society B: Biological Sciences* 288: e20210684. https://doi.org/10.1098/rspb.2021.0684

Okanishi M., Fujita T., Maekawa Y. & Sasaki T. 2017. Non-destructive morphological observations of the fleshy brittle star, *Asteronyx loveni* using micro-computed tomography (Echinodermata, Ophiuroidea, Euryalida). *ZooKeys* 663: 1–19. https://doi.org/10.3897/zookeys.663.11413

Pineda-Enriquez T. 2013. *Filogenia del género Ophiolepis Müller & Troschel, 1840 (Ophiuroidea: Ophiolepididae) inferida por caracteres morfológicos*. MSc Thesis. Universidad Nacional Autónoma de México.

Polly P.D., Lawing A.M., Fabre A.-C. & Goswami A. 2013. Phylogenetic Principal Components Analysis and geometric morphometrics. *Hystrix, the Italian Journal of Mammalogy* 24: 33–41. https://doi.org/10.4404/hystrix-24.1-6383

Ronquist F., Huelsenbeck J.P., Teslenko M., Zhang C. & Nylander J.A.A. 2020. *MrBayes version 3.2 Manual: Tutorials and Model Summaries*.
Available from https://nbisweden.github.io/MrBayes/manual.html [accessed 19 Apr. 2024].

Schoener A. 1967. Post-larval development of five deep-sea ophiuroids. *Deep-Sea Research* 14: 645–660.

Schoener A. 1969. Atlantic ophiuroids: some post-larval forms. *Deep-Sea Research* 16: 127–140.

Sereno P.C. 2007. Logical basis for morphological characters in phylogenetics. *Cladistics* 23: 565–587. https://doi.org/10.1111/j.1096-0031.2007.00161.x

Simões T.R., Vernygora O.V., de Medeiros B.A.S. & Wright A.M. 2023. Handling logical character dependency in phylogenetic inference: extensive performance testing of assumptions and solutions using simulated and empirical data. *Systematic Biology* 2 (3): 662–680. https://doi.org/10.1093/sysbio/syad006

Smith A.B., Paterson G.L.J. & Lafay B. 1995. Ophiuroid phylogeny and higher taxonomy: morphological, molecular and palaeontological perspectives. *Zoological Journal of the Linnean Society* 114: 213–243. https://doi.org/10.1111/j.1096-3642.1995.tb00117c.x

Stöhr S. 2005. Who's who among baby brittle stars (Echinodermata: Ophiuroidea): postmetamorphic development of some North Atlantic forms. *Zoological Journal of the Linnean Society* 143: 543–576. https://doi.org/10.1111/j.1096-3642.2005.00155.x

Stöhr S. 2011. New records and new species of Ophiuroidea (Echinodermata) from Lifou, Loyalty Islands, New Caledonia. *Zootaxa* 3089 (1): 1–50. https://doi.org/10.11646/zootaxa.3089.1.1

Stöhr S. & Martynov A. 2016. Paedomorphosis as an evolutionary driving force: insights from deep-sea brittle stars. *PLoS One* 11: e0164562. https://doi.org/10.1371/journal.pone.0164562

Stöhr S. & O'Hara T.D. 2021. Deep-sea Ophiuroidea (Echinodermata) from the Danish Galathea II Expedition, 1950–52, with taxonomic revisions. *Zootaxa* 4963 (3): 505–529. https://doi.org/10.11646/zootaxa.4963.3.6

Stöhr S., O'Hara T.D. & Thuy B. 2012a. Global diversity of brittle stars (Echinodermata: Ophiuroidea). *PLoS One* 7: 1–14. https://doi.org/10.1371/journal.pone.0031940

Stöhr S., Sautya S. & Ingole B. 2012b. Brittle stars (Echinodermata: Ophiuroidea) from seamounts in the Andaman Sea (Indian Ocean): first account, with descriptions of new species. *Journal of the Marine Biological Association of the United Kingdom* 92 (5): 1195–1208. https://doi.org/10.1017/S0025315412000240

Stöhr S., Boissin E. & Hoareau T.B. 2013. Taxonomic revision and phylogeny of the *Ophiocoma brevipes* group (Echinodermata, Ophiuroidea), with description of a new subgenus (*Breviturma*) and a new species. *European Journal of Taxonomy* 68: 1–26. https://doi.org/10.5852/ejt.2013.68

Stöhr S., Clark E.G., Thuy B. & Darroch S.A.F. 2019. Comparison of 2D SEM imaging with 3D micro-tomographic imaging for phylogenetic inference in brittle stars (Echinodermata: Ophiuroidea). *Zoosymposia* 15: 146–158. https://doi.org/10.11646/zoosymposia.15.1.17

Stöhr S., Weber A.A.-T., Boissin E. & Chenuil A. 2020. Resolving the *Ophioderma longicauda* (Echinodermata: Ophiuroidea) cryptic species complex: five sisters, three of them new. *European Journal of Taxonomy* 600: 1–37. https://doi.org/10.5852/ejt.2020.600

Stöhr S., O'Hara T.D. & Thuy B. 2022. World Ophiuroidea Database. *World Ophiuroidea Database*. https://doi.org/10.14284/358

Stürtz B. 1890. Neuer Beitrag zur Kenntnis paläozoischer Seesterne. *Palaeontographica* 36: 203–250.

Sumida P.Y.G., Tyler P.A., Gage J.D. & Nørrevang A. 1998. Postlarval development in shallow and deep-sea ophiuroids (Echinodermata: Ophiuroidea) of the NE Atlantic Ocean. *Zoological Journal of the Linnean Society* 124: 267–300. https://doi.org/10.1111/j.1096-3642.1998.tb00577.x

Thuy B. & Stöhr S. 2011. Lateral arm plate morphology in brittle stars (Echinodermata: Ophiuroidea): new perspectives for ophiuroid micropalaeontology and classification. *Zootaxa* 3013 (1): 1–47. https://doi.org/10.11646/zootaxa.3013.1.1

Thuy B. & Stöhr S. 2016. A new morphological phylogeny of the Ophiuroidea (Echinodermata) accords with molecular evidence and renders microfossils accessible for cladistics. *PLoS One* 11: e0156140. https://doi.org/10.1371/journal.pone.0156140

Thuy B. & Stöhr S. 2018. Unravelling the origin of the basket stars and their allies (Echinodermata, Ophiuroidea, Euryalida). *Scientific Reports* 8: e8493. https://doi.org/10.1038/s41598-018-26877-5

Thuy B., Numberger-Thuy L.D. & Pineda-Enríquez T. 2021. New fossils of Jurassic ophiurid brittle stars (Ophiuroidea; Ophiurida) provide evidence for early clade evolution in the deep sea. *Royal Society Open Science* 8: e210643. https://doi.org/10.1098/rsos.210643

Thuy B., Eriksson M.E., Kutscher M., Lindgren J., Numberger-Thuy L.D. & Wright D.F. 2022. Miniaturization during a Silurian environmental crisis generated the modern brittle star body plan. *Communications Biology* 5: 1–9. https://doi.org/10.1038/s42003-021-02971-9

Thuy B., Knox L., Numberger-Thuy L.D., Smith N.S. & Sumrall C.D. 2023. Ancient deep ocean as a harbor of biotic innovation revealed by Carboniferous ophiuroid microfossils. *Geology* 51 (2): 157–161. https://doi.org/10.1130/G50596.1

Ubaghs G. 1941. Description de quelques ophiures de Famennien de la Belgique. *Bulletin du Musée royal des Sciences naturelles de Belgique* 17: 1–31.

Ung V., Dubus G., Zaragueta-Bagils R. & Vignes-Lebbe R. 2010. Xper2: introducing e-taxonomy. *Bioinformatics* 26: 703–704. https://doi.org/10.1093/bioinformatics/btp715

Vadon C. 1988. Paedomorphosis and phylogenetic relationships in Ophiuridae. *In*: Burke R.D., Mladenov P.V., Lambert P. & Parsley R.L. (eds) *Sixth International Echinoderm Conference*: 323. Balkema, Melbourne.

Ware J.L. & Barden P. 2016. Incorporating fossils into hypotheses of insect phylogeny. *Current Opinion in Insect Science* 18: 69–76. https://doi.org/10.1016/j.cois.2016.10.003

Wilkie I.C. & Brogger M.I. 2018. The peristomial plates of ophiuroids (Echinodermata: Ophiuroidea) highlight an incongruence between morphology and proposed phylogenies. *PLoS One* 13: e0202046. https://doi.org/10.1371/journal.pone.0202046

Wright A.M. & Hillis D.M. 2014. Bayesian analysis using a simple likelihood model outperforms parsimony for estimation of phylogeny from discrete morphological data. *PLoS One* 9: e109210. https://doi.org/10.1371/journal.pone.0109210

Manuscript received: 14 July 2023
Manuscript accepted: 29 January 2024
Published on: 14 May 2024
Topic editor: Magalie Castelin
Section editor: Didier Van Den Spiegel
Desk editor: Kristiaan Hoedemakers

Printed versions of all papers are also deposited in the libraries of the institutes that are members of the *EJT* consortium: Muséum national d'histoire naturelle, Paris, France; Meise Botanic Garden, Belgium; Royal Museum for Central Africa, Tervuren, Belgium; Royal Belgian Institute of Natural Sciences, Brussels, Belgium; Natural History Museum of Denmark, Copenhagen, Denmark; Naturalis Biodiversity Center, Leiden, the Netherlands; Museo Nacional de Ciencias Naturales-CSIC, Madrid, Spain; Leibniz Institute for the Analysis of Biodiversity Change, Bonn – Hamburg, Germany; National Museum of the Czech Republic, Prague, Czech Republic.

Supp. file 1. Final character matrix of 69 species (including eight fossils) and 153 characters. https://doi.org/10.5852/ejt.2024.933.2525.11331

Supp. file 2. Computer generated descriptions (from Xper2) of all species included in the character matrix. Question marks indicate unknown characters, but were also used for absent characters that have no neomorphic character statement (see Material and methods).
https://doi.org/10.5852/ejt.2024.933.2525.11333

Appendix

Morphological character descriptions

Character statements modified from Thuy & Stöhr (2016) and (Thuy & Stöhr 2018), in part after Thuy *et al*. (2021). New character statements are marked with an asterisk, modified character descriptions are marked by a hashtag.

1. D-P-1: Dorsal disc, scalation: few thin scales (0), many thin scales (1), thick scales (2), very few thin/small scales or none (3).

2. D-P-3: Dorsal disc scales, size (excluding central primary plate and primary radial plates): variable (0), uniform (1).

3. D-P-4: Dorsal disc scales, stereom structure: no tubercles (0), with smooth tubercles (1).

4. D-P-5: Central primary plate, relative size: larger than disc scales (0), of same size/undistinguishable (1)

5. D-P-6: Primary radial plates, relative size: larger than scales (0), of same size/undistinguishable (1).

6. D-P-7: Primary radial plates, position: at a distance from CCP (0), in contact with CCP (1).

7. D-GS-1: Dorsal disc covering, nature: without granules/spines (0), with granules only (1), with both granules and spines (2), with spines only (3).

8. D-GS-2: Dorsal disc granules/spines, extension: sparse all over with underlying plates/scales visible or restricted to disc margin (0), forming dense cover completely hiding underlying plates/scales (possible exception: radial shields) (1).

9. D-GS-5: Radial shield, granule/spine covering: naked (0), at least partly covered (1).

10. D-GS-6: Dorsal disc granules/spines, differentiation: uniform (0), modified (e.g., enlarged) at disc edge (1).

11. D-RS-3: Radial shields (in articulated disc plating), length: less than one third of the disc radius (0), between one third and half of the disc radius (1), more than half of the disc radius (2).

12. D-RS-4: Radial shield pairs (in articulated disc plating), proximity: completely separated (0), separated distally (1), separated proximally (2), in contact over entire length (3).

13. D-RS-5: Radial shield, shape (macerated): scalene ("oblique") triangular (0), isosceles ("mirror-symmetric") triangular to pear-shaped (1), "half-circle" (straight inner, convex outer edge, not always as wide as a true half-circle) (2), bar-like (3).

14. D-RS-6: Radial shield abradial edge, shape: entire (0), with extension(s) (regular outline enlarged) (1), incised/irregular (2).

15. #D-RS-7: Radial shield, exposure: central part of RS to almost entire RS exposed (0), distal portion of RS exposed (1), distal-adradial portion of RS exposed (2), completely covered by scales (3).

16. *D-RS-9: Muscle attachment area on inner RS, shape: round, flat (0), crater-like depression with proximal protruding edge/rim (1), large depression (e.g., *Gorgonocephalus*) (2).

17. *D-RS-10: RS inner articulation, shape: one condyle (0), two condyles/sours with depression between them (1), no special structure (2), smooth patch (3).

18. *D-RS-11: RS inner distal edge, shape: groove and lip-shaped edge (0), other shape (1).

19. *D-RS-12: Conspicuous pore in inner side of RS: absent (0), present (0).

20. VI-2: Ventral interradii, covering: with granules (0), with spines (1), naked (2), with tubercles (3).

21. VI-3: Genital slit, length: shorter than half interradius (0), longer than half the length of an interradius or divided into two openings (1), lost (2).

22. *OR-GP-1: Oral GP: absent (0), present (1).

23. *OR-GP-2: Oral GP, shape: bar-like (0), oval (1), L-shaped (2), rectangular (3), comma-shaped (4), drop-shaped (5).

24. *OR-GP-3: Rectangular oral GP, details: with folded edge (0), convex (1), with processes (2).

25. *OR-GP-4: Oval oral GP, details: pyramid-like raised (0), with notch (1).

26. *AD-GP-1: Adradial GP, shape: bar-like (0), multi-layered (1), stout, half as wide as long (2), blade-like, straight (excl. distal dorsalwards curving end) (3), wrench-shaped (4), comma-shaped (5), cleaver-shaped (6), cup-shaped (7).

27. *AD-GP-2: AdGP to RS articular structures, shape: single condyle (0), 2 condyles (1), flat (2), condylar process (3).

28. *AD-GP-3: Bar-like adGP subtypes, shape: distally inflated (0), distally not inflated (1), club-like (2).

29. *AD-GP-4: Additional structures on adGP, shape: patch of different stereom (0), process (1).

30. AB-GP-1: Abradial plate relative length: shorter than half the adradial plate length (0), longer than half the adradial plate length (1), as long as adradial plate (2).

31. #AB-GP-2: Abradial genital plate shape: strong, curved scale (0), thin, as wide as long (1), sabre- or sickle-shaped (2), twisted (3), triangular to pear-shaped (4), blade-like, straight (5), trapezoid to rectangular (6), scoop-shaped (7), cup-shaped (8), thin curved scale (9).

32. AB-GP-3: Shape of adradio-distal tip of abradial genital plate: straight or convex (0), concave (1), fused to adGP (2).

33. AB-GP-6: Abradial genital plate covering: fully covered (0), exposed (not covered by disc plates/ scales) (1).

34. AB-GP-7: Abradial genital plate papillae/granules, nature: disc granules (1), papillae (2).

35. AB-GP-8: AbGP papillae, extension: restricted to ventral disc (0), extending to latero-dorsal disc edge (1).

36. AB-GP-9: Ventral genital papillae, shape: granule-like (0), spine-like (1), block-like (2).

37. AB-GP-10: Conspicuous perforation in adradial surface: absent (0), present (1).

38. *AB-GP-11: Longitudinal groove in abradial surface: absent (0), present (1).

39. *AB-GP-12: Distalmost genital papillae (on dorsal disc), shape: block-like (0), spine-like (1).

40. *AB-GP-13: AbGP crosses adGP: no (0), yes (1).

41. M-OAS-1: Oral shield, length (distance between proximal tip of oral shield and disc margin): covering less than one third of interradius (0), longer than one third of the length of an interradius (1).

42. M-OAS-2: Oral shield, shape: longer than wide (0), as long as wide (1), wider than long (2).

43. M-OAS-3: Madreporite, size: similar to other oral shields (0), larger than remaining oral shields (1).

44. *M-OAS-4: Madreporite inner side, structure: 1–2 openings (0), meshwork of openings (1), several pores (2).

45. *M-OAS-5: Madreporite inner opening, position: proximal (0), central (1), distal (2), centro-distal (3).

46. M-OAS-6: Adoral shields, proximity: separated (0), meeting proximal to oral shield (1).

47. M-OAS-8: Oral shield proximal portion, shape: evenly convex (0), obtuse angle with straight to convex sides (1), obtuse angle with concave sides (2), acute to right angle with straight to convex sides (3), acute to right angle with concave sides (4).

48. M-OAS-9: Oral shield distal portion, shape: evenly convex (0), square-shaped (1), with narrower distalward projection (2).

49. M-SP-1: Second oral tentacle pore position: shallow and oblique (0), deep inside mouth slit (1).

50. M-PaT-1: Lateral papillae, arrangement: single row along jaw edge (0), multiple rows covering jaws (1).

51. #M-PaT-2: Ventralmost tooth, position: exposed (0), obscured by tooth papillae (1).

52. M-PaT-3: Buccal scale, shape: smaller papilla (*Ophiura*) (0), pointed wide, higher on oral plate (*Amphiura*) (1), single wide papilla (*Amphilepis*) (2), lost (3).

53. #M-PaT-4: Infradental papillae, position: lateral, close to dental plate (0), lateral, at distance from dental plate (1), below teeth (2).

54. M-PaT-5: Adoral shield spine, shape: spiniform (0), scale-like or like other papillae (1), scale-like, much larger/wider than other papillae (2).

55. #M-PaT-6: Second degree adoral shield spine, position: at oral plate (0), at 2nd tentacle pore (1).

56. #M-PaT-7: Additional lateral oral papillae (Ophiacanthida), shape: block-shaped (0), rounded (1), spiniform (2).

57. M-PaT-8: Teeth, shape: spine-like, thin and sharply pointed (0), with round or slightly pointed tip (but never spine-like) (1), with square tip (2).

58. *M-Pa-T-9: Infradental papillae, relative size: similar to other oral papillae (0), larger than other oral papillae (1).

59. *M-Pa-T-10: Second degree adoral shield spine, number: single (0), multiple (1).

60. *M-Pa-T-11: Lyman's ossicle, position: oblique in mouth slit (0), in line with other papillae at oral plate (1).

61. *M-PaT-12: Tooth papillae, number: 2 (0), >2 (1).

62. *M-PaT-13: Accessory oral papillae: absent (0), present (1).

63. M-DP-1: Dental plate, shape: entire (0), several pieces (1).

64. M-DP-2: Dental plate, geometry: equal width all over (0), ventral half widest (1), dorsal half widest (2).

65. M-DP-3: Tooth sockets on dental plate, pattern: single column throughout (0), multiple columns or cluster on max half of plate length (1), multiple columns throughout (2).

66. M-DP-5: Tooth sockets on dental plate, predominant shape: surrounded by a more or less continuous, protruding ring (0), simple opening (1), surrounded by separate, weakly protruding knobs and/or ridges (2), surrounded by strongly protruding knobs and/or ridges (3).

67. M-DP-7: Tooth socket, depth: depression or perforating DP without septum (0), at least some perforating DP with septum (1).

68. M-OP-1: Oral plate, shape: as high as long or higher (0), longer than high (1)

69. M-OP-2: Abradial muscle fossa, shape: large, well defined flange (0), central depression (1).

70. M-OP-3: Abradial muscle attachment area, stereom structure: normal stereom (0), rib-like branching structures (1).

71. M-OP-4: Adradial muscle attachment area, position: ventral, lining ventral or ventro-distal edge of articulation area (0), middle, vertical and lining less than two thirds of distal edge of adradial articulation area (1), middle, vertical and lining more than two thirds of distal edge of adradial articulation area (2), dorsal, large spoon-shaped depression (3), flange over most of lateral surface, with striations (4)

72. A-G-2: Integument of arms, structure: naked (0), bearing granules (1).

73. A-G-3: Arms, shape: simple (0), branched (1).

74. A-VP-3: Proximal VAPs (in articulated plating), position: separated by lateral arm plates (0), potentially in contact (1).

75. A-VP-4: Distal edge of proximal VAPs (in macerated plate), shape: convex to straight (0), concave or incised (1).

76. A-VP-5: Proximal edge of proximal VAPs (macerated plate), shape: convex to straight (0), concave or incised (1).

77. A-VP-6: Distal portion of proximal VAPs (in macerated plate), dimensions: as wide as proximal portion or narrower (0), wider than proximal portion (1).

78. A-VP-7: Lateral edge of proximalmost VAPs (in macerated plate) with clear incisions/notches for tentacle openings: no (0), yes (1).

79. A-VP-8: Edge of tentacle notches with sockets/articulations for tentacle scales (e.g., *Ophiomyces*): absent (0), present (1).

80. A-VP-10: Proximal VAPs, ornamentation: without conspicuous ornamentation (0), with tubercules or striation (1)

81. A-VP-12: Spurs at proximal edge of ventral arm plates (macerated): absent (0), present (e.g., *Ophioderma*) (1).

82. A-DP-2: DAPs per segment, number: single (0), multiple (1), none (2).

83. A-DP-3: Proximal DAP series, position: separated (0), in contact (1).

84. A-DP-4: Proximal DAPs, shape: fan-shaped (0), trapezoid with smooth proximal edge (1), oval semi-circular (2)

85. A-DP-8: Proximal DAPs, ornamentation: without conspicuous ornamentation (0), tuberculous (1), with striation (2).

86. A-DP-10: Spurs at proximal edge of DAP (macerated): absent (0), present (1).

87. *A-DP-11: Accessory dorsal arm plates: absent (0), present (1).

88. A-S-1: Arm spine position: mainly lateral (0), at proximal segments only on ventral side of arms (e.g., *Asteronyx*) (1).

89. A-S-2: Arm spines, orientation: predominantly parallel to arm axis (adpressed) (0), predominantly erect, standing perpendicular to arm axis (1).

90. A-S-3: Longest arm spines, length: shorter than half a segment (0), between half a segment and one segment (1), between one and two segments (2), longer than two segments (3).

91. A-S-4: Arm spines, interior structure: massive (0), with a lumen (1).

92. A-S-5: Arm spines, surface ornamentation: smooth (0), with lateral thorns (1), with scale-like tubercles (2).

93. A-S-7: Arm spines, cross section shape: round (0), laterally flattened (1).

94. A-S-8: Tip of arm spines, shape: blunt (0), pointed (1).

95. A-S-10: Hook-shaped arm spines, position: at no segments (0), only at distal segments (0), at proximal to distal segments (1).

96. A-S-11: Hook-shaped arm spines, shape: regular arm spines with bent tip and/or saw-toothed edge (0), true, hyaline hook (1), both modified regular spines and true hooks (2).

97. A-S-13: Arm spines, size pattern: ventralmost spine(s) longest (0), median spine(s) longest (1), dorsalmost spine(s) longest (2), equal (3).

98. A-S-14: Arm spines at proximal to median arm segments, number changes: decreasing distalwards (0), constant (e.g., *Ophiura*) (1).

99. A-TS-3: Tentacle scales, shape: operculiform (nearly as long as wide) (0), leaf-like (slightly longer than wide and blunt) (1), spine-like (more than two times as long as wide and pointed) (2), ventral spine closing tentacle opening (3), flat, elongated (4).

100. A-TS-4: Tentacle scales, size: not accurately closing tentacle pore (0), accurately closing tentacle pore (1).

101. A-TS-5: Tentacle scales, ornamentation: without longitudinal striation (0), with longitudinal striation (1).

102. A-TS-6: Tentacle scales, placement: only at LAP (0), at both LAP and VAP (1), only at VAP (2).

103. A-V-1: Dorso-distal muscular fossae, distalwards projection: not projecting (0), far from distal edge of zygocondyles (short keel, e.g., *Ophiacantha*) (1), almost beyond zygocondyles (intermediate keel, e.g., *Ophiodoris*) (2), beyond zygocondyles (extended keel, e.g., *Ophiothrix*) (3).

104. A-V-2: Vertebrae: lateral saddle between muscular fossae, structure: with single ridge (0), with multiple knobs (e.g., *Gorgonocephalus*) (1).

105. A-V-4: Zygocondyles (two major articular knobs of distal surfaces of vertebrae) in proximal vertebrae, position: nearly parallel (0), dorsalwards converging (1).

106. A-V-6: Zygosphene fused with pair of zygocondyles, size: not projecting beyond ventral edge of zygocondyles or projecting beyond ventral edge of zygocondyles with projecting part shorter than zygocondyles (0), projecting beyond ventral edge of zygocondyles with projecting part as long as zygocondyles (1), projecting beyond ventral edge of zygocondyles with projecting part longer than zygocondyles (2).

107. *A-V-7: Vertebrae, needle-like thorns in dorsal groove: absent (0), present (1).

108. LAP-G-1: LAPs, position: only lateral (0), arched (wrapped around the arm) (1).

109. LAP-G-3: LAPs with constriction (dorsal and/or ventral edge(s) concave): absent (0), present (1).

110. LAP-G-4: Ventro-proximalwards projection on ventral portion of LAP: absent (0), present (1).

111. LAP-G-5: Ventralwards projection on ventro-distal tip of LAP (e.g., *Ophiopallas*): absent (0), present (1).

112. LAP-G-6: Dorsal edge distalwards ascending: absent (0), present (1).

113. *LAP-G-7: First LAPs, shape: like following LAPs (0), wing-like folded (1), elongated, blade-like (2).

114. LAP-O-2: Outer surface trabecular intersections, shape: not protruding (0), protruding to form only knobs approximately the same size as stereom pores (1), protruding to form knobs larger than stereom pores on most of outer surface of LAP (2), protruding to form knobs larger than stereom pores on small part of outer surface of LAP (3).

115. #LAP-O-8: Outer surface, structure: normal stereom (0), vertical striation formed by merged knobs (1), vertical striation formed by regular ridges (2), with pointed thorns (3).

116. LAP-O-10: Distalwards pointing, scale-like structures on outer surface stereom: absent (0), present (1).

117. LAP-PE-1: Proximal edge of outer LAP surface lined by discernible band of different (e.g., more finely meshed) stereom structure, position: no discernible band (0), only in central part (1), over most of the proximal edge (2).

118. LAP-PE-2: Spurs on proximal edge of outer LAP surface other than ventro-proximal one, size: more than two small (shorter than one fourth of LAP width) (0), one or two large (wider than one fourth of LAP width) (1), one or two small (shorter than one fourth of LAP width) (2) .

119. LAP-PE-3: Oblique, elongated spur on ventro-proximal tip of outer surface of LAP: absent (0), present (1).

120. LAP-PE-4: Proximal outer surface edge of LAP, central part extension: not protruding (0), protruding (1).

121. LAP-PE-8: Proximal edge of outer LAP surface with horizontal striation, extension: restricted to small area (e.g., between spurs) (0), along most of the edge (1).

122. LAP-SA-1: Spine articulations, position: on same level as remaining outer surface (0), on elevated portion of LAP bordered proximally by ridge (1), on elevated portion of LAP not bordered proximally by ridge (2), in notches of distal LAP edge (3).

123. LAP-SA-4: Spine articulations, separation from distal edge: by the usual outer surface stereom (0), separated from the distal edge by a thin projection of the distal LAP portion (e.g., *Ophiomyces*) (1), directly adjacent to the distal edge of LAP (2).

124. LAP-SA-5: Spine articulation series, extension: restricted to (the ventral or central) portion of the distal edge (0), arranged over entire distal LAP edge (1).

125. LAP-SA-6: Spine articulation, size: dorsalwards increasing in size (0), ventralwards increasing in size (1), middle spine articulation(s) larger (2), all similar (3).

126. LAP-SA-7: Spine articulations, distance: dorsalwards increasing (0), ventralwards increasing (1), equidistant (2), only two (3).

127. LAP-SA-8: Nerve and muscle openings, separation: by small ridge if at all (0), by large, prominent ridge or regular stereom (1).

128. LAP-SA-9: Nerve opening, size: smaller than muscle opening (0), approximately as large as muscle opening (1).

129. #LAP-SA-10: Articular structures, shape: like surrounding stereom (e.g., *Ophiura*) (0), elevated lobes (1).

130. LAP-SA-11: When dorsal and ventral lobes absent, proximal edge of muscle opening, structure: even (0), denticulate (1).

131. LAP-SA-12: Dorsal and ventral lobes, connection: simply separated (0), separated by one or several knobs or by denticulate stereom (1), merged at their proximal tips by smooth connection (2).

132. LAP-SA-13: Dorsal and ventral lobes, size: one lobe clearly larger than the other (0), equal-sized (1).

133. LAP-SA-14: Dorsal and ventral lobes, orientation to each other: shifted (e.g., *Ophiacantha*) (0), parallel (e.g., *Amphiura*) (1).

134. LAP-SA-15: Dorsal and ventral lobes, shape: at least one lobe bent (0), straight (1).

135. LAP-SA-16: Dorsal and ventral lobes, stereom structure: with perforations (0), massive (1).

136. LAP-SA-17: Lobes, orientation on plate: nearly horizontal (0), tilted (1), nearly vertical (2).

137. LAP-SA-19: Sigmoidal fold, expression: weakly developed (0), fully developed (1).

138. LAP-SA-20: When dorsal and ventral lobes absent, muscle opening encompassed by: simple stereom (e.g., *Euryale*), poorly defined circular elevation (e.g., *Asteronyx*) and/or vertical ridge distally and wavy ridge proximally (e.g., *Gorgonocephalus*) (0), vertical mouth-shaped, sharply defined elevation (1).

139. LAP-SA-21: When dorsal and ventral lobes absent, orientation of ridge distally bordering muscle opening: vertical (0), oblique (1).

140. LAP-SA-22: When dorsal and ventral lobes absent, shape of ridge distally bordering muscle opening: slender (0), thick, lip-shaped and strongly protruding (1).

141. LAP-TP-1: Tentacle opening beyond first segments under disc, shape: notch (0), within-plate perforation (1).

142. LAP-TP-2: Tentacle notch, direction: ventralwards (0), ventro-distalwards (1), distalwards, close to horizontal midline of LAP (2).

143. LAP-TP-3: Tentacle notch externally lined by narrow groove: no (0), yes (e.g., *Aganaster*, basalmost segments in *Ophiomusium*) (1).

144. LAP-TP-4: Inner side of tentacle notch with horizontally stretched stereom: no (0), yes (e.g., *Ophioscolex*) (1).

145. LAP-I-1: Inner side of LAP, main structure: more or less continuous ridge (0), two separate (rarely merged) central knobs (e.g., *Amphiura*) (1).

146. LAP-I-3: Ridge on inner side of LAP, shape: entire (0), with ventral tip of ventro-proximalwards pointing part of ridge separated from remaining ridge (1), with separate knob on ventral tip of LAP (e.g., *Ophioderma*) (2), ridge separated into two halves (3).

147. LAP-I-5: Ridge on inner side of LAP, stereom structure: the same stereom as remaining inner surface of LAP (0), more compact or more densely meshed stereom (1).

148. LAP-I-6: Ridge on inner side of LAP, shape: without major kink and with tongue-shaped dorsal tip (0), with kink between dorso-proximalwards pointing dorsal portion and ventro-proximalwards pointing ventral portion, and with tongue-shaped dorsal tip (1), with two kinks and dorsal tip with ventro-proximalwards pointing projection (2), with two kinks and dorsal kink with ventro-proximalwards pointing projection (3).

149. LAP-I-7: Large dorsal contact surface with opposite LAP: absent (0), present (1).

150. LAP-I-8: Large ventral contact surface with opposite LAP: absent (0), present (1).

151. LAP-I-9: Two central knobs on inner side of LAP, shape: simple (0), with a knob (1), with a ridge (2).

152. LAP-I-10: Additional dorsal structure on inner side of LAP merged with proximal one of the two central knobs: absent (0), present (1).

153. LAP-I-15: Perforations on inner side of LAP, shape: single small, or inconspicuous (0), vertical row without furrow (1), vertical row with furrow (2), single, large and conspicuous (3).